

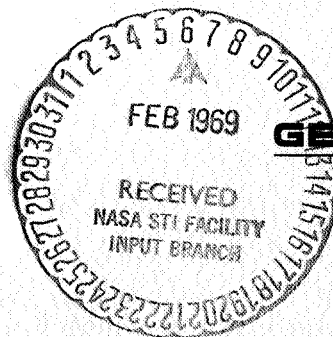
N 69 2028 4

NASA CR 100366

REPORT GDC-BKM68-055  
CONTRACT NAS3-8711

AC-16  
FINAL GUIDANCE EQUATIONS AND  
PERFORMANCE ANALYSIS

CASE FILE  
COPY



**GENERAL DYNAMICS**  
*Convair Division*

REPORT GDC-BKM68-055

**AC-16**  
**FINAL GUIDANCE EQUATIONS AND**  
**PERFORMANCE ANALYSIS**

Prepared Under  
Contract NAS3-8711

August 1968

Prepared by  
CONVAIR DIVISION OF GENERAL DYNAMICS  
San Diego, California

Prepared by *R.E. Roberts* Checked by *R.E. Roberts*  
*for* R. E. Seiley *for* D. H. Flowers  
Sr. Guidance Design Specialist  
Analysis Engineer

Approved by *R.P. Day* Approved by *J.B. Anthony*  
R. P. Day N. B. Anthony  
Group Engineer Assistant Chief Engineer  
Guidance Analysis Flight Mechanics - LVP

Security Classification Approved  
per Requirements of Paragraph 10, DOD 5220.22-M

*D.J. Hallman*  
*for* D. J. Hallman,  
Supervisor, Technical Reports

## FOREWORD

This report presents the guidance equations and constants for AC-16, the specifications and test plan for the equations, and the results of the performance analysis. The data from the performance analysis verify that the guidance equations satisfy all requirements for the AC-16 mission.

This report fulfills the data documentation requirements for Item 57, Contract NAS3-8711.

## ACKNOWLEDGMENTS

This report was prepared by members of the Centaur Guidance Analysis - LVP Group. The following personnel contributed to the designated sections of this report.

F. Backus	Appendix E
R. Roberts	Section 2, Appendixes A, B, C, F
R. Seiley	Sections 1 through 8, Appendixes A through D
A. Wilmot	Section 2

## TABLE OF CONTENTS

<u>Section</u>		<u>Page</u>
1	GUIDANCE EQUATION SPECIFICATIONS. . . . .	.1-1
1.1	MISSION REQUIREMENTS . . . . .	.1-1
1.2	EQUATION INPUT CONSTRAINTS. . . . .	.1-1
1.3	EQUATION OUTPUT REQUIREMENTS . . . . .	.1-2
1.4	EQUATION DESIGN OBJECTIVES. . . . .	.1-4
2	GUIDANCE EQUATIONS . . . . .	.2-1
2.1	NAVIGATION AND COORDINATE COMPUTATIONS . . . . .	.2-1
2.2	PITCH STEERING . . . . .	.2-5
2.2.1	Pitch Steering Law . . . . .	.2-5
2.2.2	Evaluation of Acceleration Integrals . . . . .	.2-7
2.2.3	Angular Momentum to be Gained and Time to Go . . . . .	.2-9
2.2.4	True Anomaly to Go and True Anomaly at Cutoff . . . . .	.2-13
2.2.5	Desired Cutoff Position and Radial Velocity . . . . .	.2-16
2.3	YAW STEERING. . . . .	.2-18
2.4	STEERING VECTOR COMPUTATION. . . . .	.2-22
2.5	BOOSTER PHASE . . . . .	.2-24
2.5.1	Booster Steering . . . . .	.2-24
2.5.2	BECO Discrete . . . . .	.2-25
2.5.3	Ground Test Requirements . . . . .	.2-26
2.6	SUSTAINER PHASE . . . . .	.2-27
2.6.1	Pitch Steering . . . . .	.2-27
2.6.2	Sustainer Yaw Steering . . . . .	.2-29
2.6.3	SECO Backup Discrete . . . . .	.2-30
2.7	POST INJECTION PHASE . . . . .	.2-30
2.7.1	Spacecraft Separation Attitude . . . . .	.2-31
2.7.2	Vehicle Retrothrust Attitude Vector . . . . .	.2-31
2.8	MAIN ENGINE CUTOFF . . . . .	.2-32
2.8.1	Cutoff Bias, $J_2$ . . . . .	.2-32
2.9	INITIALIZATION AND EQUATION INPUT . . . . .	.2-34
2.10	PROGRAM BRANCHES . . . . .	.2-38
3	TARGETING . . . . .	.3-1
3.1	MISSION REQUIREMENTS . . . . .	.3-2
3.2	POWERED FLIGHT TRAJECTORY TARGETING . . . . .	.3-2

## TABLE OF CONTENTS, Contd

<u>Section</u>		<u>Page</u>
3.3	SPACECRAFT ATTITUDE AND REORIENT VECTORS . . . . .	3-7
3.4	TARGETING PROCEDURES . . . . .	3-9
4	TARGET SPECIFICATION . . . . .	4-1
5	PERFORMANCE AND ACCEPTANCE CRITERIA . . . . .	5-1
6	GUIDANCE EQUATION TEST PLAN . . . . .	6-1
6.1	SIMULATION TEST PLAN . . . . .	6-1
6.1.1	Targeting Check Simulation . . . . .	6-1
6.1.2	Flight Computer Interpretive Simulations . . . . .	6-1
6.1.3	Non-Nominal Performance Simulations . . . . .	6-2
6.1.4	Omnibus Dispersions . . . . .	6-2
6.2	SIMULATION GROUND RULES . . . . .	6-3
6.2.1	Targeting Check Simulation Groundrules . . . . .	6-5
6.2.2	Flight Computer Interpretive Simulation Groundrules . . . . .	6-5
6.2.3	Non-Nominal Engineering Simulation Groundrules . . . . .	6-5
6.2.4	Omnibus Simulation Groundrules . . . . .	6-7
7	SOFTWARE PERFORMANCE EVALUATION . . . . .	7-1
7.1	TARGETING ACCURACY . . . . .	7-1
7.2	CUTOFF STEERING ERROR . . . . .	7-1
7.3	NON-NOMINAL PERFORMANCE RESULTS . . . . .	7-6
7.4	FLIGHT COMPUTER COMPUTATIONAL EFFECTS . . . . .	7-6
7.5	VELOCITY QUANTIZATION AND NOISE EFFECTS . . . . .	7-7
7.6	PU NULL EFFECTS . . . . .	7-7
7.7	GROSSLY PERTURBED INTERPRETIVE COMPUTER SIMULATION RESULTS . . . . .	7-11
7.8	HEATING DATA . . . . .	7-11
7.9	SUMMARY OF RESULTS . . . . .	7-11
8	GUIDANCE-AUTOPILOT EVENT COMPATIBILITY . . . . .	8-1
8.1	GUIDANCE AND AUTOPILOT BECO COMPATIBILITY . . . . .	8-1

## TABLE OF CONTENTS, Contd

<u>Section</u>		<u>Page</u>
8.2	GUIDANCE AND AUTOPILOT SECO- BACKUP COMPATIBILITY . . . . .	8-2
8.3	GUIDANCE AND AUTOPILOT MECO COMPATIBILITY . . . . .	8-2
8.4	GUIDANCE AND AUTOPILOT PU NULL COMPATIBILITY . . . . .	8-3
8.5	GUIDANCE AND AUTOPILOT REORIENT COMPATIBILITY . . . . .	8-4
8.6	COMPATIBILITY OF DOGLEG MANEUVER AND FAIRING JETTISON TIMES . . . .	8-4
9	REFERENCES . . . . .	9-1

Appendix

A	GUIDANCE EQUATION FLOW DIAGRAMS FOR AC-17 . . . . .	A-1
B	GUIDANCE CONSTANTS . . . . .	B-1
C	TELEMETRY SEQUENCE . . . . .	C-1
D	INFLIGHT DISCRETES . . . . .	D-1
E	TIME-TO-GO ERROR RESULTING FROM THRUST PERTURBATION DUE TO NULLING PROPELLANT UTILIZATION VALVE . . . . .	E-1
F	SIGMATOR VELOCITY FILTERING TECHNIQUE . .	F-1



## LIST OF FIGURES

<u>Figure</u>		<u>Page</u>
2-1	Orbital Geometry . . . . .	2-14
2-2	$a_{mw}$ vs Time From Go-Inertial . . . . .	2-25
2-3	Geometry for Range Safety Constraint of Sustainer Yaw Steering . . . . .	2-29
2-4	Vehicle Retrothrust Attitude Vector. . . . .	2-31
2-5	MECO Time Sequence . . . . .	2-33
3-1	Definition of Fixed $\bar{l}_n$ Vector . . . . .	3-3
3-2	Definition of Target Vector . . . . .	3-5
3-3	Reorient Attitude Vector Geometry . . . . .	3-8
3-4	OAQ Targeting Procedure . . . . .	3-10
7-1	Injection Radius Error, $\Delta r_m$ , versus Time-to-go at Enter Cut . . . . .	7-3
7-2	Deviation in $(r_a - r_p)$ versus Time-to-go at Enter Cut . . . . .	7-4
7-3	Deviation in Apogee Radius, $r_a$ , versus Time-to-go at Enter Cut . . . . .	7-4
7-4	Orbital Period Error versus Time-to-go at Enter Cut . . . . .	7-5
7-5	Heat Flux versus Time . . . . .	7-13
7-6	Heat Parameter versus Time . . . . .	7-14
8-1	Guidance Autopilot BECO Compatibility . . . . .	8-1
8-2	Guidance Autopilot SECO-Backup Compatibility . . . . .	8-2
8-3	Guidance and Autopilot MECO Compatibility . . . . .	8-3
8-4	Guidance and Autopilot PU Null Compatibility . . . . .	8-3
8-5	Guidance and Autopilot Reorient Compatibility . . . . .	8-4
8-6	Compatibility of Dogleg Maneuver and Fairing Jettison Times . . . . .	8-5
A-1	Explicit Equation Modular Blocks . . . . .	A-2
A-2	Initialization . . . . .	A-3
A-3	Initialization, Cont. . . . .	A-4

## LIST OF FIGURES, Contd

<u>Figure</u>		<u>Page</u>
A-4	Navigation Equations . . . . .	A-5
A-5	Coordinate System Equations . . . . .	A-6
A-6	Booster Logic . . . . .	A-7
A-7	Sustainer-Centaur Logic . . . . .	A-8
A-8	Time-to-Go Equations . . . . .	A-9
A-9	Pitch Steering Coefficients . . . . .	A-10
A-10	Yaw Steering Coefficients . . . . .	A-11
A-11	Steering Equations . . . . .	A-12
A-12	Parking Orbit Equations . . . . .	A-13
A-13	Post Injection Equations . . . . .	A-14
E-1	Thrust vs Time-to-Go During Nulling of PU Valve .	E-1
E-2	Probability-Density-Function (p.d.f.) for Thrust Shift Due to PU Valve Final Null Angle Shift . . .	E-5
E-3	Probability-Density-Function (p.d.f.) for Error in TTG Due to PU Valve Final Null Angle Shift . . .	E-6

## LIST OF TABLES

<u>Table</u>		<u>Page</u>
2-1	Program Logic Branches . . . . .	2-39
4-1	AC-16 Target Specifications . . . . .	4-1
6-1	Omnibus Perturbations . . . . .	6-4
6-2	Orbit Parameters for Targeting Evaluation . . .	6-6
6-3	Orbit Parameters for Interpretive Simulation . .	6-7
6-4	Dispersion List . . . . .	6-8
7-1	Targeting Accuracy . . . . .	7-2
7-2	AC-16 3-Sigma Dispersion Results . . . . .	7-8
7-3	Computational Effects . . . . .	7-10
7-4	Grossly Perturbed I.C.S. Results . . . . .	7-12
7-5	Summary of Guidance Equation Performance Results	7-15
B-1	Switching Constants . . . . .	B-2
B-2	Initialization Constants . . . . .	B-4
B-3	Equation Input Constants . . . . .	B-5
B-4	Definition of J Constants . . . . .	B-8
C-1	Telemetry Sequence . . . . .	C-1
D-1	Inflight Discretes . . . . .	D-1
E-1	Thrust Shift, $F_{LO}$ , Due to PU Valve Final Null Angle Shift . . . . .	E-5

## LIST OF SYMBOLS

$A, B$	Pitch steering coefficients.
$a_o$	Integral of thrust acceleration.
$\bar{a}_\omega$	Acceleration compensated for platform drift.
$\bar{a}_T$	Thrust acceleration corrected for scale factor, bias, and misalignment.
$a_T$	Thrust acceleration magnitude.
$a_{TI}$	Thrust acceleration magnitude at cutoff.
$\bar{C}$	Angular momentum vector.
$C$	Angular momentum.
$C_d$	Desired angular momentum of the nominal cutoff conic.
$C_1$	Instantaneous rate of change of true anomaly.
$C_2$	Rate of change of true anomaly at $T/2$ .
$C_r$	Parking orbit pitch steering coefficient.
$C_n$	Parking orbit yaw steering coefficient.
$DT$	Elapsed time interval from a reference time $t_C$ .
$d_j$	Guidance system compensation coefficients ( $j=1$ through 22).
$e$	Eccentricity of the injection transfer orbit.
$E_j$	Guidance switching constants ( $j = 1$ through 31).
$E_{PY}$	Booster switching parameter.
$\bar{f}$	Guidance-computed desired thrust pointing direction.
$\bar{f}^*$	Guidance-computer desired pointing direction for the vehicle roll axis.
$\bar{g}$	Gravitational acceleration vector.
$G$	Gravitational - centrifugal acceleration.
$G_I$	Gravitational - centrifugal acceleration at cutoff.
$h_d$	Injection orbit vis-viva energy integral.
$I_j$	Guidance initialization constants ( $j = 1$ through 11).

$J_j$	Guidance launch-day-dependent constants ( $j = 1$ through 60).
$K_j$	Guidance equation input constants ( $j = 1$ through 31).
$K_{18}$	Vehicle exhaust velocity.
$K_Y$	Yaw steering coefficient.
$P_j$	Computer roundoff constants.
$P$	Semi latus rectum of the desired nominal conic.
$\bar{r}_m$	Instantaneous position vector.
$r_m$	Instantaneous position vector magnitude.
$r_p$	Perigee radius of the injection orbit.
$\dot{r}_m$	Instantaneous radial velocity.
$\dot{r}_d$	Desired radial velocity at cutoff.
$r_d$	Desired position magnitude at cutoff.
$T$	Time to go.
$t_i$	Guidance time for $i^{\text{th}}$ cycle.
$t_\lambda$	Sigmator time associated with LOT.
$t_\sigma$	Vehicleborne computer sigmator time.
$t_C$	Reference time for time switching events.
$t_e$	Time into the launch window.
$t_{gc}$	Parking orbit time to go until MES II.
$\bar{v}_m$	Instantaneous velocity vector.
$\bar{v}_\omega$	Velocity compensation for platform drift.
$\bar{v}_\sigma$	Integral of accelerometer outputs
$v_{mt}$	Tangential component of velocity.
$V_c$	Nominal injection conic parameter = $\frac{eC_d}{P}$
$y_1, y_2$	Yaw steering coefficients.
$\bar{\alpha}_1$	Error vector sustainer phase angle of attack control.
$\alpha_1$	Magnitude of $\bar{\alpha}_1$ .
$\alpha_m$	Maximum permissible value of $\alpha_1$ .
$\beta_1, \beta_2, \beta_3$	Post injection phase attitude command components.
$\Delta t$	Computer cycle time duration.

$\Delta t_{co}$	Centaur MECO cutoff time interval.
$\Delta \eta$	True anomaly to go until cutoff.
$\Delta r$	Position to be gained.
$\Delta \dot{r}$	Radial velocity to be gained.
$\overline{\Delta f}$	Integral steering vector.
$\epsilon_Y$	Yaw error signal.
$\eta_A$	True anomaly of the target vector.
$\eta_T$	Predicted true anomaly at cutoff.
$\theta$	Instantaneous range angle to the target vector.
$\lambda$	Co-latitude
$\omega_{PB}$	Booster pitch rate.
$\omega_{YB}$	Booster yaw rate.
$\omega_d$	Gyro torquing rate.
$\omega_p$	Platform drift rate.
$\tau$	Hypothetical burn time to zero weight ( $\tau = W/\dot{W}$ )
$\bar{l}_a, \bar{l}_{a2}$	Unit target vectors for first and second burn.
$\bar{l}_{aT}$	Unit thrust acceleration vector.
$\bar{l}_n$	Unit vector normal to the flight plane.
$\bar{l}_t$	Unit tangential vector.
$\bar{l}_{np}$	Unit earth rotational axis.
$\bar{l}_r$	Unit radial vector.

## Subscripts

(u, v, w)	Inertial coordinates.
(t, n, r)	Rotating tangential, normal, radial coordinates.
i	i <sup>th</sup> cycle value.
i-1	Cycle prior to i <sup>th</sup> cycle.
$\sigma$	Sigmator data.



## SUMMARY

The final guidance equations presented in this report have been designed as a common set of explicit equations suitable for the ATS-D, E, OAO-A2 and Mariner '69 missions. This report is specifically oriented to the AC-16/OAO-A2 mission. It thoroughly describes the equations and targeting for this mission. The applications and performance capability of the equations for ATS-D are thoroughly documented in Reference 8. A subsequent report will describe aspects of the equations peculiar to the Mariner mission. This report presents the following information for the AC-16/OAO-A2 mission:

- a. Equation Specifications: Trajectory, vehicle, payload, and hardware constraints or requirements that the equation design must satisfy.
- b. Equation Design: The form of the equations, as mechanized for the vehicleborne computer, that satisfies the equation specifications and performance criteria.
- c. Performance and Acceptance Criteria: A set of maximum deviations from critical trajectory, environmental, and payload capability parameters that fixes the standard for equation performance.
- d. Target Specifications: The required orbit parameters to which the equations must be targeted.
- e. Inflight Equation Test Plan: A specification of the trajectory simulations required for a comprehensive evaluation of guidance equation performance.
- f. Performance Evaluation of Inflight Equations: A presentation of the data obtained from the simulations specified in the test plan.
- g. Targeting Techniques: A discussion of the method of targeting the AC-16 mission.

An evaluation of the results of the performance analysis shows that all guidance equation specifications have been fulfilled. The RSS of the guidance equation error sources is shown to result in achieving the specified target orbit parameters with the following accuracy:



$\Delta$ altitude: 0.22 n.mi.

$\Delta$ inclination: 0.009 deg

$\Delta(r_a - r_p)$ : 2.22 n.mi.

Grossly perturbed interpretive simulation trajectories demonstrated the gross performance and computational scaling of the guidance equations to be adequate in that reasonable orbits were obtained for all perturbed trajectories and no arithmetic operation exceeded its scale factor.

## SECTION 1

### GUIDANCE EQUATION SPECIFICATIONS

#### 1.1 MISSION REQUIREMENTS

The AC-16 guidance equations are designed to satisfy the requirements of the OAO-A2 mission for direct ascent into a circular orbit. These requirements include:

- a. Payload injection into the required target orbit with an accuracy such that guidance software errors, when combined with all hardware errors, shall not exceed the orbit parameter tolerances given by the target specification.
- b. Ensure that closed loop steering commands do not significantly degrade the payload capability of the vehicle.
- c. Provide open loop booster pitch and yaw steering signals.
- d. Provide a yaw maneuver (dogleg) capability satisfying range safety requirements.
- e. Orient the spacecraft along the required attitude vector prior to spacecraft separation.
- f. Orient the Centaur vehicle along the required attitude vector prior to the start of retrothrust.

#### 1.2 EQUATION INPUT CONSTRAINTS

The guidance equations are constrained to accept as input seven quantities from the vehicleborne computer sigmator track. These quantities are  $t_{\sigma}$ ,  $\bar{v}_{\sigma}$ , and  $\bar{r}_{\sigma}$ . However, by virtue of the design of the navigational equations, the quantity  $\bar{r}_{\sigma}$  is not utilized. The velocity vector,  $\bar{v}_{\sigma}$ , is obtained from the appropriate sigmator sector that sums incremental velocity pulses from the guidance accelerometers. The instantaneous time,  $t_{\sigma}$ , is obtained from the appropriate sigmator sector that accumulates time pulses from the computer clock.

More specifically, the input consists of:

- $t_G$ : Accumulated time since the reference zero time. Time pulses are accumulated on the sigmator short line at the rate of 1300/sec and updated on the long line every half drum revolution.
- $\bar{v}_G$ : Accumulated velocity since the reference zero time. This velocity is nominally quantized to 0.11 ft/sec and updated on the long line every half drum revolution.

### 1.3 EQUATION OUTPUT REQUIREMENTS

The guidance equations are required to provide the following output:

- a. Booster Phase Turning Rates. Throughout the booster phase, preprogrammed pitch and yaw rates are output as a function of time from 2-inch motion. The rates for pitch and yaw are output via the v and u steering modules, respectively. All preprogrammed rates are rounded-off to 10 bits in order to satisfy the steering module digital/analog converter limitations.
- b. Booster Phase Test Steering Vector. For ground checkout purposes only, a steering vector is output approximately 179 seconds after go inertial. This 179 seconds is an accumulation of  $T_C$  initialized to 9 seconds and of the  $E_{30}$  test value of 167 seconds. During actual flight, BECO occurs nominally 152.9 seconds after 2-inch motion as calculated by the guidance equations. Upon issuing BECO or sensing an acceleration decay, the booster phase of the guidance equations is exited. Since the  $E_{30}$  test would be passed 167 seconds after 2-inch motion, the issuing of the booster phase test steering vector during actual flight is virtually precluded. For flight,  $T_C$  is initialized as 100 sec. Thus if after entering flight mode a prelaunch hold longer than approximately 115 seconds occurs, guidance will erroneously implement pitch and yaw rates; to prevent this occurrence during an actual launch, the maximum prelaunch hold after go inertial is restricted to 115 seconds.
- c. Booster Phase Test Discretes. For ground checkout purposes only, a sequence of discretes will be issued after approximately 234 seconds from go inertial. This 234 seconds is an accumulation of  $T_C$  initialized to 9 seconds and the  $E_{31}$

test value of 222 seconds. The restriction that the prelaunch hold be less than 115 seconds and the nature of the guidance equations during the booster phase prohibit the erroneous issuing of these discretes during the actual flight. The sequence of test discretes is: L0, L1, L3, L6, L8, L10, L12, L16.

- d. Reference Steering Vector. Throughout the closed loop phases of flight (BECO to MECO) the steering vector  $\bar{f}^*$  is output once per compute cycle. This vector is in the drifting u, v, w coordinates, with a nominal magnitude of 0.409259 (equivalent to 11.05 volts) and a maximum magnitude of 0.413. The computed values of  $\bar{f}^*$  are truncated at 11 bits in order to satisfy the digital/analog converter limitations.
- e. Post Injection Phase Reference Vectors.
  1. Spacecraft Separation Attitude Vector. On the first compute cycle after MECO, a vector corresponding to the vehicle roll axis nominal attitude at MECO is output as the spacecraft separation attitude vector. The impulse imparted to the spacecraft at separation along this vector nominally provides the incremental velocity (2.18 ft/sec) required to attain the target orbit conditions. This vector is also the Centaur vehicle attitude vector from separation until the start of reorientation to the retrothrust attitude vector at a fixed time from MECO.
  2. Centaur Vehicle Retrothrust Attitude Vector. At MECO + 356 seconds the guidance equations output a reference attitude vector along which retrothrust occurs. This reference vector is the instantaneous negative radius vector biased by an angle,  $\alpha$ , in the direction of  $-\bar{v}_m$ . Both the separation and retrothrust attitude reference vectors are updated and output each compute cycle. The vectors are in drifting u, v, w coordinates, each having a nominal magnitude of 0.409259 (11.05 volts). The components of both vectors are truncated at 11 bits in order to satisfy the digital/analog converter limitations.

- f. Platform Torquing. Immediately after entering Flight Mode, zero is stored on the torquing pots. No inflight torquing rates are applied to the platform, since the measured drifts are compensated for analytically in the navigational equations.
- g. Discretes. The following discretes are required of the inflight guidance program:

<u>Discrete</u>	<u>Line Designation</u>	<u>Minimum Duration</u>
Flight mode acceptance	L9	9.0 ms
BECO	L3	9.0 ms
SECO (backup)	L6	9.0 ms
Null PU	L0	9.0 ms
MECO	L16	1.1 ms

(Not program controlled)

- h. Telemetry Format. Each telemetry sequence is preceded by a sequence start marker, and each data word in the sequence is preceded by an identification discrete. The start of inflight telemetry is identified by a master sequence start discrete. Telemetry markers are:
1. Master Sequence Start. Fifty binary ones (400 W.T.) issued once during the prelaunch phase of the equations upon entering flight mode.
  2. Sequence Start. Twenty-eight binary ones (224 W.T.) issued once per compute cycle preceding the first telemetered word in the sequence.
  3. Data Word Marker. Twenty-five data bit words, preceded by a 110 marker (16 W.T. discrete - line L14).

#### 1.4 EQUATION DESIGN OBJECTIVES

- a. Commonality. The AC-16/OAO-A2 guidance equations are designed to be compatible with the requirements of the ATS-D&E and Mariner Mars '69 missions. This provides a common set of explicit guidance equations for all three missions.
- b. Program Storage Requirements. The AC-16 guidance equations are designed to require not more than 2240 words of permanent storage in the GPK-33 computer, and not more than 200 words of temporary storage.

## SECTION 2

### GUIDANCE EQUATIONS

The AC-16 guidance equations are a generalized set of one stage explicit equations having the capability of guiding either single or two-burn Centaur stages. The Atlas sustainer phase guidance employs much of the Centaur phase equations, with some simplifying assumptions to avoid the problem of integrating across the Atlas-Centaur acceleration discontinuity. The Atlas booster phase is open loop. The equations are designed to satisfy the requirements of the OAO; ATS-D, E; and Mariner '69 missions. As such they provide a common guidance program for all three missions, and necessarily contain more capability than required for the OAO mission alone.

In this section the basic explicit guidance equations for both pitch and yaw steering are developed in detail. Following this development is a discussion of the requirements and equations for the booster and post-MECO phases. In addition, the equations for the guided sustainer phase and the assumptions and simplifications which permit utilizing much of the Centaur phase equations are also discussed in detail.

The equations are given in codable form in Appendix A.

#### 2.1 NAVIGATION AND COORDINATE COMPUTATIONS

The guidance computations and navigation measurements are accomplished in an earth-centered inertial coordinate system  $(u, v, w)$ , established just prior to launch as:

$\bar{1}_w$  = unit local vertical at the launch site

$\bar{1}_u$  = unit platform azimuth alignment direction

$\bar{1}_v = \bar{1}_w \times \bar{1}_u$

The  $\bar{1}_u$  direction is optically aligned. It is assumed that there is no inflight torquing of the platform gyros, and that analytic compensation is employed in the navigation equations for measurable platform drifts.

The guidance equations utilize the output from the accelerometers in the form of accumulated velocity pulses,  $\bar{v}_\sigma$ . This quantity is read from a special purpose track of the flight computer called the sigmator, which also accumulates time pulses from the vehicleborne clock. The navigational data required by the guidance equations is thus:

$t_\sigma$  instantaneous computer time.

$\bar{v}_\sigma$  velocity resulting from all non-gravitational accelerations acting on the vehicle.

The  $\bar{v}_\sigma$  data is accumulated on the sigmator long line and read in a manner which automatically provides a filter for accelerometer limit cycle noise. This is discussed in detail in Appendix F. From this data thrust acceleration,  $\bar{a}_T$ , is computed as

$$\bar{a}'_T = \begin{bmatrix} d_1 \\ d_2 \\ d_3 \end{bmatrix} \frac{\Delta \bar{v}_\sigma}{\Delta t} + \begin{bmatrix} d_7 \\ d_8 \\ d_9 \end{bmatrix}$$

$$\bar{a}_T = \begin{bmatrix} a'_{Tu} - d_{19} a'_{Tv} \\ a'_{Tv} + (d_{19} + d_4) a'_{Tu} \\ a'_{Tw} + d_5 a'_{Tu} + d_6 a'_{Tv} \end{bmatrix}$$

where

$d_1, d_2, d_3$  = accelerometer scale factors

$d_4, d_5, d_6$  = accelerometer misalignments

$d_7, d_8, d_9$  = accelerometer bias

$d_{19}$  = optical mirror misalignment

Thus the velocity data read from the sigmator is corrected for known guidance system errors. The d values are computed by the preflight calibration and alignment program.

Thrust acceleration is used to compute the platform drift vector,  $\bar{\omega}_p$ , as:

$$\bar{\omega}_p = \begin{bmatrix} d_{10} + d_{11} a_{TV} - d_{12} a_{Tu} \\ -d_{13} - d_{14} a_{Tu} - d_{15} a_{TV} \\ d_{16} + d_{17} a_{TV} - d_{18} a_{Tw} \end{bmatrix}$$

This drift vector results from fixed torque drift and mass unbalance of the gyros, and is used to correct position and velocity for platform drift, since the platform is not torqued in flight.

Position, gravity, and velocity in inertial coordinates are then obtained as:

#### Position

$$\Delta \bar{r}_{mi} = \left( \bar{v}_{mi-1} + \bar{r}_{mi-1} \times \bar{\omega}_{pi} + \frac{\Delta \bar{v}_m}{2} \right) \Delta t$$

$$\bar{r}_{mi} = \bar{r}_{mi-1} + \Delta \bar{r}_m$$

$$r_m = |\bar{r}_{mi}|$$

#### Gravity

$$\cos \lambda = \frac{\bar{r}_m}{|\bar{r}_m|} \cdot \bar{1}_{np}$$

$$\bar{1}_{np} = \text{unit earth rotational vector}$$

$$g_r = \frac{-K_1}{r_m^2} + \frac{K_2}{r_m^4} \left( \frac{5 \cos^2 \lambda - 1}{2} \right)$$

$$g_n = \frac{-K_2}{r_m^4} \cos \lambda$$

$$K_1, K_2 = \text{constants}$$



$$\bar{g} = g_r \frac{\bar{r}_m}{|\bar{r}_m|} + g_n \bar{l}_{np}$$

### Velocity

$$\Delta \bar{v}_{mi} = \left( \bar{a}_{Ti} + \bar{v}_{mi-1} \times \bar{\omega}_{pi} + \frac{\bar{g}_i + \bar{g}_{i-1}}{2} \right) \Delta t$$

$$\bar{v}_{mi} = \bar{v}_{mi-1} + \Delta \bar{v}_{mi}$$

In addition to correcting position and velocity for platform drift, it is necessary to correct other inertial vectors used by the guidance equations.

In particular, the earth rotational vector,  $\bar{l}_{np}$ , and the target vector,  $\bar{l}_a$ , must be converted to drifting "inertial" coordinates as

$$\bar{l}_{np} = \bar{l}_{np} + (\bar{l}_{np} \times \bar{\omega}_p) \Delta t$$

$$\bar{l}_a = \bar{l}_a + (\bar{l}_a \times \bar{\omega}_p) \Delta t$$

The vector  $\bar{l}_{a2}$ , also converted to drifting coordinates, is the second-burn target vector for ATS missions and therefore not utilized by OAO.

The computation of inflight steering commands is greatly facilitated by using the following rotating tangential, normal, radial (t, n, r) coordinate system:

$$\bar{l}_r = \frac{\bar{r}_m}{r_m}$$

$$\bar{l}_n = \frac{\bar{l}_r \times \bar{v}_m}{|\bar{l}_r \times \bar{v}_m|}$$

$$\bar{l}_t = \bar{l}_n \times \bar{l}_r$$

In this system the radial and tangential required velocity components are easily obtained from conic equations.

These navigation and coordinate computations are performed on each compute cycle.

To compensate for predictable computational (truncation) errors in the flight computer, roundoff bits ( $p_i$ ) are added to certain navigational quantities. The parameters affected are the following:

$\Delta \bar{r}_m$ ( $\bar{p}_1$ ):	to compensate for truncation due to the right shift before adding $\Delta \bar{r}_m$ to $\bar{r}_{mi-1}$
$r_m^2$ ( $\bar{p}_2$ ):	to compensate for multiply truncation errors in the dot product $r_m^2 = \bar{r}_m \cdot \bar{r}_m$
$\Delta \bar{v}_m$ ( $\bar{p}_3$ ):	to compensate for truncation due to the right shift before adding $\Delta \bar{v}_m$ to $\bar{v}_{mi-1}$
$\bar{l}_a, \bar{l}_{a2}$ ( $\bar{p}_4$ ):	to compensate for multiply truncation errors in the products $(\bar{l}_a \times \bar{\omega}_p)\Delta t$ and $(\bar{l}_{a2} \times \bar{\omega}_p)\Delta t$

## 2.2 PITCH STEERING

**2.2.1 PITCH STEERING LAW.** Pitch steering is based upon integrating the radial acceleration out to cutoff then predicting the desired cutoff position and radial velocity,  $r_d, \dot{r}_d$  respectively. These quantities are then used to form error signals  $\Delta r, \Delta \dot{r}$ , which represent position and velocity to be gained, from which the pitch steering command,  $f_r$ , is generated.

The explicit pitch steering law is derived from the radial acceleration, given by

$$\ddot{r} = a_{Tr} - \frac{K_1}{r^2} + \frac{C^2}{r^3}$$

where  $a_{Tr}$  is the radial component of thrust acceleration,  $a_{Tr} = \bar{a}_T \cdot \bar{l}_r$ , and  $C$  is angular momentum  $= |\bar{r} \times \bar{v}|$ . Let  $a_{Tr} = a_T f_r$ , where  $a_T$  is the total thrust acceleration. Then  $f_r$  is the control function for the pitch steering. If we let  $f_r$  be given by

$$f_r = A + Bt + \frac{\left( \frac{K_1}{r^2} - \frac{C^2}{r^3} \right)}{a_T} \quad (1)$$

then  $\ddot{r}$  becomes

$$\ddot{r} = (A + Bt) a_T$$

where A and B are as yet unspecified constants. Integrating  $\ddot{r}$  from  $t_0$  to T, i.e. from "now",  $t_0$ , to cutoff, T, we have

$$\begin{aligned}\dot{r}(T) &= \dot{r}(t_0) + A \int_{t_0}^T a_T dt + B \int_{t_0}^T a_T t dt \\ r(T) &= r(t_0) + \dot{r}(t_0) T + A \int_{t_0}^T \int_{t_0}^T a_T dt dt + B \int_{t_0}^T \int_{t_0}^T a_T t dt dt\end{aligned}\tag{2}$$

Thus if  $\dot{r}(T)$  and  $r(T)$  are known, the above equations can be solved for A and B. If we let  $r(T) = r_d$ ,  $\dot{r}(T) = \dot{r}_d$  and

$$\begin{aligned}a_0 &= \int_{t_0}^T a_T dt \\ a_1 &= \int_{t_0}^T a_T t dt \\ b_0 &= \int_{t_0}^T \int_{t_0}^T a_T dt dt \\ b_1 &= \int_{t_0}^T \int_{t_0}^T a_T t dt dt\end{aligned}$$

then the equations of (2) become

$$\begin{aligned}\dot{r}_d &= \dot{r} + A a_0 + B a_1 \\ r_d &= r_m + \dot{r} T + A b_0 + B b_1\end{aligned}\tag{3}$$

Solving (3) for A and B, we have

$$\begin{aligned} B &= \frac{b_0 \Delta \dot{r} - a_0 \Delta r}{b_0 a_1 - a_0 b_1} \\ A &= \frac{\Delta \dot{r} - a_1 B}{a_0} \end{aligned} \quad (4)$$

where

$$\Delta \dot{r} = \dot{r}_d - \dot{r}$$

$$\Delta r = r_d - r_m - \dot{r} T$$

and T is time-to-go until cutoff.

Since the steering command is to be implemented now, i.e., at  $t = 0$ , and will be changed on the next compute cycle, the steering command  $f_r$  becomes

$$f_r = A + \frac{\left( \frac{K_1}{r^2} - \frac{C^2}{r^3} \right)}{a_T} \quad (5)$$

with A given by (4).

**2.2.2 EVALUATION OF ACCELERATION INTEGRALS.** This computation of  $f_r$  requires knowledge of the time-to-go, T, to main engine cutoff, the integrals  $a_0$ ,  $a_1$ ,  $b_0$ ,  $b_1$  and the predicted true anomaly at cutoff,  $\eta_T$ , from which  $r_d$  and  $\dot{r}_d$  are obtained.

To evaluate the integrals, we introduce the variable

$$\tau = \frac{w}{\dot{w}} = \text{weight/weight flow.}$$

Then since

$$a_T = \frac{Th}{w/g} = \frac{g Th}{\tau \dot{w}}$$

we have

$$a_T = \frac{v_e}{\tau}$$

Since  $\tau$  is a linear function of time (for constant weight flow) the acceleration at time  $t$  is

$$a_T(t) = \frac{v_e}{\tau - t} \quad (6)$$

Substituting this into the integral for  $a_0$ , we have

$$\begin{aligned} a_0 &= \int_0^T a_T dt = \int_0^T \frac{v_e}{\tau - t} dt \\ a_0 &= -v_e \ln \left( 1 - \frac{T}{\tau} \right) = \Delta v \end{aligned} \quad (7)$$

Similiarly

$$\begin{aligned} a_n &= \int_0^T t^n a_T(t) dt = a_{n-1} \tau - \frac{v_e T^n}{n} \\ n &= 1, 2, 3, \dots \\ b_0 &= \int_0^T \int_0^T a_T(t) dt dt = a_0 T - a_1 \\ b_n &= \int_0^T \int_0^T t^n a_T(t) dt dt = b_{n-1} \tau - \frac{v_e T^{n+1}}{n(n+1)} \\ n &= 1, 2, 3, \dots \end{aligned} \quad (8)$$

Thus if we can solve for  $T$ , we can evaluate the integrals (7) and (8).

Due to scaling requirements and computational (truncation) errors in the flight computer, the steering coefficients  $A$  and  $B$  are not computed from Equations 4. To retain sufficient computational significance as cutoff is approached it is necessary to rescale the quantities  $\Delta r$  and  $T$ . To facilitate this rescaling, Equations 4, 7, and 8 are combined to give  $A$  and  $B$  as follows:

$$\begin{aligned}
 x_d &= v_e T \left( \tau - \frac{v_e T}{a_0} - \frac{T}{2} \right) \\
 B &= \frac{\left( T - \tau + \frac{v_e T}{a_0} \right) \Delta \dot{r} - \Delta r}{x_d} \\
 A &= \frac{\Delta \dot{r}}{a_0} - B \left( \tau - \frac{v_e T}{a_0} \right)
 \end{aligned} \tag{4'}$$

These equations are equivalent to Equations 4, but do not require the explicit computation of  $a_1$ ,  $b_0$ , and  $b_1$ .

**2.2.3 ANGULAR MOMENTUM TO BE GAINED AND TIME TO GO.** Computation of the time to go is based upon the angular momentum to be gained,  $\Delta c$ , where

$$\Delta c = c_d - c$$

$c$  is the instantaneous angular momentum given by

$$c = |\bar{r}_m \times \bar{v}_m| = \sqrt{(\bar{r} \times \bar{v}) \cdot (\bar{r} \times \bar{v})}$$

and  $c_d$  is the desired angular momentum of the nominal conic at cutoff, computed from

$$c_d = \sqrt{K_1 p}$$

where

$$K_1 = \text{earth's gravitational constant}$$

From the definition of angular momentum

$$c = r_m v_{mt}$$

where  $v_{mt}$  is tangential velocity. Differentiating,

$$\dot{c} = \dot{r}_m v_{mt} + r_m \dot{v}_{mt}$$

$$\dot{c} = r_m a_T f_t$$

where  $a_T f_t$  is the  $t$  component of  $\bar{a}_T$ ; i.e.,  $\bar{a}_T \cdot \bar{l}_t = a_{Tt} = a_T f_t$ . Thus  $f_t$  is the  $t$  component of the unit thrust pointing direction  $\bar{f}$ .

Therefore, the angular momentum to be gained,  $\Delta c'$ , is

$$\Delta c' = \int_0^T \dot{c} dt = \int_0^T r_m(t) a_T(t) f_t(t) dt \quad (9)$$

This integral is evaluated using Simpson's numerical integration formula. The integrand is computed at  $t = 0$  and  $t = T$ , and three equally spaced points in between. For this an estimate of the time to go,  $T'$ , is required. This is obtained as

$$T' = T_{i-1} - \Delta t$$

where  $\Delta t$  is the compute cycle length and  $T_{i-1}$  is the previous cycle's  $T$ . The integrand involves radial distance, acceleration magnitude, and the tangential component of the unit steering vector.  $r_m(t)$  is obtained by dividing the difference between the present  $r_m$  and the desired cutoff radius,  $r_d$ , into four equal intervals. Thus

$$r_m(t)_j = r_m + (j-1) \frac{(r_d - r_m)}{4} \quad (10)$$

$$j = 1, \dots, 5$$

The acceleration magnitude as a function of  $t$  is obtained from Equation 6. Thus at the five points used to evaluate the integral we have

$$a_T(t)_j = \frac{v_e}{\tau - \frac{(j-1) T'}{4}} \quad (11)$$

$$j = 1, \dots, 5$$

Equation 11 requires knowledge of the parameter  $\tau$ . To obtain  $\tau$  we update the magnitude of the acceleration vector,  $\bar{a}_T$ , computed in the navigational equations for the 1/2 cycle computational lag. (Recall that  $\bar{a}_T = \frac{\bar{v}_\sigma - \bar{v}_{\sigma i-1}}{\Delta t}$ , and is therefore valid half

way between the  $i-1$  and  $i^{\text{th}}$  compute cycles). Thus the updated  $|\bar{a}_T|$  is given by

$$a_T = |\bar{a}_T| + \dot{a}_T \frac{\Delta t}{2}$$

$$a_T = |\bar{a}_T| + \frac{|\bar{a}_T| \Delta t}{2 \left( \tau_{i-1} - \frac{\Delta t}{2} \right)}$$

Then, from Equation 6 we have

$$\tau_i = \frac{v_e}{a_T}$$

The pitch and yaw steering laws employed in the equations compute the radial and normal steering commands,  $f_r$  and  $f_n$  respectively. The tangential component,  $f_t$ , is obtained from a square root as

$$f_t = \sqrt{1 - f_r^2 - f_n^2}$$

Therefore

$$f_{t(t)_j} = \sqrt{1 - \left( f_r + \dot{f}_r \frac{(j-1) T'}{4} \right)^2 - \left( f_n + \dot{f}_n \frac{(j-1) T'}{4} \right)^2} \quad (12)$$

$$j = 1, \dots, 5$$

Equation 12 requires the steering derivatives  $\dot{f}_r$  and  $\dot{f}_n$ . These derivatives are obtained from

$$f_r = A + Bt + \left( \frac{K_1}{r^2} - \frac{C^2}{r^3} \right) / a_T$$

$$\dot{f}_r = B + \frac{\left( \frac{K_1}{r^2} - \frac{C^2}{r^3} \right) / a_T \Big|_{t=T'} - \left( \frac{K_1}{r^2} - \frac{C^2}{r^3} \right) / a_T \Big|_{t=0}}{T'} \quad (13)$$



$$\dot{f}_r = B + \frac{\left(\frac{K_1}{r_d^2} - \frac{C_d^2}{r_d^3}\right) / \left(\frac{v_e}{\tau - T'}\right) - \left(\frac{K_1}{r^2} - \frac{C^2}{r^3}\right) / a_T}{T'}$$

and

$$f_n = K_y y_1 \text{ (see Section 2.3)}$$

$$\dot{f}_n = K_y y_2 \quad (14)$$

Using Equations 10, 11, and 12, the integrand in Equation 9 at each of the five points of evaluation becomes

$$P_j = r_m(t)_j a_T(t)_j f_t(t)_j \quad (15)$$

$$j = 1, \dots, 5$$

Finally, using Simpson's integration rule we have

$$\Delta c' = \frac{(P_1 + 4P_2 + 2P_3 + 4P_4 + P_5) T'}{12} \quad (16)$$

Equation 16 gives the angular momentum to be gained assuming a time to go,  $T'$ , which was decremented from the previous cycle, and the steering derivatives given by Equations 13 and 14. The true angular momentum to be gained is  $\Delta c = c_d - c$ . Thus the difference between  $\Delta c$  and  $\Delta c'$  can be used to adjust the estimated time to go  $T'$ . This time adjustment is

$$T_A = \frac{\Delta c - \Delta c'}{\dot{c}(T)} = \frac{\Delta c - \Delta c'}{P_5}$$

Finally then the time to go is

$$T = T' + T_A \quad (17)$$

Having time to go,  $T$ , and  $\tau$  we are in a position to evaluate the acceleration integral  $a_0$ . From Equation 7,

$$a_0 = -v_e \ln \left( 1 - \frac{T}{\tau} \right)$$

The logarithm above is evaluated using a numerical approximation given in Reference 1. Because of the range of the quantity  $\left( 1 - \frac{T}{\tau} \right)$ , and to facilitate the numerical approximation,  $a_0$  is rewritten as

$$a_0 = v_e \ln(10) \log_{10} \left( \frac{\tau}{\tau - T} \right)$$

The logarithm is now approximated as

$$\begin{aligned} \log_{10} \frac{\tau}{\tau - T} &= \frac{1}{2} + \alpha_1 \left( \frac{x - \sqrt{10}}{x + \sqrt{10}} \right) + \alpha_3 \left( \frac{x - \sqrt{10}}{x + \sqrt{10}} \right)^3 + \dots \\ &\quad + \alpha_9 \left( \frac{x - \sqrt{10}}{x + \sqrt{10}} \right)^9 \end{aligned}$$

where  $x = \frac{\tau}{\tau - T}$  and the coefficients  $\alpha$  are given in Reference 1.

In the flight program the constant  $v_e \ln 10$  is included in the polynomial coefficients.

**2.2.4 TRUE ANOMALY TO GO AND TRUE ANOMALY AT CUTOFF.** For ATS and Mariner missions, the pitch steering coefficients A and B require the calculation of the true anomaly at cutoff,  $\eta_T$ . This calculation is not necessary for the determination of OAO pitch steering coefficients since  $\eta_T$  is meaningless for circular orbit missions. However, because of the equation design ground rule of commonality, this calculation is made for the OAO mission. It does not alter the desired values of  $\dot{r}_d$  and  $r_d$  because  $e = 0$ . This independence of  $\dot{r}_d$  and  $r_d$  from  $\eta_T$  for OAO is shown in Section 2.2.5.

For the sake of completeness, the discussion of orbital parameter equations, carried over in this report from Reference 8, includes the calculation of  $\eta_T$ .

Figure 2-1 defines some of the orbital geometry parameters, including  $\eta_T$ , and illustrates their relationships to the target vector,  $\bar{1}_a$ .

In Figure 2-1:

- $\bar{i}_a$  = unit target vector
- $\bar{i}_r$  = unit instantaneous position vector
- $\bar{i}_{r(T)}$  = unit predicted position vector at cutoff
- $\bar{i}_{rp}$  = unit perigee vector

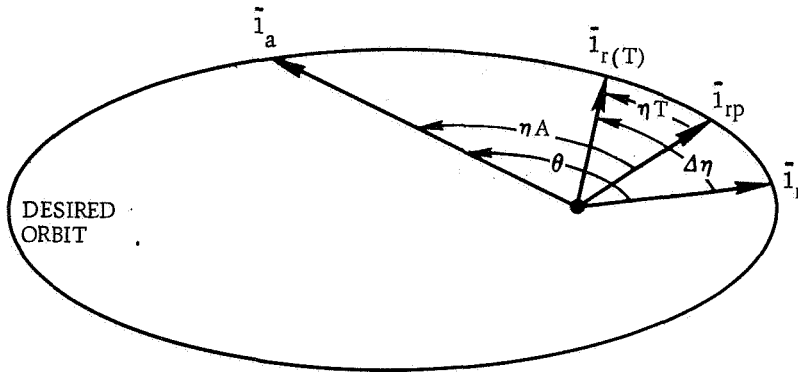


Figure 2-1. Orbital Geometry

- $\Delta\eta$  = predicted true anomaly to go to cutoff
- $\eta_T$  = predicted true anomaly at cutoff
- $\eta_A$  = true anomaly of the target vector (a constant)
- $\theta$  = instantaneous range angle to the target vector

From Figure 2-1 it can be seen that the true anomaly at cutoff is

$$\eta_T = \eta_A + (\Delta\eta - \theta) \quad (18)$$

The range angle  $\theta$  is easily obtained as

$$\begin{aligned} \cos \theta &= \bar{i}_r \cdot \bar{i}_a \\ \sin \theta &= \sqrt{1 - \cos^2 \theta} \end{aligned} \quad (19)$$

Since  $\eta_A$  is an equation input constant, it remains only to compute  $\Delta\eta$ , the predicted burn arc to go until cutoff.  $\Delta\eta$  can be predicted from the time to go and angular momentum.

$$\Delta\eta = \int_0^T \dot{\eta}(t) dt \quad (20)$$

But

$$\dot{\eta}(t) = \frac{c(t)}{r_m^2(t)}$$

The integral in Equation 20 is evaluated using a three points Simpson's integration formula as

$$\Delta\eta = \left[ \dot{\eta}(0) + 4\dot{\eta}\left(\frac{T}{2}\right) + \dot{\eta}(T) \right] \frac{T}{6}$$

The terms  $\dot{\eta}(0)$  and  $\dot{\eta}(T)$  are easily obtained as

$$\dot{\eta}(0) = \frac{c}{r_m^2}$$

$$\dot{\eta}(T) = \frac{c_d}{r_d^2}$$

Here  $c_d$  is the angular momentum of the desired conic and  $r_d$  is the predicted cutoff position from the previous cycle.  $\dot{\eta}$  at the midpoint,  $\frac{T}{2}$ , is obtained by integrating  $\dot{c}$  from  $t=0$  to  $t=\frac{T}{2}$  and adding to the instantaneous  $c$ ; i.e.,

$$c\left(\frac{T}{2}\right) = c + \int_0^{T/2} \dot{c} dt$$

From the time to go computations we obtain  $\dot{c}(t) = r_m(t) a_T(t) f_t(t)$ . Therefore, using Equation 15 we have

$$c\left(\frac{T}{2}\right) = c + (P_1 + 4P_2 + P_3) \frac{T}{12}$$

Therefore

$$\dot{\eta}\left(\frac{T}{2}\right) = \frac{c\left(\frac{T}{2}\right)}{\left(\frac{r_m + r_d}{2}\right)^2}$$

Sine and cosine of  $\Delta\eta$  are approximated from series as

$$\sin \Delta\eta = \Delta\eta - \frac{\Delta\eta^3}{6}$$

$$\cos \Delta\eta = 1 - \frac{\Delta\eta^2}{4} + \frac{\Delta\eta^4}{24}$$

Finally then, combining Equations 18, 19, and 21 we have

$$\begin{aligned}\sin \eta_T &= \sin \eta_A \cos (\Delta\eta - \theta) + \cos \eta_A \sin (\Delta\eta - \theta) \\ \cos \eta_T &= \cos \eta_A \cos (\Delta\eta - \theta) - \sin \eta_A \sin (\Delta\eta - \theta)\end{aligned}$$

**2.2.5 DESIRED CUTOFF POSITION AND RADIAL VELOCITY.** Under the equation design ground rule of commonality, the desired cutoff radius magnitude,  $r_d$ , and the desired radial velocity at cutoff,  $\dot{r}_d$ , are obtained from the following:

$$\begin{aligned}\dot{r}_d &= \left( \frac{e c_d}{p} \right) \sin \eta_T \\ r_d &= \frac{p}{1 + e \cos \eta_T} \quad (\text{From } T = J_{29} \text{ to } T = 0)\end{aligned}$$

Since for circular orbit missions,  $e=0$ ,  $\dot{r}_d$  and  $r_d$  for OAO become:

$$\begin{aligned}\dot{r}_d &= 0 \\ r_d &= p\end{aligned}$$

Thus, by virtue of  $e=0$ ,  $\dot{r}_d$  and  $r_d$  are not affected by the value of  $\eta_T$ .

The parameters  $e$ ,  $p$ , and  $c_d$  are computed from input constants during the initialization phase which for OAO are the parameters  $h_d$  and  $r_p$ , where  $r_p$  is actually the desired circular orbit radius. The trajectory parameters used in Equation 23 are calculated as follows:

$$\begin{aligned}e &= 1 + \frac{h_d r_p}{K_1} \quad (= 0 \text{ for OAO}) \\ p &= r_p (1 + e) \quad (= r_d \text{ for OAO}) \\ c_d &= \sqrt{K_1 p}\end{aligned}$$

where

$K_1$  = earth's gravitational constant

During the early phase of Centaur steering, the value of  $r_d$  is modified by a linearly decreasing (in time) term in order to minimize the payload loss due to pitch steering. This pitch profile shaping is peculiar to the OAO mission because of its steep ascent trajectory. (It is by-passed in the ATS and Mariner applications of the equations).

The modification of  $r_d$  for OAO is given by the following:

$$r_d = r_{d(T)} - c_{dr} (T - J_{29}) \quad (23B)$$

where

$r_{d(T)}$  is given by Equation 23

$c_{dr}$  = input gain constant,  $K_{12}$

$T$  = time-to-go to cutoff

$J_{29}$  = time-to-go at which  $r_d = r_{d(T)}$

The constants  $c_{dr}$  and  $J_{29}$  in Equation 23B are selected to result in a commanded radial thrust pointing direction history ( $f_r$  versus  $T$ ) approximating that of the calculus of variations (OPSEC) trajectory for OAO. This modification minimizes a payload penalty of approximately 14 lb that would otherwise accrue from a purely explicit determination of the OAO pitch steering coefficients.

In summary then, the pitch steering calculations proceed as follows:

- a. Compute the orbit parameters  $e$ ,  $p$ ,  $c_d$  from Equation 24 in initialization.
- b. Compute  $T$  using Equations 10 through 17.
- c. Compute  $a_0$  from Equation 7.
- d. Compute range angle from Equation 19, true anomaly to go from Equation 20 and  $\eta_T$  from Equation 22.
- e. Compute  $\dot{r}_d$ ,  $r_d$  from Equation 23 (or 23B).

f. Compute A and B from Equation 4'.

g. Compute  $f_r$  from Equation 5.

### 2.3 YAW STEERING

The objective of yaw steering is primarily the control of the final orbit inclination. This primary function is deferred to the Centaur phase of flight after nose fairing jettison. The sustainer phase yaw steering is discussed later in Section 2.6.2.

During the Centaur phase of flight, the error signal used for yaw steering is given by

$$\epsilon_y = \bar{l}_n \cdot \bar{l}_a \quad (25)$$

where

$$\bar{l}_n = (\bar{r}_m \times \bar{v}_m) / |\bar{r}_m \times \bar{v}_m|$$

The function of the yaw steering is to drive  $\epsilon_y$  to zero at cutoff. This is accomplished in a manner which minimizes payload loss due to out of plane steering.

Following is a derivation of the yaw steering command,  $f_n$ . The problem is solved using the calculus of variations and Lagrange multipliers.

The error signal  $\epsilon_y$  provides the constraint equation, by requiring that  $\epsilon_y(T) = 0$ .

The yaw error is

$$\epsilon_y = \bar{l}_n \cdot \bar{l}_a$$

Therefore

$$\begin{aligned} \dot{\epsilon}_y &= \left( \frac{d}{dt} \bar{l}_n \right) \cdot \bar{l}_a \\ &\approx \begin{pmatrix} -a_{Tn}/v_{mt} \\ 0 \\ 0 \end{pmatrix} \cdot \bar{l}_a \\ &= \frac{-a_{Tn}}{v_{mt}} \bar{l}_t \cdot \bar{l}_a \end{aligned}$$

We want

$$\epsilon_y \Big|_{t=0} + \int_0^T \dot{\epsilon}_y dt = 0$$

Therefore

$$\begin{aligned} \bar{l}_n \cdot \bar{l}_a \Big|_0 &= \int_0^T \frac{a_{Tn}}{v_{mt}} (\bar{l}_t \cdot \bar{l}_a) dt \\ \bar{l}_n \cdot \bar{l}_a \Big|_0 &= \int_0^T a_T (\bar{f} \cdot \bar{l}_n) \frac{(\bar{l}_t \cdot \bar{l}_a)}{v_{mt}} dt \end{aligned} \quad (26)$$

Equation 26 serves as the constraint equation when minimizing the payload loss due to out of plane steering

The acceleration loss due to out of plane steering can be approximated as

$$\begin{aligned} \Delta a &= a_T \left[ 1 - \sqrt{1 - (\bar{l}_n \cdot \bar{f})^2} \right] \\ &\approx a_T \left[ 1 - 1 + \frac{1}{2} (\bar{l}_n \cdot \bar{f})^2 \right] \\ &= \frac{a_T}{2} (\bar{l}_n \cdot \bar{f})^2 \end{aligned}$$

Thus the velocity loss is

$$\Delta V_L = \int_0^T \frac{a_T}{2} (\bar{f} \cdot \bar{l}_n)^2 dt$$

which is equivalent to a payload loss of

$$\Delta m = \frac{m_T}{v_e} \int_0^T \frac{a_T}{2} (\bar{l}_n \cdot \bar{f})^2 dt \quad (27)$$



We want to minimize Equation 27 subject to the constraint of Equation 26, with the control variable being  $f_n = \bar{f} \cdot \bar{l}_n$ . Therefore, define  $\Gamma$  as

$$\Gamma(\bar{l}_n \cdot \bar{f}) = \int_0^T a_T \left[ \frac{m_T}{2 v_e} (\bar{l}_n \cdot \bar{f})^2 + \lambda (\bar{f} \cdot \bar{l}_n) \frac{(\bar{l}_t \cdot \bar{l}_a)}{v_t} \right] dt - \lambda (\bar{l}_n \cdot \bar{l}_a) \Big|_0$$

where  $\lambda$  is undetermined.

To minimize payload loss, we need to minimize  $\Gamma$ . Therefore, taking differentials,

$$\delta \Gamma(\bar{l}_n \cdot \bar{f}) = \int_0^T a_T \left[ \frac{m_T}{v_e} (\bar{l}_n \cdot \bar{f}) + \lambda \frac{(\bar{l}_t \cdot \bar{l}_a)}{v_t} \right] \delta (\bar{l}_n \cdot \bar{f}) dt$$

For a minimum  $\delta \Gamma = 0$ . Since  $\delta (\bar{l}_n \cdot \bar{f})$  is arbitrary, we must have

$$\bar{l}_n \cdot \bar{f} = -\lambda \left( \frac{\bar{l}_t \cdot \bar{l}_a}{v_t} \right) \frac{v_e}{m_t} \quad (28)$$

Using the constraint equation (26) we get

$$\bar{l}_n \cdot \bar{l}_a \Big|_0 = -\lambda \frac{v_e}{m_T} \int_0^T a_T \left( \frac{\bar{l}_t \cdot \bar{l}_a}{v_t} \right)^2 dt$$

Therefore

$$\lambda = \frac{-\frac{m_T}{v_e} \bar{l}_n \cdot \bar{l}_a}{\int_0^T a_T \left( \frac{\bar{l}_t \cdot \bar{l}_a}{v_t} \right)^2 dt} \quad (29)$$

Substituting Equation 29 into Equation 28, we get for the normal steering command

$$\bar{l}_n \cdot \bar{f} = f_n = \frac{\frac{(\bar{l}_n \cdot \bar{l}_a) (\bar{l}_t \cdot \bar{l}_a)}{v_t}}{\int_0^T a_T \left( \frac{\bar{l}_t \cdot \bar{l}_a}{v_t} \right)^2 dt} \quad (30)$$

To evaluate the integral in the denominator, we assume

$$\frac{\bar{l}_t \cdot \bar{l}_a}{v_t} = y_1 + y_2 t$$

$$\therefore y_1 = \left[ \frac{\bar{l}_t \cdot \bar{l}_a}{v_t} \right]_{t=0}$$

$$y_2 = \frac{\left[ \frac{\bar{l}_t \cdot \bar{l}_a}{v_t} \right]_{t=T} - y_1}{T}$$

Then

$$f_n = \frac{\epsilon_y y_1}{\int_0^T a_T (y_1^2 + 2y_1 y_2 t + y_2^2 t^2) dt}$$

$$f_n = \frac{\epsilon_y y_1}{y_1^2 a_0 + 2y_1 y_2 a_1 + y_2^2 a_2} = K_y y_1 \quad (31)$$

where  $a_0$ ,  $a_1$ ,  $a_2$  are given by Equations 7 and 8.

However, since the integrals  $a_1$  and  $a_2$  are not computed directly, the term  $K_y$  in the above equation is actually computed as

$$K_y = \frac{\epsilon_y}{a_0 \left[ y_1^2 + 2y_1 y_2 \left( \tau - \frac{v_e T}{a_0} \right) + y_2^2 \left( \tau^2 - \frac{v_e T}{a_0} \tau - \frac{v_e T^2}{2a_0} \right) \right]} \quad (32)$$

From the definition of  $\bar{l}_a$  we can obtain  $y_1$  and  $y_2$  as

$$y_1 = \left[ \frac{\bar{l}_t \cdot \bar{l}_a}{v_t} \right]_{t=0} \approx \frac{\sin \theta}{v_t}$$

$$y_2 = \frac{\left[ \frac{\bar{l}_t \cdot \bar{l}_a}{v_t} \right]_{t=T} - y_1}{T} = \frac{-\sin(\Delta\eta - \theta) \frac{r_d}{c_d} - y_1}{T} \quad (33)$$

In summary then, the normal steering command  $f_n$  is obtained as follows:

- a. Compute  $\epsilon_y$  from Equation 25.
- b. Use the  $a_0$ ,  $T$ ,  $\tau$  previously computed.
- c. Compute  $y_1$ ,  $y_2$  from Equation 33.
- d. Compute  $f_n$  from Equations 31 and 32.

#### 2.4 STEERING VECTOR COMPUTATION

The pitch and yaw steering computations compute the radial and normal steering components,  $f_r$  and  $f_n$ . Since the steering vector  $\bar{f}$  is a unit vector, the tangential component is given by

$$f_t = \sqrt{1 - f_r^2 - f_n^2}$$

The steering vector is then computed as follows:

$$\bar{f} = f_t \bar{1}_t + f_n \bar{1}_n + f_r \bar{1}_r \quad (34)$$

The vector  $\bar{f}$  is the ideal thrust pointing direction. However, to provide a tighter steering loop an integral control term  $\Delta\bar{f}$  is computed and added to  $\bar{f}$  to provide a second order steering system. The integral control term is given by

$$\Delta\bar{f} = \int_0^t (\bar{1}_{a_T} \times \bar{f}) \times \bar{f} dt$$

where

$$\bar{1}_{a_T} = \frac{\bar{a}_T}{a_T}$$

$\Delta\bar{f}$  is computed as

$$\Delta\bar{f} = K_7 \Delta t (\bar{f} - \bar{1}_{a_T}) + \Delta\bar{f}_{i-1} \quad (35)$$

where  $K_7$  is an input integral gain constant.

The output steering command is then proportional to the vector sum

$$\bar{Q} = \bar{f} + \Delta \bar{f}$$

This vector is unitized by approximating its magnitude as

$$|\bar{Q}| = \sqrt{\bar{Q} \cdot \bar{Q}} \approx \frac{\bar{Q} \cdot \bar{Q} + 1}{2}$$

The commanded thrust pointing direction which is output to the control system is then computed as

$$\bar{f}^* = K_8 \frac{\bar{Q}}{(\bar{Q} \cdot \bar{Q} + 1)} + \bar{p}_5 \quad (36)$$

where  $K_8$  is twice the steering gain constant.

The constant  $\bar{p}_5$  is a roundoff bit used to compensate for the truncation which results from extracting 11 bits of the  $\bar{f}^*$  components before storing them on the steering pots. This roundoff is required for the spacecraft attitude vector which is output after MECO II using Equation 36. The roundoff reduces by 50% the pot truncation error contribution to the spacecraft attitude vector.

The steering equations include a limit on the angle of attack to control the atmospheric heating which could arise from implementing the guidance commanded thrust attitude. During the sustainer phase when the altitude is below a specified input value ( $K_{27}$ ) an error signal is computed as the vector difference between the desired guidance steering vector,  $\bar{f}$ , and the unit velocity vector,  $\bar{1}_{v_m}$ , as

$$\bar{\alpha}_1 = \bar{f} - \bar{1}_{v_m} \quad (37)$$

If the magnitude of this vector exceeds a specified maximum value,  $\alpha_m$ , the steering vector  $\bar{f}$  is modified. The upper bound,  $\alpha_m$ , is a polynomial in altitude given by

$$\alpha_m = K_4 + K_5 (K_{27} - r_m) + K_6 (K_{27} - r_m)^2 \quad (38)$$

If  $|\bar{\alpha}_1| > \alpha_m$  we set

$$\bar{f} = \bar{1}_{v_m} + \alpha_m \frac{\bar{\alpha}_1}{|\bar{\alpha}_1|} \quad (39)$$

During the portion of the trajectory when  $r_m < K_{27}$ , no integral control is employed and Equation 39 is used to compute the output steering command,  $\bar{f}^*$ , given by Equation 36.

## 2.5 BOOSTER PHASE

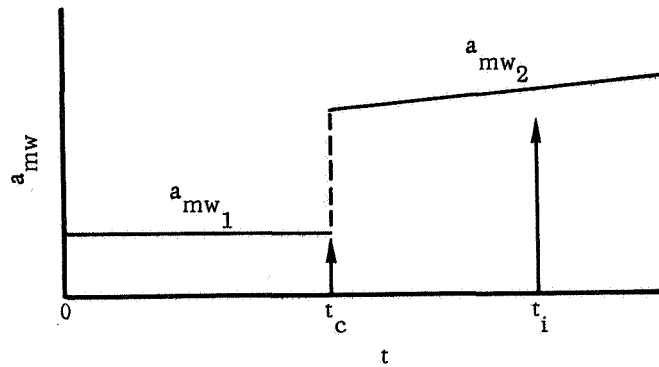
The booster phase guidance equations have three functions:

- a. Issue open loop pitch and yaw rates.
- b. Monitor the acceleration and issue the BECO discrete.
- c. Provide a reference steering vector and sequence of discretized for ground checkout.

**2.5.1 BOOSTER STEERING.** The guidance equations output open loop pitch and yaw steering rates, via the v and u steering pots respectively. These rates are a sequence of 10 constant values output at fixed time intervals from 2-inch motion. The time slots are permanent storage constants, but the rates are loaded on the computer temporary storage tracks. This permits the rates to be selected as a function of the wind conditions on the day of launch, and thus increases the launch availability, since each set of rates is designed for a particular wind profile.

The booster steering function requires the guidance equations to sense the 2-inch motion event and establish a reference time for outputting the pitch and yaw rates. This is accomplished using the w component of total velocity and acceleration, as follows.

Figure 2-2 sketches the  $a_{mw}$  history. On the pad between the go-inertial time and 2-inch motion time,  $t_c$ , the acceleration is a known constant. At  $t = t_c$  a sharp step increase in  $a_{mw}$  occurs. This step increase can be detected by observing  $a_T^2$  in the navigational equations. On each cycle preceding 2-inch motion,  $a_T^2$  is tested against

Figure 2-2.  $a_{mw}$  vs. Time From Go-Inertial

$E_3$  (an input constant). When  $a_T^2 > E_3$ , the time,  $t_i$ , and velocity,  $v_{mw}$ , are used in a linear relationship to obtain  $t_c$  as

$$v_{mw} = a_{mw1} t_c + a_{mw2} (t_i - t_c)$$

$$t_c = \frac{v_{mw} - a_{mw2} t_i}{(a_{mw1} - a_{mw2})} \quad (40)$$

The two acceleration terms in Equation 40 are input constants. Since  $a_{mw2}$  may be mission dependent (as a function of the payload) it is input as a J-constant on temporary storage. Equation 40 is thus mechanized as

$$t_c = \frac{v_{mw} + J_{33} t_i}{(J_{33} + K_{14})}$$

**2.5.2 BECO DISCRETE.** The booster phase equations monitor the acceleration for the purpose of issuing the BECO discrete and switching to the closed loop sustainer-Centaur phase, as follows:

$$a_T^2 > E_6: \quad \text{issue BECO and switch to sustainer-Centaur phase}$$

$$a_T^2 < E_7: \quad \text{switch to sustainer-Centaur phase}$$

The constant  $E_6$  is obtained as follows:

$$E_6 = \left\{ \left[ g_d - \dot{a}_T (1 + k_1 + k_2) \right] 32.174 \right\}^2$$

where

$$g_d = \text{desired BECO acceleration (g's)} = 5.7$$

$$k_1 = \text{time interval from the } \bar{v}_0 \text{ pickup to the acceleration test (compute cycles)} = 0.972$$

$$k_2 = \text{electromechanical timer delay (compute cycles)} = 0.072$$

$$\dot{a}_T = \text{rate of change of } a_T \text{ (g's/compute cycle)} = 0.227$$

The one compute cycle subtracted from  $g_d$  results from the acceleration lag (half compute cycle) and the sampling bias (half compute cycle), designed to minimize BECO sampling errors. Therefore

$$E_6 = \{ [5.7 - 0.227(1. + 0.972 + 0.072)] 32.17 \}^2$$

$$E_6 = 28,500. (\text{ft/sec}^2)^2$$

**2.5.3 GROUND TEST REQUIREMENTS.** The guidance equations are required to provide a reference steering vector and a sequence of discretely for systems level ground checkout (see Section 1.3). Since during ground tests the equations cycle through only the navigation, coordinate, and booster equations, the test vector and discretely are located in the booster phase.

After approximately 179 seconds from go inertial the equations will issue the L3 discrete and output a steering vector given by

$$\bar{f}^* = \begin{bmatrix} K_{15} \\ K_{16} \\ K_{16} \end{bmatrix}$$

After approximately 231 seconds the equations branch to the preflight integrated test routine. This routine issues the following discretes at the given times from go inertial.

<u>Discrete</u>	<u>Time</u>	<u>Discrete</u>	<u>Time</u>
L6	238	L1	649
L6	273	L1	669
L0	549	L16	683
L16	553	L0	769
L16	583	L0	787
L0	598	L16	791
L16	638	L16	809
<u>Discrete</u>		<u>Time</u>	
L8		1335	
L10		1339	
L8		1359	
L10		1361	
L12		1361	

## 2.6 SUSTAINER PHASE

2.6.1 PITCH STEERING. Unfortunately, the preceding integration of acceleration and cutoff prediction is not valid over the two-stage sustainer-Centaur burn. The acceleration discontinuity at SECO invalidates this prediction. To utilize most of the explicit calculations necessary for the Centaur burn during the sustainer phase, and thus minimize additional program requirements for sustainer guidance, an approximation to the time to go is used to evaluate the acceleration integrals.

We make the following assumptions:

$$\begin{aligned}
 T &= J_{36} - t_i \\
 \tau &= K_{19} - (t_i - t_c) \\
 \frac{G}{a_T} &= J_{38} + J_{39} (t_i - t_c)
 \end{aligned} \tag{41}$$



where  $t_c$  = BECO time.

$K_{19}$  = average value of  $\tau$  at BECO time for OAO, ATS, Mariner trajectories

The constants  $J_{36}$  -  $J_{39}$  are equation input, mission dependent constants, obtained as follows:

$J_{36}$  = nominal MECO time less the non-guided powered flight time from SECO to MES+4

$J_{38} = \frac{G}{a_T}$ , evaluated at the end of the BECO decay

( $J_{38}$  can be modified slightly to control altitude at SECO)

$$J_{39} = \frac{\left. \frac{G}{a_T} \right|_{\text{MES}} - \left. \frac{G}{a_T} \right|_{\text{BECO}+8}}{t_{(\text{SECO})} - t_{(\text{BECO}+8)}}$$

( $J_{39}$  can be modified slightly to provide a smooth attitude transition between the sustainer and Centaur I phases.)

For the sustainer phase guidance, a one shot calculation of  $r_d$  and  $\dot{r}_d$  is made using Equation 23, with a nominal, input true anomaly to go,  $\Delta\eta$ . This one shot calculation is made on the first sustainer cycle, and the resulting  $r_d$ ,  $\dot{r}_d$  are used on all succeeding sustainer computations to obtain  $\Delta r$ ,  $\Delta \dot{r}$ . During the sustainer phase the modification of  $r_d$  given by Equation 23B is by-passed.

With  $T$ ,  $\tau$ ,  $G/a_T$ ,  $r_d$ , and  $\dot{r}_d$  derived from the simplified assumptions above, the remainder of the explicit calculations can be used to obtain  $a_0$ ,  $\Delta r$ ,  $\Delta \dot{r}$ ,  $B$ ,  $A$ , and finally the steering component,  $f_r$ .

In summary then, the sustainer pitch steering computations are as follows:

- Compute  $T$ ,  $\tau$ ,  $G/a_T$  from Equation 41.
- Estimate  $r_d$ ,  $\dot{r}_d$  using an input nominal  $\Delta\eta$ .
- Compute  $a_0$  from Equation 7.
- Compute  $A$  and  $B$  from Equation 4'.
- Compute  $f_r$  from Equation 5.

**2.6.2 SUSTAINER YAW STEERING.** During the sustainer phase of flight the yaw steering logic is designed to maintain the t, r (pitch) plane parallel to, or to the left of, the flight plane defined by range safety. This orientation of the trajectory plane during sustainer phase is in consideration of Bermuda overflight constraints, and results in a yaw right maneuver (dogleg) during the Centaur phase to achieve the required orbit inclination.

Basically, the sustainer yaw steering is mechanized in such a way as to prevent guidance from commanding a vehicle thrust pointing direction that would cause the vehicle IIP (instantaneous impact point) to violate some range safety constraint. Figure 2-3 illustrates the geometry involved. The vector,  $\bar{i}_{no} (= J_{18}, J_{19}, 0)$ , is a unit vector normal to the plane defined as the range safety limit and to the right of which flight is prohibited.

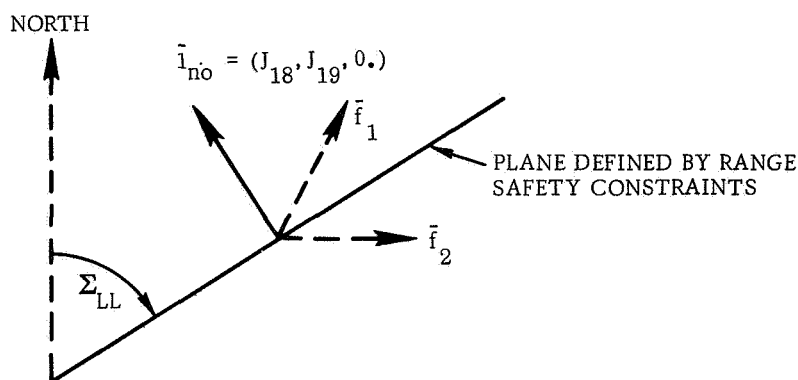


Figure 2-3. Geometry for Range Safety Constraint of Sustainer Yaw Steering

In Figure 2-3:

$\Sigma_{LL}$  = limiting launch azimuth due to range safety considerations

$\bar{i}_{no}$  = unit vector normal to plane defined by  $\Sigma_{LL}$

$\bar{f}_2, \bar{f}_1$  = steering vectors that would and would not, respectively, cause the vehicle to violate the range safety constraint

The test of acceptability of the computed desired thrust pointing direction is the algebraic sign resulting from Equation 42.

$$\bar{f} \cdot \bar{i}_{no} = f_u J_{18} + f_v J_{19} \quad (42)$$

Reference to Figure 2-3 will show that if  $\bar{f} = \bar{f}_1$  then the sign of  $\bar{f} \cdot \bar{i}_{no}$  above will be positive and this commanded thrust pointing would not cause the vehicle to steer to the right of the plane defined by  $\bar{i}_{no}$  and thus violate range safety constraints. Therefore, as long as  $\bar{f} \cdot \bar{i}_{no} \geq 0$  the guidance equations will provide yaw steering corrections in the same manner as the Centaur phase.

However, if  $\bar{f} = \bar{f}_2$  (Figure 2-3), then  $\bar{f} \cdot \bar{i}_{no} < 0$  and to command this thrust pointing direction would cause the vehicle IIP to violate the range safety constraint. In this event the usual rotating t, n, r coordinate system is abandoned by redefining the normal (n) direction as  $\bar{i}_n = \bar{i}_{no}$ . This has the effect of making the t, r plane parallel to the plane defining the range safety constraint. The yaw steering constraint is then effected by setting the normal component ( $f'_n$ ) of the steering vector to zero, which causes the thrust pointing direction to lie in the t, r plane, which is as far right as range safety considerations will permit.

Finally, once this condition ( $\bar{f} \cdot \bar{i}_{no} < 0$ ) is met several branches are set to inhibit the calculation of  $\bar{i}_n = \bar{c}/c$  in the coordinates section, and also to bypass further testing of the quantity  $\bar{f} \cdot \bar{i}_{no}$  since  $\bar{f} \perp \bar{i}_{no}$  by definition and the dot product will always be zero.

**2.6.3 SECO BACKUP DISCRETE (L6).** The sustainer phase guidance equations issue the SECO backup discrete, L6. This discrete is issued when the guidance equations sense acceleration decay. When  $a_T^2 < E_8$  (0.7 g) the L6 discrete is issued, and the equations are switched to the Centaur phase.

## 2.7 POST INJECTION PHASE

The post injection phase for the OAO mission is as follows:

- a. Align the Centaur and payload to the separation attitude vector.
- b. Separate the spacecraft.
- c. Align the Centaur to the retrothrust attitude vector.

**2.7.1 SPACECRAFT SEPARATION ATTITUDE.** On the first compute cycle after MECO the reference attitude vector for spacecraft separation is output in drifting  $u, v, w$  coordinates. This pointing direction corresponds to the nominal attitude vector at MECO. The components of this vector,  $\beta_1, \beta_2, \beta_3$ , are input as  $J$  constants. The commanded attitude in the local  $t, n, r$  coordinate system is

$$\begin{aligned} f_t &= \beta_3 = J_{51} \\ f_n &= \beta_2 = J_{50} \\ f_r &= \beta_1 = J_{49} \end{aligned} \quad (43)$$

The output steering vector is then computed using Equation 43 to obtain  $\bar{f}$  from Equation 34, and  $\bar{f}^*$  from Equation 36. The integral term  $\Delta\bar{f}$  is set to zero for the calculation of  $\bar{f}^*$ . This vector is updated each cycle so that the attitude of the spacecraft in the  $t, n, r$  system is maintained constant.

**2.7.2 VEHICLE RETROTHRUST ATTITUDE VECTOR.** At a fixed time from MECO, ( $E_t = J_{41}$ ) and following spacecraft separation, the Centaur vehicle is aligned to the instantaneous negative position vector,  $-\bar{r}_m$ , biased by an angle,  $\alpha$ , in the direction of  $-\bar{v}_m$ . Figure 2-4 illustrates the inplane relationship of the retrothrust attitude vector to  $-\bar{r}_m$  and  $-\bar{v}_m$ .

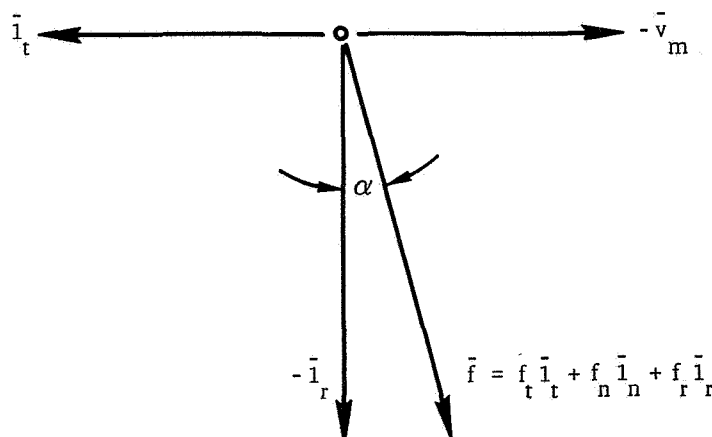


Figure 2-4. Vehicle Retrothrust Attitude Vector

The angle  $\alpha$  is selected to maximize the probability of achieving a range of acceptable spacecraft-to-Centaur vehicle post-separation viewing histories.

The components of this vector in the t, n, r coordinate system are input as J constants as follows:

$$\begin{aligned} f_t &= J_{52} \\ f_n &= J_{53} \\ f_r &= J_{54} \end{aligned} \tag{44}$$

The output steering vector is then computed obtaining  $\tilde{f}$  from Equation 34 and finally  $\bar{f}^*$  from Equation 36. The vector is updated each compute cycle so that the vehicle attitude relative to the t, n, r system is constant during the period of retrothrust.

## 2.8 MAIN ENGINE CUTOFF

The guidance equations issue the Centaur main engine cutoff discrete. The discrete time is computed from the time to go given by Equation 17. When  $T < J_{55}$ , an input constant, the term  $\Delta t_{co}$  is computed as

$$\Delta t_{co} = T - (t_\sigma - t_i) - J_2$$

Here  $(t_\sigma - t_i)$  is the elapsed time from the start of the compute cycle, which is the reference time for T, and  $J_2$  is a constant used to bias off computational errors and flight computer delays (such as the short line lags). Minus  $\Delta t_{co}$  is then placed on the signator countdown sector, which triggers MECO on the overflow.

Due to the presence of velocity quantization errors and accelerometer limit cycle noise, it is necessary to filter the  $\bar{v}_\sigma$  data in order to obtain a sufficiently accurate computation of T for cutoff purposes. Recall that  $a_T$  is used in the computation of  $\Delta c'$  to obtain T. This filtering is discussed in detail in Appendix F, and results in the desired accuracy for T.

**2.8.1 CUTOFF BIAS,  $J_2$ .** The cutoff time bias  $J_2$  is used to compensate for computational lags in the flight computer, flight computer truncation, countdown uncertainties and the MECO engine decay. For the OAO, the value of  $J_2$  is derived as follows:

- a. Computational Delays. The sequence of events which occurs on the cutoff cycle is shown in Figure 2-5.

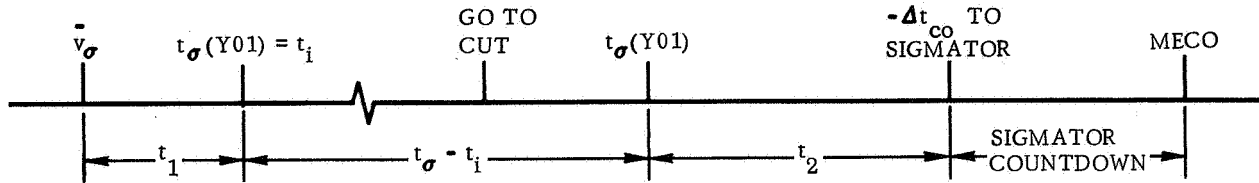


Figure 2-5. MECO Time Sequence

- The program is coded such that  $t_\sigma$  and  $\bar{v}_\sigma$  are effectively read simultaneously in the navigational equations. Therefore, including short line lags,  $t_1 = 0$ .  $t_2$  is also a function of the program coding and, including short line lags,  $t_2 = 0.03375$ . The interval  $t_\sigma - t_i$  is variable with drum speed and is computed by the program.
- b. Countdown Loop. The cutoff time to go stored on the sigmator is incremented every eight word times, and the MECO discrete is issued when the overflow from negative to positive occurs. Consequently, the cutoff could occur from 0 to 8 word times late. Therefore an average value of 4 word times is biased off as  $t_{cd} = 0.0006$ .
- c. Computational Errors. Truncation and computational errors in the navigational data,  $\bar{r}_m$  and  $\bar{v}_m$ , contribute to an error in the calculated angular momentum-to-be-gained,  $\Delta C$ . This error in turn results in a cutoff error, if uncorrected, of  $-0.0075$  sec. This is an early cutoff, and therefore an amount  $t_c = -0.0075$  is included in  $J_2$ .

$\Delta t_{co}$  is right shifted four times prior to being stored on the sigmator countdown. This causes data to be shifted out in an amount ranging from 0 to  $P_{24}$  of the shifted quantity. Therefore an average error is biased off. Since a negative number is placed on the sigmator, the right shift decreases the  $(-\Delta t_{co})$  and therefore causes a late cutoff. The average error thus introduced is  $P_{24}/2$  scaled to 12905.55077. Therefore an error  $t_s$  due to the shift is biased off as  $t_s = 0.0004$ .

- d. MECO Decay and Separation  $\Delta V$ . The OAO trajectory is targeted for a circular orbit after spacecraft separation. Therefore cutoff is biased to occur early according to the velocity added by the shutdown impulse,  $\Delta v_d$ , and the spacecraft separation spring impulse,  $\Delta v_s$ , as follows:

$$t_{ds} = \frac{\Delta v_d + \Delta v_s}{a_T} = 0.1273 \text{ sec}$$

where  $\Delta v_d = 8.97 \text{ ft/sec}$

$\Delta v_s = 2.18 \text{ ft/sec}$

$a_T = \text{nominal thrust acceleration at cutoff} = 87.7 \text{ ft/sec}^2$

- e.  $J_2$ . The value of  $J_2$  is thus

$$\begin{aligned} J_2 &= t_1 + t_2 + t_{cd} + t_c + t_s + t_{ds} \\ &= 0. + 0.03375 + 0.0006 - 0.0075 + 0.0004 + 0.127 \\ &= 0.154 \text{ sec} \end{aligned}$$

## 2.9 INITIALIZATION AND EQUATION INPUT

The guidance equations are initialized prior to liftoff. This initialization includes navigational data, conic calculations, square root start-up values, and program branch settings. Also, by virtue of commonality the launch time,  $t_e$ , is calculated, even though OAO is not a launch-on-time mission.

- a. Calculation of Launch Time,  $t_e$ .

$$t_e = t_\lambda + t_\sigma + J_1$$

$t_\lambda$  = sigmator time at receipt of LOT signal

$t_\sigma$  = sigmator time at time of entering flight mode

$J_1$  = negative of the time from LOT to  $t_e = 0$

Since the mission-dependent orbital parameters,  $h_d$ ,  $r_p$ ,  $e$ , etc. for OAO are really input constants, the J-value coefficients of the  $t_e$  terms in the prelaunch polynomials are set to zero. Therefore the value of  $t_e$  has no effect on the OAO trajectory.

- b. Sigmator Initialization. After the calculation of  $t_e$ , the sigmator is initialized as

$$\bar{v}_\sigma = \bar{0}$$

$$t_\sigma = 0$$

$$\bar{\omega}_d = \bar{0}$$

MECO countdown sector = 0

- c. Navigational Equations. The initialization of the navigational data is as follows:

$$\text{Time: } t_i = 0$$

$$\text{Earth rotational axis: } \bar{1}_{np} = \begin{bmatrix} J_{45} \\ J_{46} \\ J_{47} \end{bmatrix}$$

$$\text{Position: } \bar{r}_m = \begin{bmatrix} J_{43} \\ J_{44} \\ I_2 \end{bmatrix}$$

$$\text{Velocity: } \bar{v}_{\sigma i-1} = \bar{0}$$

$$\bar{v}_m = \begin{bmatrix} K_{13} \ 1_{npv} \\ -K_{13} \ 1_{npv} \\ 0 \end{bmatrix}$$

$$\Delta \bar{v}_m = \bar{0}$$

$$\text{Gravity: } \bar{g} = \begin{bmatrix} 0 \\ 0 \\ I_7 \end{bmatrix}$$

- d. Conic Calculations and Targeting Input.

$$\text{Target vector: } \bar{1}_a = \begin{bmatrix} J_6 \\ J_{11} \\ \sqrt{1 - J_6^2 - J_{11}^2} \end{bmatrix}$$



Energy:  $h_d = J_{16} + J_{17} t_e$

Perigee radius:  $r_p = J_{24} + J_{25} t_e + J_{26} t_e^2$

Eccentricity:  $e = \frac{h_d r_p}{K_1} + 1$

Semi-latus rectum:  $p = r_p (1 + e)$

Target vector true anomaly:  $\cos \eta_A = J_{32}$

$$\sin \eta_A = \sqrt{1 - \cos^2 \eta_A}$$

Desired cutoff angular momentum:  $c_d = \sqrt{K_1 p}$

Sustainer phase true anomaly to go:  $\Delta \eta = J_{28}$

Start up acceleration for Centaur phase time to go:  $C_{AT} = J_{31}$

Pitch steering parameter:  $V_c = \frac{e C_d}{p}$

Spacecraft separation attitude:  $\beta_1 = J_{49}$

$$\beta_2 = J_{50}$$

$$\beta_3 = J_{51}$$

e. Square Root Start up Values

$$a_T = I_1$$

$$r_m = I_2$$

$$\alpha_1 = I_3$$

$$C_d = I_4$$

$$V_m = I_5$$

$$C = I_6$$

$$f_t = 1$$

$$\sin \eta_A = 1$$

$$l_{aw} = 1$$

$$\sin \theta = 1$$

f. Program Branch Settings (see equation flow charts, Appendix A).

$$\text{Branch 1} = 0$$

$$\text{Branch 2} = J_{21} = 0$$

$$\text{Branch 3} = 0$$

$$\text{Branch 4} = 0$$

$$\text{Branch 5} = 0$$

$$\text{Branch 6} = 0$$

$$\text{Branch 7} = 0$$

$$\text{Branch 8} = 0$$

$$\text{Branch 9} = J_{22} = 0$$

$$\text{Branch 10} = 0$$

$$\text{Branch 11} = 0$$

$$\text{Branch 12} = 0$$

$$\text{Branch 13} = 0$$

$$\text{Branch 14} = 0$$

$$\text{Branch 15} = 0$$

$$\text{Branch 16} = J_{23} = 1$$

$$\text{Branch 17} = 0$$

$$\text{Branch 18} = 0$$

$$\text{Branch 19} = 1$$

$$\text{Branch 20} = 1$$

$$\text{Branch 21} = 0$$

It should be noted that not all branches need be initialized prior to liftoff. To conserve computer temporary storage some are initialized at BECO, and others at SECO, depending upon where the branch is used in the flight program.

## 2.10 PROGRAM BRANCHES

The AC-16 guidance flight program contains 22 logic branches. The branches control program flow according to the mission and phase of flight. Table 2-1 defines the logic and their path options.

Table 2-1. Program Logic Branches

Branch	Function Definition
1	<p>Flight phase switching branch, executed after navigation and coordinates are completed.</p> <p>= 0 Performs liftoff time test and then switches to Booster section.</p> <p>= 1 Booster section .</p> <p>= 2 Sustainer section.</p> <p>= 3 Centaur A, where an elapsed time test is interrogated to enable the test for MECO backup. After this test is performed the equations cycle thru time to go and compute steering coefficients.</p> <p>= 4 Centaur B, where the acceleration test to issue MECO backup is performed, prior to entering time to go and steering coefficients.</p> <p>= 5 Parking Orbit section.</p> <p>= 6 Post-Injection section.</p>
2	<p>The mission targeting branch, executed during initialization. Certain mission-dependent quantities are initialized prior to entering Branch 2. These are <math>\cos \eta_A</math>, <math>l_{aw}</math>, <math>\sin \theta</math>, <math>\sin \eta_A</math>. Branch 2, then, controls the ultimate algebraic sign of <math>l_{aw}</math>, <math>\sin \theta</math>, and <math>\sin \eta_A</math>; the ultimate setting of Branch 19, and the ultimate value of <math>\cos \eta_A</math>.</p> <p>= 0 OAO mission; <math>l_{aw}</math> sign set positive.</p> <p>= 1 ATS mission; signs of <math>\sin \theta</math> and <math>\sin \eta_A</math> set negative; Branch 19 set to 1 (so that PU discrete is not issued for ATS first burn); <math>\beta_{tnr}</math> components of third burn pointing vector are computed.</p> <p>= 2 Mariner mission; computes <math>\cos \eta_A = -1/e</math>; and computes the u, v components of Mariner target vector.</p> <p>= 3 Used as an iterative loop to compute square roots required for <math>l_{aw}</math>, <math>\sin \eta_A</math>, and <math>C_d</math>.</p> <p>= 4 Used as iterative loop for square roots required for <math>\sin \eta_A</math> and <math>C_d</math> prior to ATS second burn.</p>
3	<p>Control switch for computing <math> \bar{a}_T </math></p> <p>= 0 <math> \bar{a}_T </math> computed if <math>\bar{a}_T \cdot \bar{a}_T</math> exceeds <math>E_2</math>.</p> <p>= 1 <math>\bar{a}_T</math> set to <math>\bar{0}</math> (used in ATS parking orbit to "switch out" accelerometers).</p>

Table 2-1. Program Logic Branches, Contd

Branch	Function Definition
4	<p>Control switch for <math>\bar{l}_n</math>.</p> <p>= 0 True <math>\bar{l}_n</math> computed.</p> <p>= 1 Use predetermined <math>\bar{l}_n</math> (<math>l_{nu} = J_{18}</math>, <math>l_{nv} = J_{19}</math>, <math>l_{nw}:\text{true}</math>) (for dogleg yaw steering).</p>
5	<p>Mission dogleg branch.</p> <p>= 0 Test <math>\bar{f}</math> for dogleg limit</p> <p>= 1 Bypass dogleg test</p>
6	<p>Booster steering and test branch.</p> <p>= 0-9 Issue booster pitch, yaw steering</p> <p>= 10 Issue test <math>\bar{f}^*</math> for FACT plugs-out test</p> <p>= 11 Go to integrated test (in preflight section for FACT test)</p>
7	<p>Booster enable test branch.</p> <p>= 0 Interrogate BECO discrete enable test.</p> <p>= 1 Bypass BECO enable test.</p>
8	<p>Controls bypassing of selected steering coefficient computations.</p> <p>= 2 Normal route used during Centaur phase; computes <math>\Delta\eta</math>, <math>\sin \Delta\eta</math>, <math>\cos \Delta\eta</math>, <math>r_d</math>, <math>\dot{r}_d</math>.</p> <p>= 0 Same as 2 except <math>\Delta\eta</math> computation bypassed; (instead <math>\Delta\eta</math> input as <math>J_{28}</math>).</p> <p>= 1 Bypasses all of above computations (used during ATS 2nd burn startup).</p>
9	<p>Mission switching branch used on cutoff cycle.</p> <p>= 0 Switches to post-injection computations.</p> <p>= 1 Switches equations to parking orbit after MECO I for ATS.</p>
10	<p>Allows initialization for ATS second burn to be performed without issuing flight mode accept discrete.</p>

Table 2-1. Program Logic Branches, Contd

Branch	Function Definition
10 Contd	<p>= 0 Issue flight mode accept discrete (just after first initialization is complete).</p> <p>= 1 Initializes <math>\sin \theta</math>, <math>\cos \theta</math> for ATS second burn, and sends equations to steering coefficient section.</p>
11	<p>Dogleg control switch.</p> <p>= 0 Use <math>f_n'</math> as determined from guidance yaw steering</p> <p>= 1 Set <math>f_n' = 0</math>, and use preset <math>\bar{l}_n = (J_{18}, J_{19}, l_{nw})</math> determined from input J's.</p>
12	<p>Controls switching of equations in post-injection branch.</p> <p>= 0 Compute spacecraft separation attitude vector.</p> <p>= 1 Compute vehicle retrothrust attitude vector.</p> <p>= 2 Issue "unlock vent valve" (L8) discrete, based on elapsed time from MECO (<math>J_{30}</math>). (ATS)</p> <p>= 3 Issue, one cycle after L8, the "power changeover discrete" (L10). (ATS)</p>
13	<p>Steering coefficient switching branch.</p> <p>= 0 Normal routing; compute A, B, and <math>f_r</math></p> <p>= 1 Used during ATS second burn startup; allows equations to compute a new <math>\Delta r</math>, <math>\Delta \dot{r}</math>, and <math>(G/a_T)</math> so that second burn startup <math>\bar{f}</math> vector can be computed.</p> <p>= 2 Used on second iteration during ATS second burn startup; switches equations to startup yaw computations without destroying start up pitch components, previously computed.</p>
14	<p>Integral control branch.</p> <p>= 0 Allows integral control enable test to be interrogated.</p> <p>= 1 Bypasses computations which update <math>\Delta \bar{f}</math>.</p>
15	<p>Parking orbit switching branch. (ATS only)</p> <p>= 0 Enables setup of attitude vector change from first MECO to coast phase <math>\bar{l}_v</math> vector.</p>

Table 2-1. Program Logic Branches, Contd

Branch	Function Definition
15 Contd	<p>= 1 Enables interrogation of time delay test (<math>J_9</math>) which delays parking orbit range angle test until vehicle is in correct quadrant; also enables <math>t_{gc}</math> test, which when passed allows second burn startup attitude vector to be computed.</p> <p>= 2 Enables range angle test used for second MES startup sequence discrete.</p> <p>= 3 Enables acceleration test used to detect main engine start for second burn, thereby switching the equations to the steering mode.</p>
16	<p>Post-injection mission dependent branch used to compute the spacecraft separation vector; set via <math>J_{23}</math>.</p> <p>= 2 ATS mission; enables computation of first (temporary) separation vector (90 deg from last MECO <math>\bar{f}</math> vector).</p> <p>= 0 ATS mission; enables computation of second (permanent) separation vector.</p> <p>= 1 OAO, Mariner missions; enables computation of separation vector.</p>
17	<p>Switching branch used in time-to-go section; enables sharing of <math>f_t</math> computation with STEER.</p> <p>= 0, 1, 2 Loops equations through numerical integration computation for <math>\Delta c</math> actual.</p> <p>= 3 Completes numerical integration for <math>\Delta c</math>, and computes <math>T_A</math> correction to initial time to go estimate.</p> <p>= 4 Routes the equations back to STEER after computing <math>f_t</math> (using the same square root computation as time to go)</p>
18	<p>Steering enable branch used in steering equations.</p> <p>= 0 Normal route; compute <math>\bar{f}</math> vector.</p> <p>= 1 Used during ATS second burn restart computation; computes pitch and yaw rates of change required to reorient the vehicle prior to second MES.</p>

Table 2-1. Program Logic Branches, Contd

Branch	Function Definition
18 Contd	<p>= 2 Enables interrogation of time delay test; used to delay admittance of guidance steering for first Centaur burn until all attitude disturbing transients (caused by MES, and/or nose fairing eject) have been damped.</p>
19	<p>PU discrete issuing branch - issues L0 discrete (which nulls the PU valve) <math>E_9</math> seconds prior to cutoff.</p> <p>= 0 issue discrete (OAO, Mariner, ATS second burn).</p> <p>= 1 Do not issue discrete (ATS first burn).</p>
20	<p>Post-injection switching branch — set to 1 just prior to entering post injection for the first time.</p> <p>= 1 Routes the equations back to start of basics; do not compute and issue new steering vector.</p> <p>= 0 Routes equations into steering block which computes <math>\bar{f}</math>. Computation for <math>f_t</math> (using square root) is bypassed.</p>
21	<p>ATS second burn restart switching branch; used only during computation of ATS second burn restart vector.</p> <p>= 0 Normal routing of equations to yaw steering.</p> <p>= 1 Routes equations back to initialization to compute e, p and thence to COEF to compute <math>\sin(\Delta\eta - \theta)</math> for second burn pitch and yaw steering.</p>
22	<p>Branch in COORDINATES to avoid interrupting the telemetry sequence when the <math>\bar{I}_t</math> calculation is entered from a non-standard route. If the equations fail the azimuth limit test the preset <math>\bar{I}_n</math> is used and the equations are returned to the coordinate phase to recompute <math>\bar{I}_t</math>.</p> <p>= 0 Normal route thru the remainder of the coordinate computations.</p> <p>= 1 Set one time only when <math>J_{18} f_u + J_{19} f_v &lt; 0</math>. The equations recycle through the <math>\bar{I}_t</math> computation, then return to the steering equations with <math>f'_n = 0</math>.</p>



### SECTION 3

#### TARGETING

Targeting for the AC-16/OAO mission is the generation of the mission-dependent guidance constants required for execution of the guidance equations so as to attain the target orbit.

The fundamental ground rules which affect the AC-16 targeting are:

- a. Launch at an azimuth of  $60^\circ$  with a yaw right maneuver (dogleg) after fairing jettison to achieve the required inclination of  $35^\circ$ .
- b. Inject the spacecraft into a nominally circular orbit of 417 n.mi. altitude.
- c. Orient the Centaur vehicle and payload along the required attitude vector prior to spacecraft separation.
- d. Orient the Centaur vehicle along the required attitude vector for the retrothrust sequence.

The guidance equations employ the target vector concept which, in the AC-16/OAO application of the common equations, is required for yaw steering only.

In the general (fixed) conic case, the target vector is used to define the required cutoff position and velocity in the presence of trajectory dispersions. The same is true in the case of the injection conic for launch-on-time trajectories whose elements change as launch time. Therefore in both cases the target vector enters into the formulation of both pitch and yaw steering signals required to achieve the desired cutoff conditions.

Because the OAO powered flight trajectory is independent of launch time and the target conic is circular, the desired cutoff parameters ( $r$ ,  $v$ ,  $\gamma$ ) are constants. Therefore the target vector is not required for pitch steering. The target vector is therefore selected to satisfy the requirements of yaw steering only.

### 3.1 MISSION REQUIREMENTS

The AC-16/OAO mission requires a direct ascent guided powered flight trajectory terminating with payload injection into a nominally circular orbit of 417 n.mi. The AC-16 guidance equations are specifically targeted to satisfy the following powered flight trajectory and final orbit requirements:

- a. Maintain the powered flight trajectory plane during the sustainer phase and on through fairing jettison parallel to the initial azimuth heading.
- b. After fairing jettison perform a yaw right maneuver (dogleg) to achieve the desired orbit inclination of 35 degrees.

- c. Final orbit parameters:

Injection altitude = 417 n.mi.

Injection flight path angle = 0 deg

Injection velocity = circular orbit velocity

Target orbit inclination = 35 deg.

- d. Spacecraft separation to occur along the nominal attitude vector at MECO.
- e. Retrothrust to occur along an attitude vector,  $\bar{f}$ , displaced from the negative radius vector,  $-\bar{1}_r$ , in the direction of  $-\bar{v}_m$ , by an angle  $\alpha$ .

For this mission, all of the target requirements are constants and, for the most part, the required equation input J constants are obtained directly from the target requirements. In instances where the required conic input to the equations is obtained from a polynomial in launch time, the required parameter is input as the constant term, and the coefficients of launch time are zeroed.

### 3.2 POWERED FLIGHT TRAJECTORY TARGETING

- a. Dogleg Requirements. Maintenance of the ascent trajectory plane during sustainer phase parallel to the initial azimuth direction is accomplished by employing a fixed unit normal vector,  $\bar{1}_n$ . The definition of the fixed  $\bar{1}_n$  vector is illustrated in Figure 3-1 and obtained as follows:

$$\begin{aligned}
 1_{nu} &= -\sin \ell = J_{18} \\
 1_{nv} &= \cos \ell = J_{19} \\
 1_{nw} &= 1_{nw}(\text{BECO})
 \end{aligned}
 \tag{45}$$

$1_{nw}$  at BECO is sufficiently small ( $\approx 0.5 \times 10^{-2}$ ) as to not significantly affect the direction of  $\bar{1}_n$ .

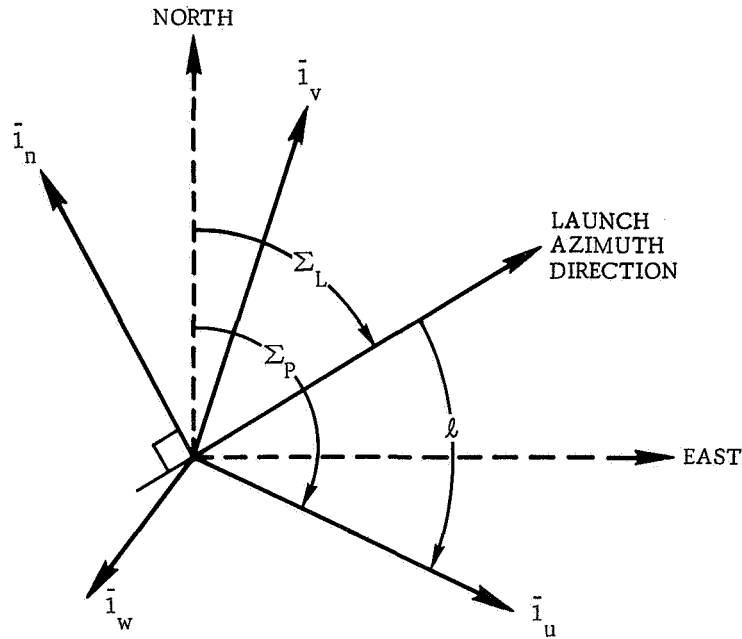


Figure 3-1. Definition of Fixed  $\bar{1}_n$  Vector

where

$$\begin{aligned}
 \bar{1}_w &= \text{unit local vertical at the launch site} \\
 \bar{1}_u &= \text{unit platform azimuth alignment direction} \\
 \bar{1}_v &= \bar{1}_w \times \bar{1}_u \\
 \Sigma_p &= \text{platform alignment azimuth} \\
 \Sigma_L &= \text{launch azimuth} \\
 \ell &= \Sigma_p - \Sigma_L
 \end{aligned}$$

Figure 3-1. Definition of Fixed  $\bar{1}_n$  Vector

b. Final Orbit Conic Calculations. The target orbit is specified by inputting to the computer the perigee radius and the orbital energy.

1. Perigee radius. The desired perigee radius, which for OAO is the specified circular orbit radius, is input to the computer as

$$r_p = J_{24}$$

2. Orbital energy. The orbital energy,  $h_d$ , is obtained as follows:

$$h_d = \frac{-\mu}{a} = \frac{-\mu}{r_p}$$

since for circular orbit  $a = r = r_p$ .  $h_d$  is input to the computer as

$$h_d = J_{16}$$

3. Eccentricity. The eccentricity is computed in the flight program initialization as

$$e = 1 + \frac{h_d r_p}{\mu}$$

Note that  $e = 0$  for OAO since  $h_d = \frac{-\mu}{r_p}$

4. Semi-latus rectum. The semi-latus rectum of the parking orbit is computed in the flight program initialization as

$$p = r_p (1 + e)$$

For OAO  $p = r_p$  since  $e = 0$ .

5. Angular momentum. The angular momentum of the parking orbit is computed in the flight program initialization as

$$C_d = \sqrt{\mu p}$$

These parameters are used to compute the desired cutoff position and radial velocity. From Equations 23,  $r_d$  and  $\dot{r}_d$  are

$$r_d = \frac{p}{1 + e \cos \eta_T} = p \quad \text{since } e = 0 \text{ for OAO}$$

$$\dot{r}_d = \frac{e C_d}{p} \sin \eta_T = 0 \quad \text{since } e = 0 \text{ for OAO}$$

where  $\eta_T$  is the predicted true anomaly at cutoff, irrelevant for OAO circular orbit.

c. Target Vector. The target vector  $\bar{l}_a$  is used for yaw steering only, the objective of which is to control the target orbit inclination. The following sequence of operations defines  $\bar{l}_a$ :

1. Locate the ascending node of the target orbit with a unit vector,  $\bar{l}_{as}$ , in the equatorial plane, at the longitude of the equatorial crossing.
2. Rotate  $\bar{l}_{as}$  about the earth rotational axis,  $\bar{l}_{np}$ , through  $90^\circ$ . This gives  $(\bar{l}_{np} \times \bar{l}_{as})$ .
3. Rotate  $(\bar{l}_{np} \times \bar{l}_{as})$  about  $\bar{l}_{as}$  through the desired inclination angle,  $i_d$ .

Figure 3-2 illustrates the definition of the target vector.

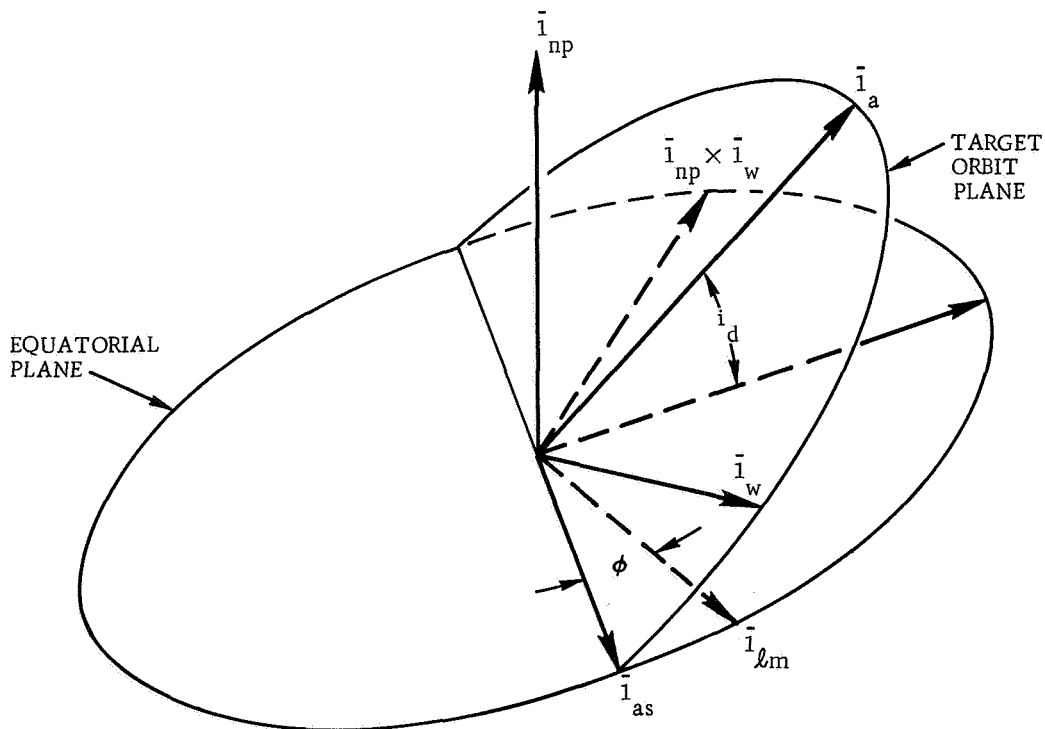


Figure 3-2. Definition of Target Vector

The target vector is therefore given by:

$$\bar{\mathbf{l}}_a = \sin i_d \bar{\mathbf{l}}_{np} + \cos i_d (\bar{\mathbf{l}}_{np} \times \bar{\mathbf{l}}_{as}) \quad (46)$$

This vector is therefore located  $90^\circ$  from the ascending node of the target orbit, and lies in a plane inclined at the desired orbit inclination. For yaw steering the error signal  $\epsilon_y$  is formed from  $\bar{\mathbf{l}}_n \cdot \bar{\mathbf{l}}_a$ . If  $\epsilon_y = 0$  at MECO, the target orbit inclination requirement is satisfied.

From Equation 46 it is seen that to obtain  $\bar{\mathbf{l}}_a$  it remains to compute  $\bar{\mathbf{l}}_{as}$ . The inclination angle  $i_d$  is a target specification and the vector  $\bar{\mathbf{l}}_{np}$  is a known constant. The vector  $\bar{\mathbf{l}}_{as}$  is a function of launch azimuth and burn arc. It may be calculated from a set of initial conditions at SECO (prior to the start of Centaur yaw steering) and the desired MECO conditions; but because OAO is a single trajectory mission, a much simpler and equally accurate method is to obtain  $\bar{\mathbf{l}}_{as}$  from the open loop reference trajectory.

Referring to Figure 3-2, the vector  $\bar{\mathbf{l}}_{as}$  is obtained as follows:

- a. From the open loop reference trajectory determine the angle  $\phi$ , which is the angle in the equatorial plane corresponding to the longitude of the target orbit ascending node relative to the launch meridian.
- b. Locate the vector  $\bar{\mathbf{l}}_{\ell m}$  in the equatorial plane at the inertially fixed launch meridian as follows:

$$\bar{\mathbf{l}}_{\ell m} = \left( \frac{\bar{\mathbf{l}}_{np} \times \bar{\mathbf{l}}_w}{|\bar{\mathbf{l}}_{np} \times \bar{\mathbf{l}}_w|} \right) \times \bar{\mathbf{l}}_{np} \quad (47)$$

where  $\bar{\mathbf{l}}_w$  = unit local vertical at the launch site.

- c. The vector  $\bar{\mathbf{l}}_{as}$  is then determined as

$$\bar{\mathbf{l}}_{as} = \cos \phi \bar{\mathbf{l}}_{\ell m} - \sin \phi \left( \frac{\bar{\mathbf{l}}_{np} \times \bar{\mathbf{l}}_w}{|\bar{\mathbf{l}}_{np} \times \bar{\mathbf{l}}_w|} \right) \quad (48)$$

In summary then,  $\bar{1}_a$  is computed as follows.

- a. Given: earth rotational axis,  $\bar{1}_{np}$ ; desired target orbit inclination,  $i_d$ ; and the unit local vertical at the launch site,  $\bar{1}_w$ .
- b. Obtain the angle  $\phi$  from the open loop reference trajectory.
- c. Compute  $\bar{1}_{as}$  as given by Equations 47 and 48.
- d. Compute  $\bar{1}_a$  as given by Equation 46.

The target vector input to the guidance program consists of the u and v components of  $\bar{1}_a$  as

$$1_{au} = J_6$$

$$1_{av} = J_{11}$$

The w component of  $\bar{1}_a$  is computed in the initialization phase as

$$1_{aw} = \sqrt{1 - 1_{au}^2 - 1_{av}^2}$$

### 3.3 SPACECRAFT ATTITUDE AND VEHICLE REORIENT VECTORS

- a. Spacecraft Separation Attitude Vector. Following MECO the Centaur aligns the spacecraft at the required attitude for separation. This vector corresponds to the nominal vehicle attitude vector at MECO as given by the direction cosines of the vehicle roll axis,  $\bar{1}_\xi$ . The required attitude direction,  $\bar{f}$ , in t, n, r, coordinates is thus given by:

$$f_t = \bar{1}_\xi \cdot \bar{1}_t$$

$$f_n = \bar{1}_\xi \cdot \bar{1}_n$$

$$f_r = \bar{1}_\xi \cdot \bar{1}_r$$

where  $\bar{1}_\xi$ ,  $\bar{1}_t$ ,  $\bar{1}_n$ ,  $\bar{1}_r$  are in inertial u, v, w coordinates and taken from the nominal trajectory at MECO.

The required attitude vector in t, n, r coordinates is therefore input to the guidance program as

$$\beta_1 = J_{51} = f_t$$

$$\beta_2 = J_{50} = f_n$$

$$\beta_3 = J_{49} = f_r$$

- b. Vehicle Reorient Vector. Following spacecraft separation and at a fixed time from MECO the vehicle is reoriented for the retrothrust sequence. The required orientation is essentially along the instantaneous negative radius vector,  $-\vec{r}_m$ , but for purposes of maximizing desirable viewing relationships between the spacecraft and the Centaur tank, the attitude vector,  $\vec{f}$ , is displaced from  $-\vec{r}_m$  by an angle  $\alpha$ . Figure 3-3 illustrates the reorient vector geometry in the plane of the orbit.

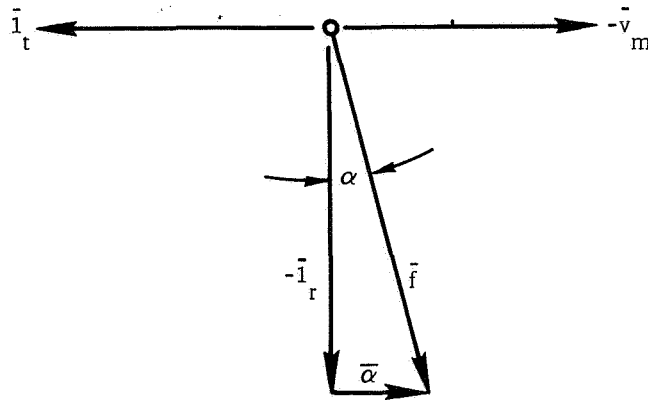


Figure 3-3. Reorient Attitude Vector Geometry

Referring to Figure 3-3, the required attitude vector for vehicle reorientation is given by

$$\vec{f}_{u,v,w} = -\vec{l}_r + \vec{\alpha} = -\vec{l}_r - \sin \alpha \vec{l}_t$$



In local t, n, r coordinates the required attitude vector is given by

$$\bar{f}_{t,n,r} = \begin{bmatrix} -\sin\alpha \\ 0 \\ -\cos\alpha \end{bmatrix} = \begin{bmatrix} J_{52} \\ J_{53} \\ J_{54} \end{bmatrix}$$

### 3.4 TARGETING PROCEDURES

The targeting procedures discussed in the previous section in most instances consist either of simple calculations or direct input of target conic parameters as J constants. For this reason and because OAO is a single trajectory mission, no automated targeting program was developed. Figure 3-4 summarizes the targeting procedures for the AC-16/OAO mission.

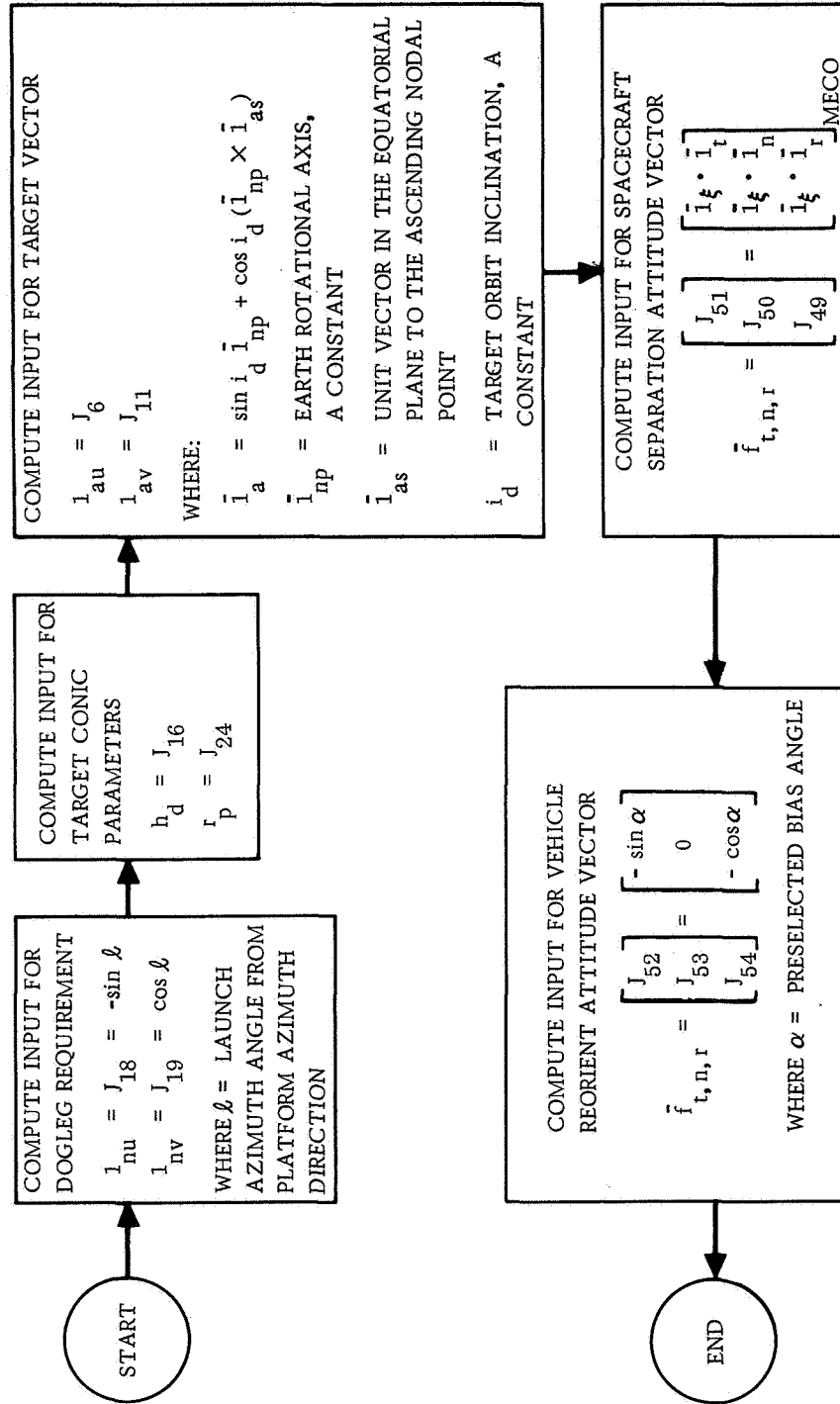


Figure 3-4. OAO Targeting Procedure

SECTION 4  
TARGET SPECIFICATION

The AC-16 mission requires a direct ascent launch to place the OAO/A-2 spacecraft into a 417 n.mi. circular orbit inclined at 35 degrees to the equatorial plane. The target specifications taken from Reference 2 are given in Table 4-1.

Table 4-1. AC-16 Target Specifications

1. Launch azimuth: 60° east of true north with a yaw maneuver performed during the Centaur powered phase to achieve the required target orbit inclination.
2. Orbit inclination: 35°
3. Injection altitude: 417 n.mi. referenced to an equatorial radius of 20,925,741 ft.
4. Injection flight path angle: 0°.
5. Injection velocity: circular orbit velocity.
6. Reorient vector bias angle: Based on a spacecraft field of view beginning at an angle 14° above the earth's horizon.
7. Spacecraft weight: 4425 lb.

The targeting was performed subject to the following ground rules:

- a. Vehicle configuration as defined in Reference 3.
- b. Flight sequence as defined in Reference 4.
- c. Launch from Complex 36B.
- d. Spacecraft  $\Delta v = 2.18$  ft/sec, based on the spacecraft weight given in Reference 2 and separation spring constants given in Reference 7.
- e. Centaur MECO decay impulse: 3055 lb-sec, including the effects of the 5.5-ms electromechanical timer delay.

## SECTION 5

### PERFORMANCE AND ACCEPTANCE CRITERIA

The performance and acceptance criteria for the AC-16 guidance equations are:

a. Injection Radius Magnitude

$$\Delta r \leq 0.5 \text{ n.mi.}$$

b. Final Orbit Inclination

$$\Delta i \leq 0.1 \text{ deg}$$

c. Final Orbit Apogee Radius

$$\Delta r_a \leq 2.0 \text{ n.mi.}$$

d. Final Orbit Apogee Radius - Perigee Radius Difference

$$\Delta(r_a - r_p) \leq 2.0 \text{ n.mi.}$$

e. Injection Weight Deviation

$\Delta W \leq 239.2 \text{ lb}$ , using the non-nominal performance data given in Reference 5, assuming uncorrelated errors and combining results in an RSS manner.

f. Heat Parameter

$$\int_0^{\text{SECO}} qv \, dt \leq 1.13 \times 10^8 \text{ lb/ft}$$

where:  $q$  = dynamic pressure

$v$  = relative velocity

g. Heat Flux

$$qv \leq 144 \text{ lb/ft-sec at fairing jettison.}$$

The error sources considered in the evaluation of the guidance equations relative to these criteria are:

- a. Targeting accuracy
- b. Cutoff steering effects
- c. Non-nominal performance effects
- d. Flight computer computational effects
- e. Velocity quantization and noise effects
- f. PU valve null effects

## SECTION 6

### GUIDANCE EQUATION TEST PLAN

The purpose of the guidance equation test plan is to specify trajectory simulations and ground rules necessary to a comprehensive evaluation of the performance of the guidance equations. In substance, the results of the specified simulation studies for the guidance equations determine the degree to which these equations satisfy mission objectives and performance specifications.

The guidance equation test plan is designed to allow separation of the effects on performance due to targeting, airborne computer computational effects, and vehicle non-nominal performance.

#### 6.1 SIMULATION TEST PLAN

6.1.1 TARGETING CHECK SIMULATION. The purpose of the targeting check simulation is to evaluate the targeting accuracy relative to the specified final orbit parameters for the AC-16 mission.

Since AC-16 is a single trajectory mission, only one targeted trajectory exists. Therefore the targeting check consists of comparing the final orbit parameters from the nominal targeted trajectory, simulated from launch to spacecraft separation, with the target specifications.

6.1.2 FLIGHT COMPUTER INTERPRETIVE SIMULATIONS. The interpretive computer simulations are performed with the guidance equations simulated exactly as in the flight computer. The purpose of the interpretive simulations is to evaluate the effect of velocity quantization and computational truncation error on guidance performance, and to verify the reliability of the guidance equations as mechanized for the flight computer.

The computational effect is evaluated by obtaining parameter differences between interpretive simulations and corresponding engineering simulations. The reliability of

the guidance equations as mechanized for the flight computer is ascertained by verifying the non-existence of computational overflows; more stringently, by verifying that no equation variable or intermediate calculation ever exceeds 90 percent of its scale factor. (The latter is accomplished automatically by a special routine in the interpretive computer simulation.)

One nominal trajectory is simulated with the interpretive computer simulation, since the powered flight trajectory is the same for all launch times.

6.1.3 NON-NOMINAL PERFORMANCE SIMULATIONS. The non-nominal engineering simulation analysis is performed to verify the capability of the equations to satisfy the performance specifications in the presence of non-nominal vehicle and environmental parameters. The non-nominal vehicle and environmental parameters introduced individually on the nominal closed loop simulation are obtained from Reference 5. The results of all non-nominal simulations are evaluated in terms of the deviation from the nominal closed loop trajectory of specified performance parameters.

The non-nominal engineering simulations generated for evaluation of the AC-16 guidance equations performance comprise a complete study consisting of simulations of all significant vehicle parameter dispersions, both positive and negative, applied to the nominal trajectory.

6.1.4 OMNIBUS DISPERSIONS. The TRAK omnibus dispersions are performed with the guidance equations simulated exactly as in the flight computer. The purpose of the omnibus dispersions is to evaluate the gross performance of the guidance equations while operating under severely perturbed trajectories. The omnibus dispersions are also a severe test on the adequacy of computational scaling.

The perturbed trajectories are obtained by introducing combinations of dispersions, classified by their effect on the trajectories as follows:

- a. High or Low: Non-nominal vehicle parameters combined to cause a correspondingly high, or low, in-plane trajectory altitude characteristic.

- b. Right or Left Lateral: Non-nominal vehicle parameters combined to introduce large velocity errors normal to the trajectory plane in the yaw right or yaw left direction respectively.
- c. Omnibus: Combinations of a and b.

The non-nominal vehicle parameters introduced for generating the extremely perturbed trajectories are listed in Table 6-1.

The perturbed trajectories for the AC-16 omnibus dispersions are generated as follows:

- a. Low left.
- b. Low right.
- c. High left.
- d. High right.

## 6.2 SIMULATION GROUND RULES

The following ground rules are common to all trajectory simulations generated for evaluating guidance performance.

- a. Vehicle configuration as defined in Reference 3.
- b. Spacecraft weight as specified by Reference 2.
- c. Flight sequence as defined in Reference 4.
- d. Launch from Complex 36B.
- e. Nominal Centaur main engine decay impulse of 3055 lb-sec including the effects of the 5.5-ms electromechanical timer delay.
- f. Nominal Centaur/spacecraft separation velocity increment of 2.18 ft/sec.
- g. Booster and sustainer propulsion systems simulated using a 12-variable sea-level model and an altitude model respectively.

The remaining ground rules, which are variable according to the simulation objectives, are given in the following sections.



Table 6-1. Omnibus Perturbations

Omnibus	Perturbations					
	Booster Pitch (%)	Centaur $I_{sp}$ (sec)	Centaur Thrust (lb)	Sustainer Centaur Thrust Misalignment (deg)		Launch Azimuth Error (deg)
				Pitch	Yaw	
Low-Left	+10	-8	-1100	3	3	-6
Low-Right	+10	-8	-1100	3	-3	+6
High-Left	-10	+8	+1100	-3	3	-6
High-Right	-10	+8	+1100	-3	-3	+6

†Signs adjusted to produce an additive effect as follows:

$d_{10}$ (deg/hr)	$d_{11}$ (deg/hr/g)	$d_{12}$ (deg/hr/g)	$d_{13}$ (deg/hr)	$d_{14}$ (deg/hr/g)	$d_{15}$ (deg/hr/g)	$d_{16}$ (deg/hr)	$d_{17}$ (deg/hr/g)	$d_{18}$ (deg/hr/g)
(1) -3	-3	+3	+3	+3	+3	-3	-3	+3
(2) +3	+3	-3	-3	-3	-3	+3	+3	-3

6.2.1 TARGETING CHECK SIMULATION GROUND RULES. In addition to the basic simulation ground rules given in Section 6.2, the following ground rules apply:

- a. Guidance equations are simulated using an ideal computer simulation.
- b. Integration step size approximating the flight computer program cycle times as follows:
  1. Booster phase: 2.0 sec.
  2. Sustainer phase: 3.0 sec.
  3. Centaur: 4.0 sec.
  4. Post-injection phase: 2.0 sec.
- c. A closed-loop Centaur cutoff is effected using the inflight MECO time-to-go calculation.
- d. Open-loop, precise booster staging at 5.7 g's.
- e. Orbit data are measured relative to the target specifications. Table 6-2 gives the parameters to be tabulated.

6.2.2 FLIGHT COMPUTER INTERPRETIVE SIMULATION GROUND RULES. In addition to the basic simulation ground rules given in Section 6.2, the following ground rules apply:

- a. The guidance equations are simulated exactly as in the flight computer; that is, the computational effects due to the 25-bit word length, fixed point arithmetic, arithmetic algorithms, and guidance integration step sizes.
- b. A closed-loop Centaur cutoff is effected using the inflight MECO time-to-go calculation.
- c. Open-loop, precise booster staging at 5.7 g's.
- d. All orbit deviations are measured relative to the closed-loop targeting check simulation. The parameters to be tabulated are given in Table 6-3.

6.2.3 NON-NOMINAL ENGINEERING SIMULATION GROUND RULES. In addition to the basic simulation ground rules given in Section 6.2, the following ground rules apply:

Table 6-2. Orbit Parameters for Targeting Evaluation

Epoch	Parameter	Units
Launch	Launch availability date	
	Go inertial time (opening)	hr:min:sec GMT
	Go inertial time (closing)	hr:min:sec GMT
	Launch azimuth	deg
	Launch pad	
MECO decay	<sup>†</sup> Burnout weight	lb
Spacecraft Separation	Time of separation from go-inertial time	sec
	Injection latitude	deg
	Injection longitude <sup>(1)</sup>	deg
	<sup>†</sup> Injection radius magnitude	n.mi.
	Injection velocity magnitude	ft/sec
	Injection flight path angle	deg
	<sup>†</sup> Orbital inclination	deg
	Longitude of the ascending node <sup>(2)</sup>	deg
	Orbital period	min
	<sup>†</sup> Apogee altitude*	n.mi.
	<sup>†</sup> (Apogee altitude - Perigee altitude)	n.mi.
Heating	<sup>†</sup> $\int_0^{\text{MECO}} qv \, dt$	lb/ft

(1) Longitude at spacecraft separation measured positive east of Greenwich.

(2) Longitude of the ascending node of the final orbit at equatorial crossing, measured positive east of the launch longitude inertially fixed at launch time.

\* Referenced to a spherical earth of radius 20,925,741 ft.

<sup>†</sup> These parameters are to be used as the acceptance criteria.

Table 6-3. Orbit Parameters for Interpretive Simulation and Non-nominal Performance Evaluation

Parameter	Units
$\int_0^{\text{SECO}} qv \, dt$	lb/ft
Weight at MECO	lb
Injection radius	ft
Apogee radius	ft
Orbit inclination	deg
Orbit period	sec
Longitude of the ascending node	deg
$\Delta(\text{apogee-perigee})$ radius	ft
Latitude at spacecraft separation	deg
Longitude at spacecraft separation	deg

- a. Guidance equations are simulated using an ideal computer simulation.
- b. Integration step size approximating the flight computer program cycle times as given by item b in Section 6.2.1.
- c. Booster cutoff is treated as a separate dispersion so that its effect is considered only once.
- d. Open-loop, precise booster staging at 5.7 g's.
- e. A non-nominal main engine decay is simulated for thrust dispersions since the engine decay simulations use the actual value of thrust.
- g. Deviations are measured from the closed-loop nominal simulation in order to separate non-nominal and targeting effects. The parameters to be tabulated are given in Table 6-3.
- h. The list of vehicle dispersions is given in Table 6-4.

6.2.4 OMNIBUS SIMULATION GROUND RULES. In addition to the basic simulation ground rules given in Section 6.2, the following ground rules apply:

- a. The guidance equations are simulated exactly as in the flight computer.
- b. A closed-loop Centaur cutoff is effected using the inflight MECO time-to-go calculation.
- c. Guidance issues the BECO discrete.
- d. The orbit parameter deviations are measured relative to closed loop targeting check simulation. The parameters to be tabulated are given in Table 6-3.

Table 6-4. Dispersion List

Dispersion	Value
1. Booster pitch	4.8%
2. Booster thrust	$\pm 3074$ lb, $\pm 0.52$ sec $I_{sp}$
3. Booster $I_{sp}$	$\pm 1.92$ sec
4. Sustainer thrust	$\pm 1130$ lb $\pm 1.36$ sec $I_{sp}$
5. Sustainer $I_{sp}$	$\pm 2.89$ sec
6. Atlas fuel weight	$\pm 1234$ lb
7. Atlas LOX weight	$\pm 1138$ lb
8. Sustainer jettison weight	$\pm 62$ damp, $+408/-90$ GO <sub>2</sub> , $\pm 226$ min propel
9. Centaur thrust	$\pm 424$ lb
10. Centaur $I_{sp}$	$\pm 3.54$ sec
11. Centaur weight	$+426/-399$ lb
12. Centaur initial attitude (pitch and yaw)	$\pm 10^\circ$
13. Booster pitch thrust misalignments	$\pm 0.5^\circ$
14. Sustainer/Centaur thrust misalignments (pitch and yaw)	$\pm 2.0$
15. BECO discrete	$\pm 0.113g$
16. Launch azimuth	$\pm 2^\circ$
17. Platform drift	$\pm 2.5^\circ/\text{hr}$ , $\pm 2.5^\circ/\text{hr-g}$
18. Drag coefficient and normal force	$\pm 10\%$
19. Atmosphere	Reference 5, Table 2-3
20. Winds (head, tail, cross)	Reference 5, Table 2-4

## SECTION 7

### SOFTWARE PERFORMANCE EVALUATION

This section gives the results of the performance analysis conducted according to the test plan given in the previous section. Evaluated in this section are:

- a. Targeting accuracy.
- b. Cutoff steering effects.
- c. Non-nominal performance capability.
- d. Flight computer computational effects.
- e. Velocity quantization and noise effects.
- f. PU null effects on cutoff accuracy.
- g. Grossly perturbed interpretive computer simulations.
- h. Heating data.

#### 7.1 TARGETING ACCURACY

The results of the targeting check trajectory are given in Table 7-1. Since the AC-16 powered flight trajectory characteristics are independent of launch time, targeting accuracy is evaluated by a single simulation. All the targeted parameters agree closely with those given in or inferred from the target specification.

#### 7.2 CUTOFF STEERING ERROR

Upon entering the cutoff equation, the steering vector is not updated in order to assure minimum vehicle turning rates during MECO decay. Such an accommodation results primarily in a pitch steering error near MECO since an essentially constant vehicle attitude is maintained during the remainder of the time to cutoff.

The extent of the cutoff steering error depends upon (1) the steering rate normally commanded near cutoff and (2) the time interval over which the steering vector is held constant prior to cutoff. The time interval can vary between 3.6 and 8 seconds for the explicit guidance equations as governed by the  $J_{55}$  time-to-go test shown in Figure A-8.

Table 7-1. Targeting Accuracy

Launch Azimuth: 60° with dogleg at SECO to achieve 35° inclination Complex 36, Pad B Launch Availability: 18 September 1968 Go Inertial Time: 07:49:09 GMT (opening) Go Inertial Time: 09:49:09 GMT (closing)			
Parameter	Value	Units	Deviation From Target Specification
Burnout Weight	10965.9	lb	**
Time of Spacecraft Separation	747.95	sec	**
Injection Latitude	34.18	deg (N)	**
Injection Longitude	300.34	deg	**
Injection Radius Magnitude	3860.90	n.mi.	-0.04 <sup>†</sup>
Injection Velocity Magnitude	24495.98	ft/sec	0.40*
Injection Flight Path Angle	-0.000156	deg	-0.000156*
Orbital Inclination	34.996	deg	-0.004 <sup>†</sup>
Longitude of the Ascending Node	308.112	deg	**
Orbital Period	100.29	min	0*
Apogee Altitude	417.12	n.mi.	0.12*
Apogee Altitude - Perigee Altitude	0.18	n.mi.	0.18 <sup>†</sup>

<sup>†</sup> Target specification parameters.

\* Parameter deviations inferred by target specifications.

\*\* Parameter deviations not required or inferred by target specification.

For OAO, the cutoff steering error contributes to errors in the inplane orbital parameters of apogee radius ( $r_a$ ), apogee radius minus perigee radius ( $r_a - r_p$ ), orbital period, and, to a lesser extent, the radius magnitude ( $r_m$ ) at orbital injection.

The cutoff steering error for OAO was evaluated parametrically by simulation of several cases of the nominal trajectory with a variable time of entering the cutoff equation in the range of 3.6 seconds to 8 seconds. The resulting errors in the in-plane parameters as functions of the time of entering cutoff are shown in Figures 7-1, 7-2, 7-3, and 7-4 for  $r_m$ , ( $r_a - r_p$ ),  $r_a$ , and orbital period, respectively. The worst case errors indicated in these figures for each parameter are summarized in Table 7-5.

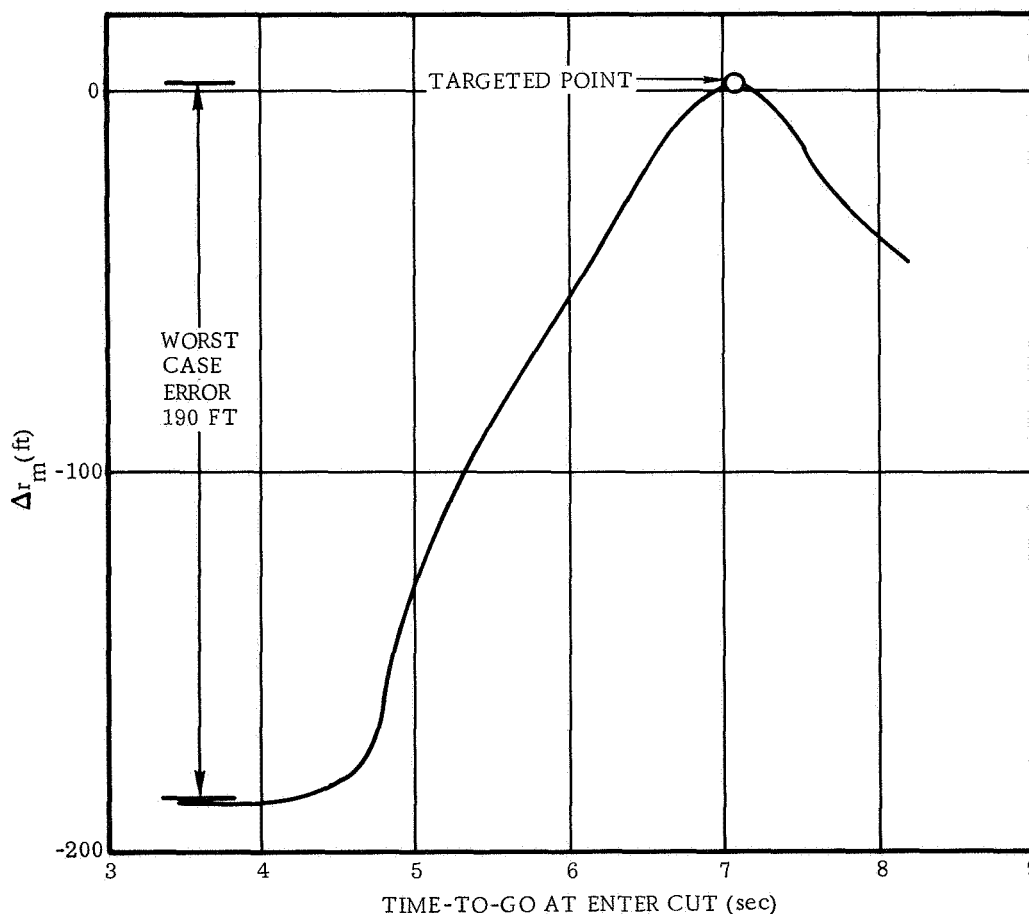


Figure 7-1. Injection Radius Error,  $\Delta r_m$ , versus Time-to-go at Enter Cut



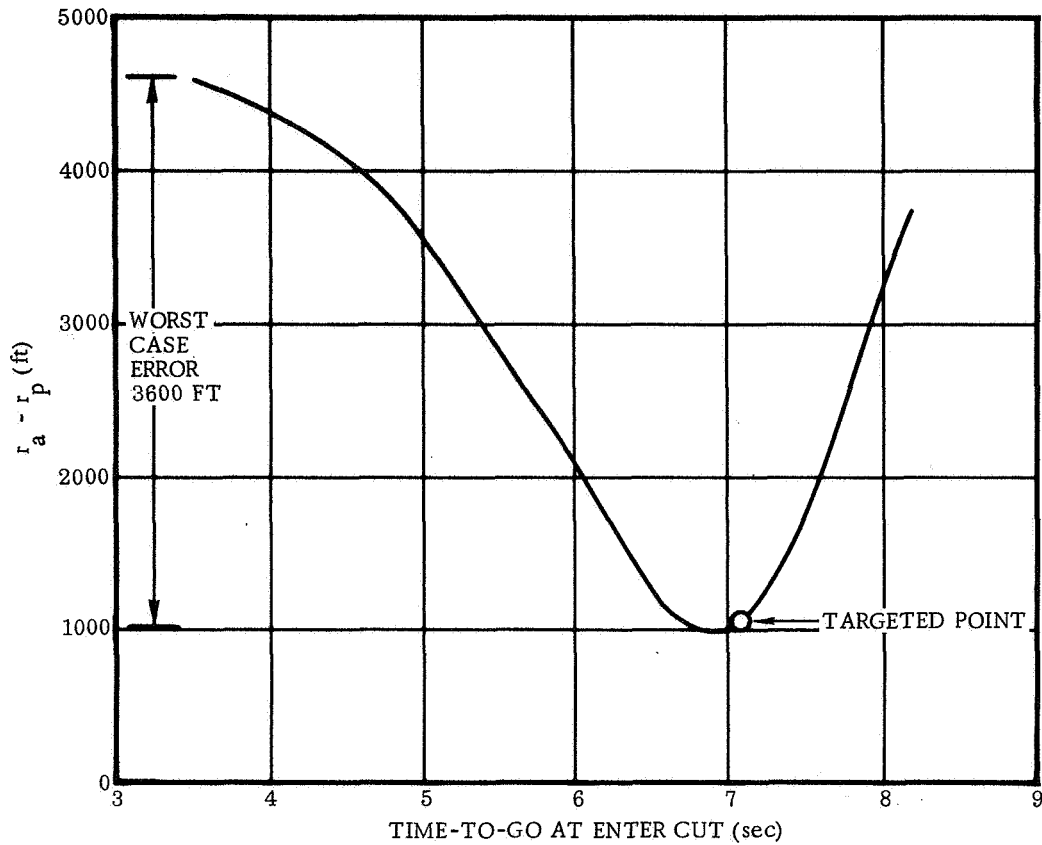


Figure 7-2. Deviation in  $(r_a - r_p)$  versus Time-to-go at Enter Cut

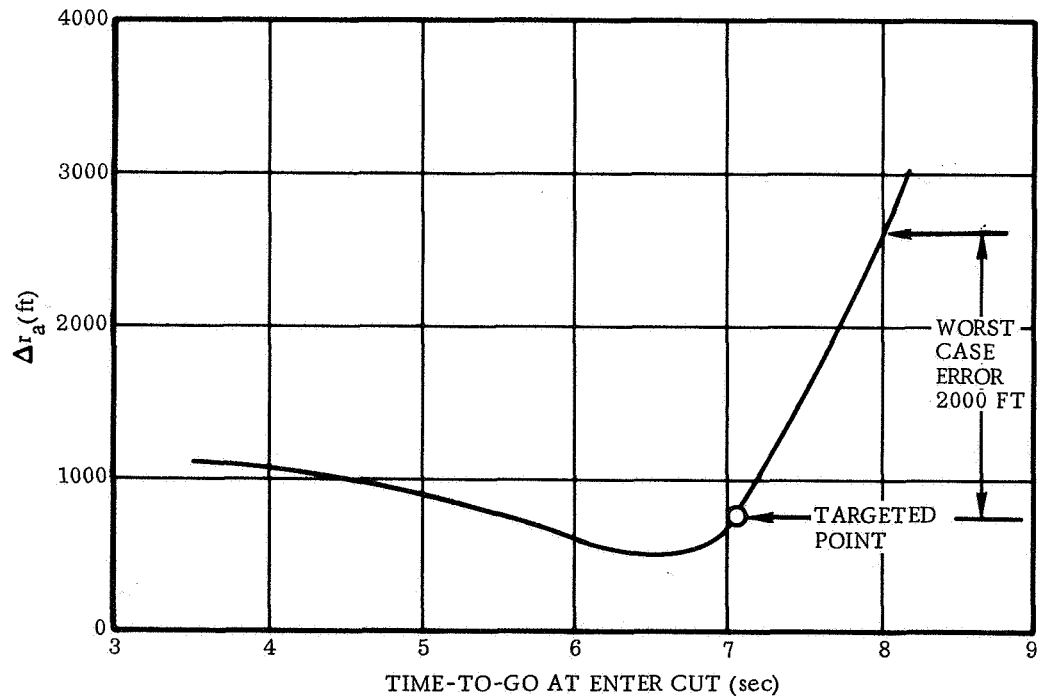


Figure 7-3. Deviation in Apogee Radius,  $r_a$ , versus Time-to-go at Enter Cut

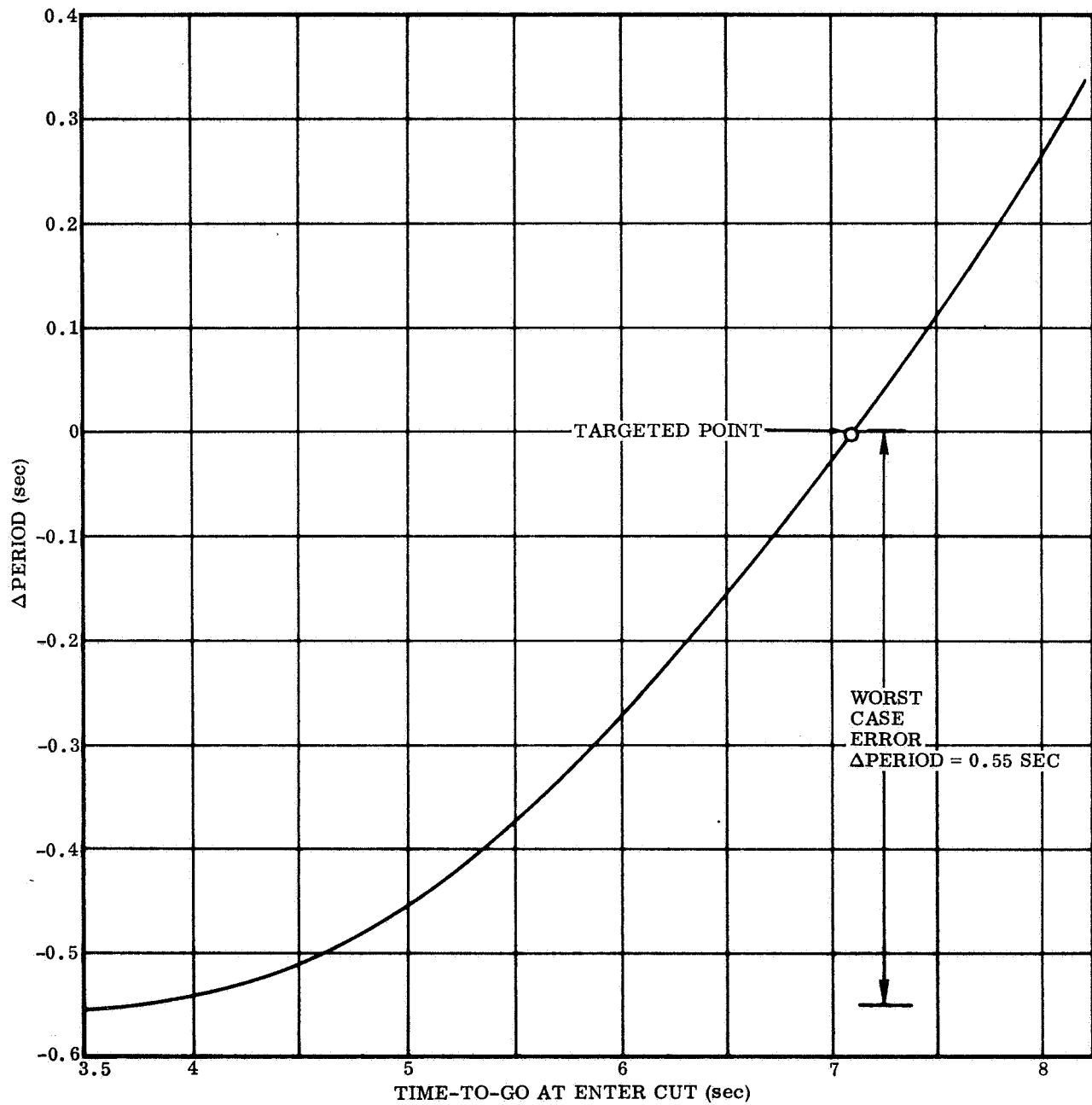


Figure 7-4. Orbital Period Error versus Time-to-go at Enter Cut

### 7.3 NON-NOMINAL PERFORMANCE RESULTS

The results of the non-nominal performance analysis are given in Table 7-2 for both the positive and negative dispersions. The results were obtained subject to the ground rules given in Section 6.

Since the cutoff steering error is evaluated separately, the inplane parameter deviations affected by this error source were adjusted as indicated by Figures 7-1 through 7-4. For example, assuming the enter cut time for a dispersion was 3.5 seconds, the correction applied to the observed ( $r_a - r_p$ ) deviation from the nominal was 3600 ft as obtained from Figure 7-2. Thus the values for the deviations in injection radius magnitude, apogee radius, apogee minus perigee radius, and orbital period in Table 7-2 represent deviations due solely to non-nominal performance.

In the software performance summary table (Section 7.9) the contribution due to non-nominal performance is obtained from the larger of the RSS's of the positive or negative dispersions or deviations, as given in Table 7-2, for each parameter except injection weight and heat parameters. For the weight contribution, the RSS of all negative weight deviations is included in the summary table. The heat parameter contribution in the summary table is the RSS of all positive heat parameter deviations.

### 7.4 FLIGHT COMPUTER COMPUTATIONAL EFFECTS

The results of flight computer computational effects are given in Table 7-3. This data is obtained by differencing the indicated parameters resulting on the nominal targeting check trajectory and a nominal interpretive computer simulation. The ground rules are given in the previous section. This data shows that the flight computer arithmetic operations do not significantly degrade the mission accuracy or performance.

## 7.5 VELOCITY QUANTIZATION AND NOISE EFFECTS

Quantization and random noise on the velocity data used by the guidance equations cause an error in the predicted time-to-go until cutoff. Although time-to-go is used in the generation of the steering coefficients, the principal effect is an error in the MECO time. For AC-16 the  $3\sigma$  cutoff error due to velocity quantization and random noise is  $\pm 0.002$  sec. (See Reference 6.) The only orbit parameters affected to any significant degree by this cutoff error is apogee radius,  $r_a$ , and  $\Delta(r_a - r_p)$ . The corresponding errors in these parameters are both  $\pm 0.10$  n.mi. These deviations are included in the summary table, 7-5.

## 7.6 PU NULL EFFECT

The propellant utilization (PU) valve is commanded to a null position upon issuance of the guidance LO discrete at a time-to-go to cutoff of  $15 \pm 2.2$  seconds. Due to the proximity of the discrete occurrence to the range of enter cut times (3.6 to 8 sec), an 11.7% probability exists of a time-to-go guidance sampling point occurring during PU valve movement to the null position. This effect and its probable contribution to an error in the guidance-predicted cutoff time is thoroughly discussed in Appendix E.

The analysis given in Appendix E shows that the  $3\sigma$  cutoff time error due to the PU null effect is 23.8 ms. For OAO, this error affects primarily cutoff velocity and in turn the inplane parameters  $r_a$  and  $(r_a - r_p)$  as follows:

$$\delta v = (\delta \Delta t_{co})(a_T) = 2.08 \text{ ft/sec}$$

where:  $\delta \Delta t_{co}$  = cutoff time error = 0.0238 sec

$a_T$  = nominal cutoff thrust acceleration = 87.6 ft/sec.

$$\delta r_a = \delta(r_a - r_p) = 4a \frac{\delta v}{v} = 7980 \text{ ft}$$

where:  $a$  = semi major axis =  $0.2346 \times 10^8$  ft

$\delta v$  = cutoff velocity error = 2.08 ft/sec

$v$  = cutoff velocity =  $0.245 \times 10^5$ .

Table 7-2. AC-16 3 $\sigma$  Dispersion Results

Dispersion	Deviations From Nominal									
	$\int_0^{\text{SECO}} qv \, dt$ (lb/ft)	Injection Weight (lb)	Radius At Injection (ft)	Apogee Radius (ft)	Inclination (deg)	Period (sec)	Long. of Ascen. Node (deg)	( $r_a - r_p$ ) (ft)	Latitude At Inject. (deg)	Longitude At Inject. (deg)
Booster Pitch	+1.8% -4.8%	-2.7 -18.1	10 9	299 -254	0.00001 0.00002	0.08 -0.04	-0.06 0.07	315 -302	0.02 -0.02	0.13 -0.14
Booster Thrust	+3074 lb -3074 lb	46.6 -49.2	-46 -99	6 -35	0.00002 0.00003	-0.02 -0.04	-0.02 0.04	124 162	0.01 -0.01	0.03 -0.03
Booster I <sub>sp</sub>	+1.92 sec -1.92 sec	85.5 -85.3	-144 -100	-25 -35	0 0.00004	-0.05 -0.04	-0.03 0.05	272 196	0.01 -0.01	0.07 -0.07
Booster Pitch Thrust Misalign.	+0.5 deg -0.5 deg	5.0 -6.2	-13 3	60 -43	0 0	0.01 0	-0.02 0.02	63 -43	0.01 -0.01	0.04 -0.04
Sustainer Thrust	+1130 lb -1130 lb	28.0 -27.4	-3 20	19 -1	-0.00003 0.00005	0.03 0.02	0.01 0.01	-4 -58	0 0	0.01 -0.01
Sustainer I <sub>sp</sub>	+2.89 sec -2.89 sec	73.9 -74.3	-55 44	-114 -22	-0.00002 0.00006	-0.02 0.02	-0.02 0.04	-75 -81	0.01 -0.01	0.06 -0.06
Atlas Fuel Wt.	+1234 lb -1234 lb	13.7 -25.0	-33 -57	-6 7	0 0.00004	0.01 -0.02	-0.01 0.03	16 166	0 -0.01	0.02 -0.03
Atlas LOX Wt.	+1138 lb -1138 lb	16.7 -18.4	-40 -22	-45 -3	-0.00002 0.00004	0 -0.01	0 0.02	-17 79	0 0	0.02 -0.02
Sustainer Jettison Weight	+696 lb -378 lb	-128.5 68.4	-2 -20	-27 10	0.00005 0.00002	-0.01 0	0.06 -0.03	31 38	-0.02 0.01	-0.10 0.05
BECO Discrete	+0.113G -0.113G	17.4 -32.0	-58 -40	71 -46	-0.00004 0.00005	0.02 -0.01	0.02 0.02	88 -41	0 0	-0.01 -0.01
Sust./Cent. Pitch Thrust Misalign.	+2.0 deg -2.0 deg	1.4 -3.5	-186 137	1009 2356	0.00010 -0.00010	-0.48 0.30	-0.01 0.01	4589 3177	0.01 -0.01	0.03 -0.03
Sust./Cent. Yaw Thrust Misalign.	+2.0 deg -2.0 deg	-13.7 10.7	56 -35	804 -43	0.00023 0.00025	0.12 -0.06	-0.25 0.25	1011 363	0.03 -0.03	-0.01 0.01
Centaur Thrust	+424 lb -399 lb	-25.3 23.5	24 48	-69 79	0.00003 0.00006	0.01 0.04	0.04 -0.07	-12 -90	-0.03 0.03	-0.22 0.22
Centaur I <sub>sp</sub>	+3.54 sec -3.54 sec	122.3 -123.4	82 24	-12 71	0.00006 0.00004	0 0.09	-0.01 0.01	32 293	0.01 -0.01	0.08 -0.08
Centaur Initial Wt.	+426 lb -426 lb	61.4 -58.9	-83 -20	14 -40	0.00003 0.00002	-0.02 -0.01	0.01 0.01	206 -17	0.01 -0.01	0.11 -0.10
Launch Azimuth	+2.0 deg -2.0 deg	28.6 -36.5	-16 58	-4 209	0.00229 0.00200	0 0.04	0.73 -0.72	90 219	-0.08 0.08	0.04 -0.04

Platform	+2.5°/hr	0	0.5	-223	-672	0.00016	-0.28	0	111	0	0
Drift D10	-2.5°/hr	0	-0.5	213	1259	-0.00014	0.28	0	1134	0	0
Platform	+2.5°/hr	0	0.4	-239	-365	0.00004	-0.19	0	296	0	0
Drift D13	-2.5°/hr	0	-0.4	229	859	-0.00003	0.19	0	764	0	0
Platform	+2.5°/hr	0	-1.1	3	-40	-0.00082	0	-0.02	-33	0	0
Drift D16	-2.5°/hr	0	1.1	-4	26	0.00083	0	0.02	50	0	0
Platform	+2.5°/hr/g	0	0.4	-219	-433	0.00006	-0.21	0	241	0	0
Drift D11	-2.5°/hr/g	0	-0.4	212	961	-0.00005	0.21	0	873	0	0
Platform	+2.5°/hr/g	0	-0.4	203	1092	0.00002	0.23	0	1009	0	0
Drift D12	-2.5°/hr/g	0	0.4	-209	-524	-0.00001	-0.23	0	300	0	0
Platform	+2.5°/hr/g	0	0.4	-189	-486	0.00002	-0.21	0	179	0	0
Drift D14	-2.5°/hr/g	0	-0.4	183	1015	-0.00001	0.22	0	945	0	0
Platform	+2.5°/hr/g	0	0.4	-193	-464	-0.00005	-0.19	0	141	0	0
Drift D15	-2.5°/hr/g	0	-0.4	186	923	0.00006	0.20	0	850	0	0
Platform	+2.5°/hr/g	0	-0.8	4	-18	-0.00081	0	-0.02	-13	0	0
Drift D17	-2.5°/hr/g	0	0.8	-5	7	0.00083	0	0.02	33	0	0
Platform	+2.5°/hr/g	0	1.9	-13	-91	0.00019	-0.03	0.03	-40	0	0
Drift D18	-2.5°/hr/g	0	-2.0	12	101	-0.00017	0.03	-0.03	95	0	0
Atmosphere	+3 sigma	$0.259 \times 10^7$	-3.8	3	3	0	0.01	0	-3	0	0
	-3 sigma	$-0.263 \times 10^7$	4.6	7	0	0.00004	0.01	0.02	14	0	0.01
Tailwind	3 sigma	$-0.105 \times 10^7$	114.0	-36	209	0.00003	0.04	-0.11	256	0.04	0.23
Headwind	3 sigma	$0.140 \times 10^7$	-64.1	84	53	0.00009	0.04	0.07	-67	-0.02	-0.13
Left Crosswind	3 sigma	$0.346 \times 10^6$	25.0	-29	-2	0.00308	0	0.85	74	-0.09	0.05
Right Crosswind	3 sigma	$0.128 \times 10^6$	-28.0	51	130	0.00147	0.04	-0.62	122	0.07	-0.04
Centaur Initial	+10 deg	0	-1.7	0	16	0	0.02	0	22	0	0.01
Pitch Attitude	-10 deg	0	-1.4	2	-33	0	0.01	0	-26	0	-0.01
Centaur Initial	+10 deg	0	-5.4	5	27	0.00001	0.02	-0.06	26	0.01	0
Yaw Attitude	-10 deg	0	2.1	-2	2	0.00003	0	0.06	22	-0.01	0
Aerodynamic	+10%	$-0.330 \times 10^6$	-48.0	56	152	-0.00001	0.04	0.02	142	-0.01	-0.04
Forces	-10%	$0.329 \times 10^6$	49.0	32	38	0.00005	0.02	0	-19	0.01	0.04
RSS	Positive Dispersions	$0.314 \times 10^7$	263.4	599	2068	0.00403	0.74	1.16	4865	0.13	0.409
Values	Negative Dispersions	$0.325 \times 10^7$	225.8	566	3334	0.00277	0.64	1.00	3866	0.13	0.352
	Positive Deviations	$0.328 \times 10^7$	239.7	549	4406	0.00404	0.66	1.16	5280	0.13	0.397
	Negative Deviations	$0.312 \times 10^7$	250.9	599	4006	0.00037	0.73	1.00	349	0.13	0.360

Table 7-3. Computational Effects

Trajectory Simulation	$\int_{\circ}^{\text{SECO}} qv \, dt$ (lb/ft)	Injected Weight (lb)	Injection Radius (ft)	Apogee Radius (ft)	Orbital Inclination (deg)	Orbital Period (sec)	Long. of Ascending Node (deg)	$r_a - r_p$ (ft)	Latitude (deg)	Longitude (deg)
Nominal Engineering	51587883.	10965.9	23459213.	23460227.	34.996	6017.51	308.112	1018.	34.18	300.34
Nominal TRAK	Not Available	10965.0	23458795.	23460775.	34.995	6017.32	308.132	3203.	34.17	300.33
Computational Error (TRAK - ENG)	-	-0.9	-418.	548.	-0.001	-0.19	0.020	2185.	-0.01	-0.01

These analytically-determined errors were verified by simulation of a nominal trajectory with the cutoff time perturbed by 24 ms, and included in the summary table, 7-5.

## 7.7 GROSSLY PERTURBED INTERPRETIVE COMPUTER SIMULATION RESULTS

The results of four grossly perturbed interpretive computer simulations are shown in Table 7-4. These simulations verify the adequacy of the program scaling and the ability of the equations to guide to a reasonably satisfactory orbit under extremely perturbed conditions. The primary contributors to the orbital errors are the Centaur  $I_{sp}$  variations and the platform drift. Since all dispersions in these simulations are much worse than  $3\sigma$ , the results are considered satisfactory. The trajectory designations HIGH, LOW, LEFT, and RIGHT are given in Table 6-1.

## 7.8 HEATING DATA

Figures 7-5 and 7-6 show the heat flux ( $qv$ ) and the heat parameter ( $\int qv dt$ ) as functions of time from liftoff. These data show that the nominal and  $+3\sigma$  values at no time violate the heat limit indicator values also shown on both figures.

## 7.9 SUMMARY OF RESULTS

Table 7-5 summarizes the simulation results and gives the overall software performance evaluation. The data in this table is extracted from Tables 7-1 to 7-3 and Figures 7-1 to 7-3. The parameters tabulated are those used for the guidance equation performance evaluation. Also shown, for reference, are the acceptance criteria that were set for the AC-16 mission prior to recognition of the PU null effect on guidance cutoff accuracy. It is seen that the  $3\sigma$  value for  $\Delta(r_a - r_p)$  exceeds the acceptance criteria for that parameter by 0.22 n.mi. However, the software accuracy requirements are fulfilled well within the software specification numbers shown in the summary table. These specification numbers represent the target specification values adjusted to delete the hardware error contributions, the resultant being a specification value that guidance software must not violate.



Table 7-4. Grossly Perturbed I.C.S. Results

Deviation From Nominal Engineering Simulation									
Dispersed Trajectory	$\Delta$ Injection Weight (lb)	$\Delta$ Injection Radius (ft)	$\Delta$ Apogee Radius (ft)	$\Delta$ Orbital Inclination (deg)	$\Delta$ Orbital Period (sec)	$\Delta$ Ascending Node (deg)	$\Delta$ ( $r_a - r_p$ ) (ft)	$\Delta$ Latitude (deg)	$\Delta$ Longitude (deg)
Low Left	-484.0	-644	1531	0.032	-0.80	-2.925	7253	0.38	0.46
Low Right	-229.1	-669	3124	0.033	-0.98	2.743	11388	-0.21	0.88
High Right	201.1	-450	488	0.029	-0.62	2.556	4249	-0.39	-0.62
High Left	3.9	-446	-326	0.013	-0.66	-3.042	2823	0.13	-0.89

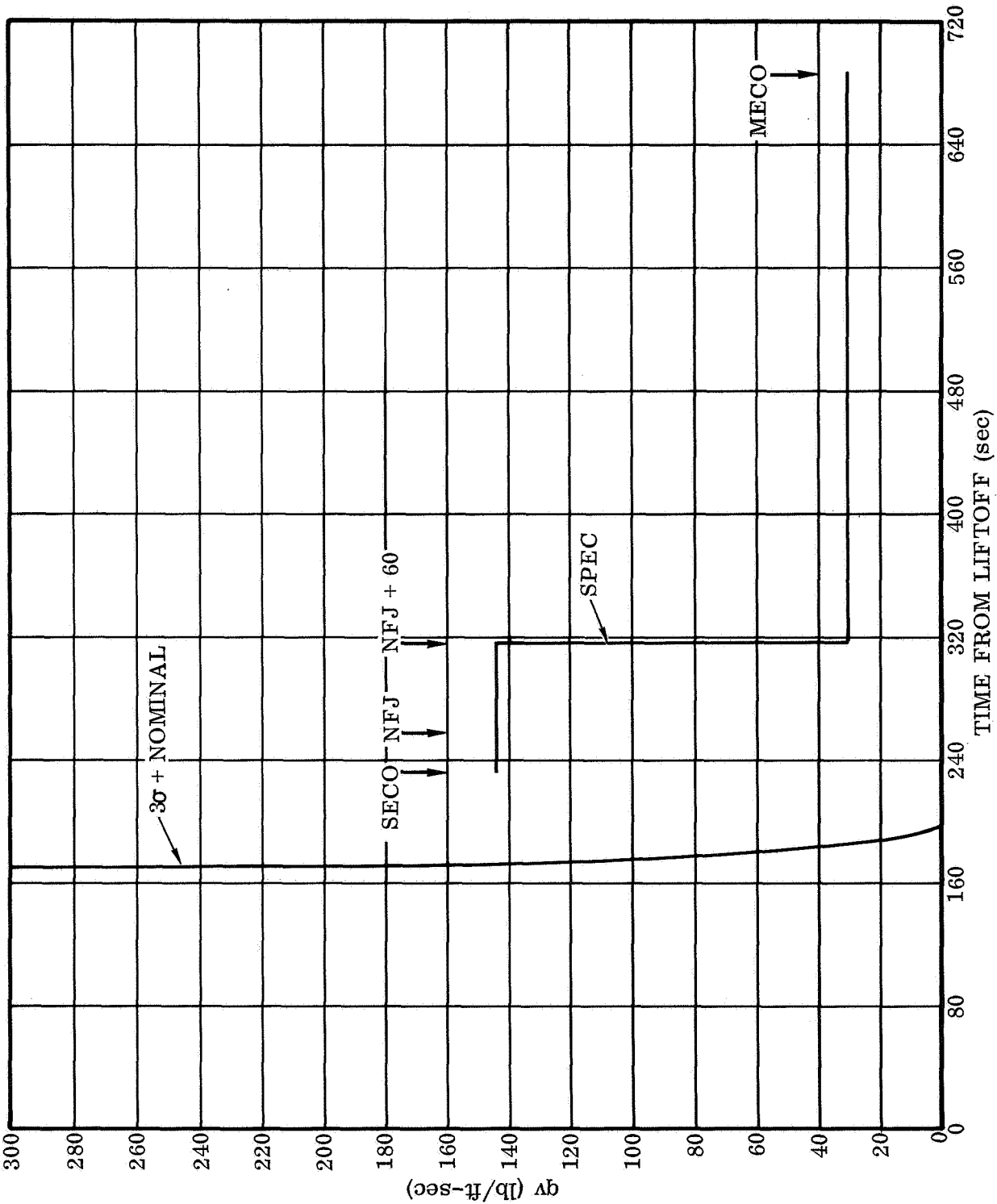


Figure 7-5. Heat Flux versus Time

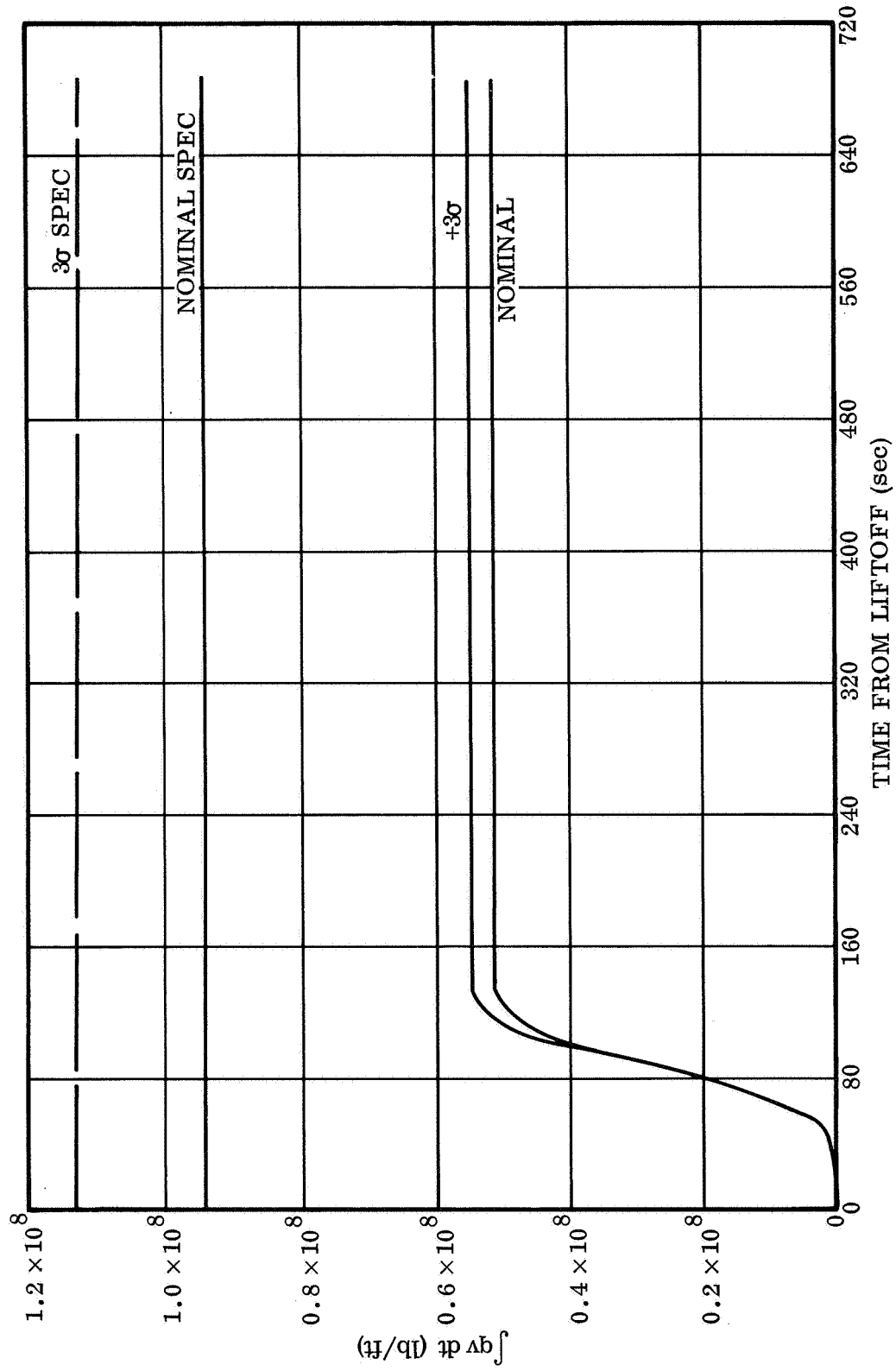


Figure 7-6. Heat Parameter versus Time

Table 7-5. Summary of Guidance Equation Performance Results

Parameter	Error Sources								Acceptance Criteria	Software Specification	
	Bias Errors			Variable Errors							
	Targeting	Computational	Sum	Non-nominal	Cutoff Steering	Velocity Noise	PU Null	RSS			
											RSS(1) ± Sum
Δ Injection Radius (n.mi.)	-0.04	-0.07	-0.11	0.10	0.03	0	0.01	0.105	0.22	0.5	4.9
Δ Orbit Inclination (deg)	-0.004	-0.001	-0.005	0.004	0	0	0	0.004	0.009	0.1	0.9
Δ Apogee Radius (n.mi.)	0.12	0.09	0.21	0.72	0.33	0.10	1.32	1.54	1.75	2.0	-
Δ (r <sub>a</sub> - r <sub>p</sub> ) (n.mi.)	0.18	0.36	0.54	0.87	0.60	0.10	1.32	1.68	2.22	2.0	14.0
Δ Injection Weight (lb)	(2)	-0.9	-0.9	250.9	1.1	0.1	1.6	250.9 235.7	251.8(3) 236.6(4)	254.2(3) 239.2(4)	239.2
Δ (∫ <sub>0</sub> <sup>SECO</sup> qv dt) (lb/ft)	0.516 × 10 <sup>8</sup>	0	0.516 × 10 <sup>8</sup>	0.328 × 10 <sup>7</sup>	0	0	0	0.328 × 10 <sup>7</sup>	0.549 × 10 <sup>8</sup>	1.13 × 10 <sup>8</sup>	1.13 × 10 <sup>8</sup>

NOTES: (1) Worst case combination tabulated.

(2) The closed loop nominal trajectory injection weight is the reference value for all weight deviations.

(3) Resulting RSS of negative weight deviations using a combined perturbation method for the sustainer jettison weight dispersion (129 lb deviation).

(4) Resulting RSS of negative weight deviations using the FPR analysis method for the sustainer jettison weight dispersion (96 lb deviation).

## SECTION 8

### GUIDANCE-AUTOPILOT EVENT COMPATIBILITY

Figures 8-1 through 8-5 illustrate the compatibility of the autopilot and guidance events as determined from guidance and trajectory simulation data and guidance and control systems requirements for AC-16 (Reference 4). The time ranges given for the guidance events are obtained from the results of the 3-sigma performance analysis and the targeted trajectory. A short discussion of each interfacing guidance and autopilot event follows.

#### 8.1 GUIDANCE AND AUTOPILOT BECO COMPATIBILITY

The guidance program issues BECO (L3 discrete) at an acceleration of  $5.7 \pm 0.113$  g's when the  $E_6$  test (see Figure A-4) is passed. The nominal time of occurrence of this guidance discrete for AC-16 is 152.90 seconds from 2-inch motion time with an uncertainty range of  $\pm 2.5$  seconds due to non-nominal performance and environmental parameters. Figure 8-1 illustrates the guidance and autopilot timing relationships for BECO.

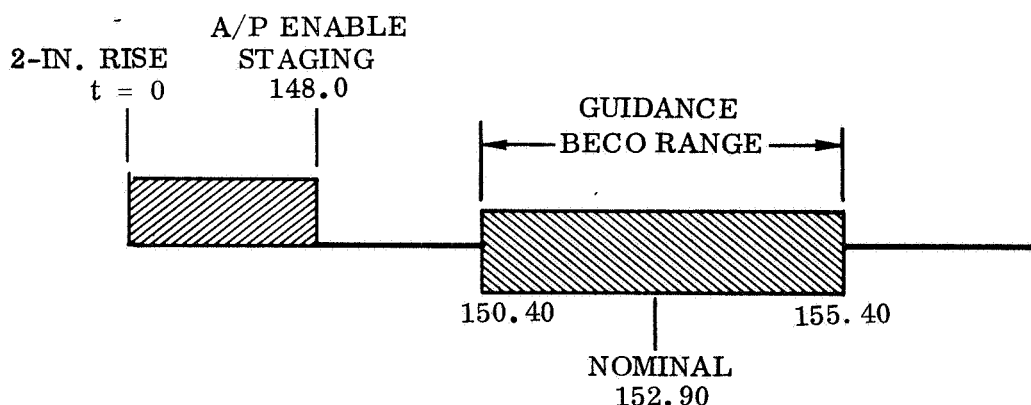


Figure 8-1. Guidance and Autopilot BECO Compatibility

## 8.2 GUIDANCE AND AUTOPILOT SECO-BACKUP COMPATIBILITY

The inflight program will issue a SECO backup discrete (L6) upon sensing acceleration decay in the sustainer phase ( $E_g$  test, Figure A-6). SECO occurs nominally at 81.8 seconds after BECO with an uncertainty of  $\pm 7.0$  seconds due to non-nominal performance and environmental parameters. Since the guidance-computed acceleration quantity is an aged quantity because of cycle time lags, the decaying acceleration will be sensed 3.45 to 8.20 seconds after SECO. This variation in the time of issuing the guidance discrete is due to the 3.07-second computer cycle length. The SECO backup discrete will, therefore, be issued between 78.25 and 97.0 seconds as exemplified by Figure 8-2.

It should be emphasized that the L6 discrete cannot cause SECO to occur. Its purpose is to start the upper stage timer and to switch the guidance equations to the Centaur phase.

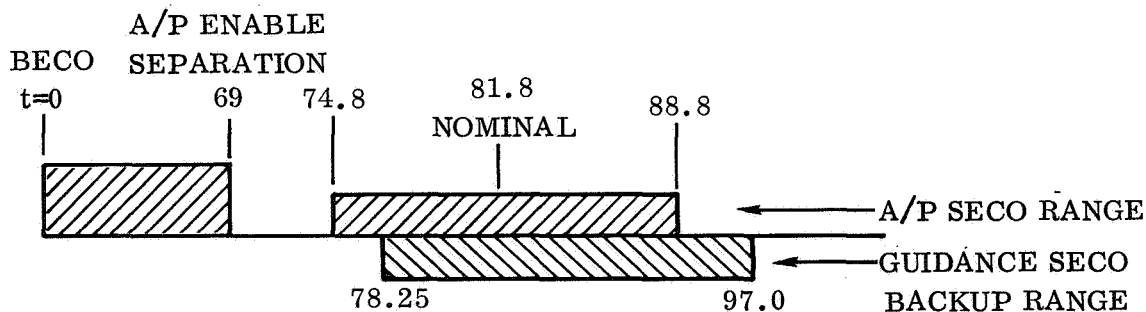


Figure 8-2. Guidance and Autopilot SECO Backup Compatibility

## 8.3 GUIDANCE AND AUTOPILOT MECO COMPATIBILITY

The guidance computer will issue a MECO discrete (L16) upon counting down the time-to-go ( $\Delta t_{co}$ ) extrapolated by the guidance equations after passing the time-to-go test ( $J_{55}$ , Figure A-5). The MECO discrete will occur nominally at 451.3 seconds after SECO with a 3-sigma uncertainty of  $\pm 8.7$  seconds. The guidance MECO discrete can therefore occur between 442.6 and 460.0 seconds after SECO. The autopilot Enable-

MECO discrete is given at 400 seconds after SECO. The guidance and autopilot MECO relationships are exemplified by Figure 8-3.

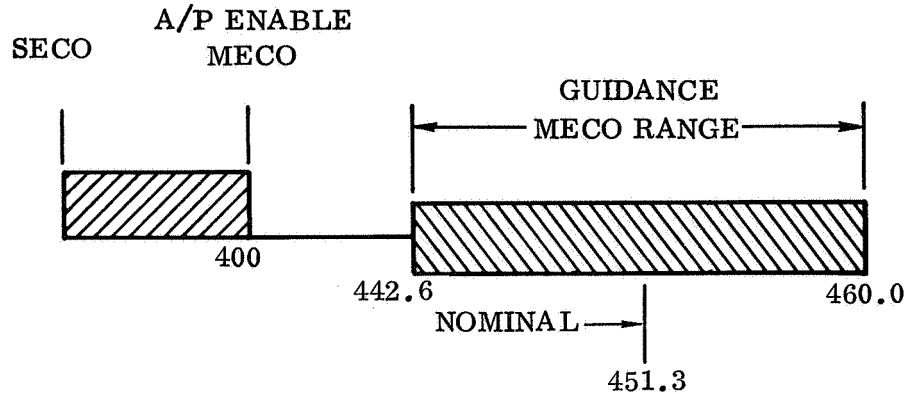


Figure 8-3. Guidance and Autopilot MECO Compatibility

#### 8.4 GUIDANCE AND AUTOPILOT PU NULL COMPATIBILITY

The guidance computer issues a PU null discrete (L0) at a guidance-predicted time-to-go of  $15 \pm 2.2$  seconds. The uncertainty of  $\pm 2.2$  seconds is due to the 4.4-second compute cycle. In addition to this uncertainty, the time of issuing the L0 discrete relative to SECO will also vary as MECO time. Therefore the PU null discrete will occur nominally at 436.3 after SECO with a 3-sigma uncertainty of  $\pm 10.9$  seconds. The L0 discrete is enabled by the autopilot at 314.5 seconds after SECO. Figure 8-4 exemplifies the relationship between guidance and autopilot PU null events.

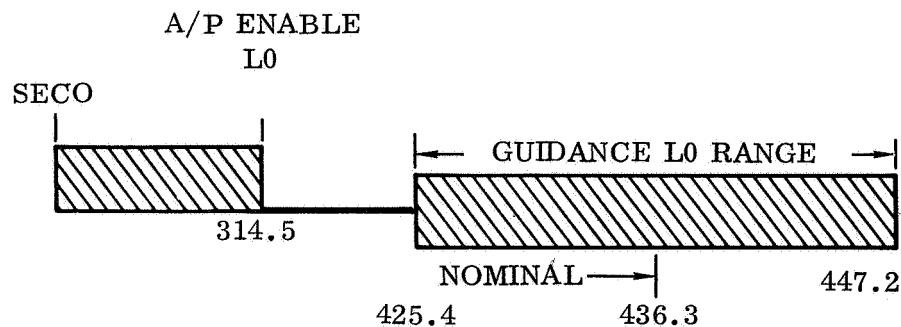


Figure 8-4. Guidance and Autopilot PU Null Compatibility

## 8.5 GUIDANCE AND AUTOPILOT REORIENT COMPATIBILITY

Guidance issues two attitude reference vectors for the reorient sequence, each of which occurs at fixed times from MECO.

The spacecraft separation attitude vector is issued on the first cycle after MECO. Therefore it will be initially output from 0 to 2.2 seconds after MECO. The 2.2-second possible delay corresponds to the compute cycle length in the post-injection phase.

The attitude vector for the vehicle retrothrust is issued by guidance nominally at 356 seconds after MECO. The compute cycle introduces an uncertainty in this time of  $\pm 1.2$  seconds. Therefore this vector can be initially output at MECO+354.8 to MECO+357.2. Figure 8-5 exemplifies the post-injection sequence.

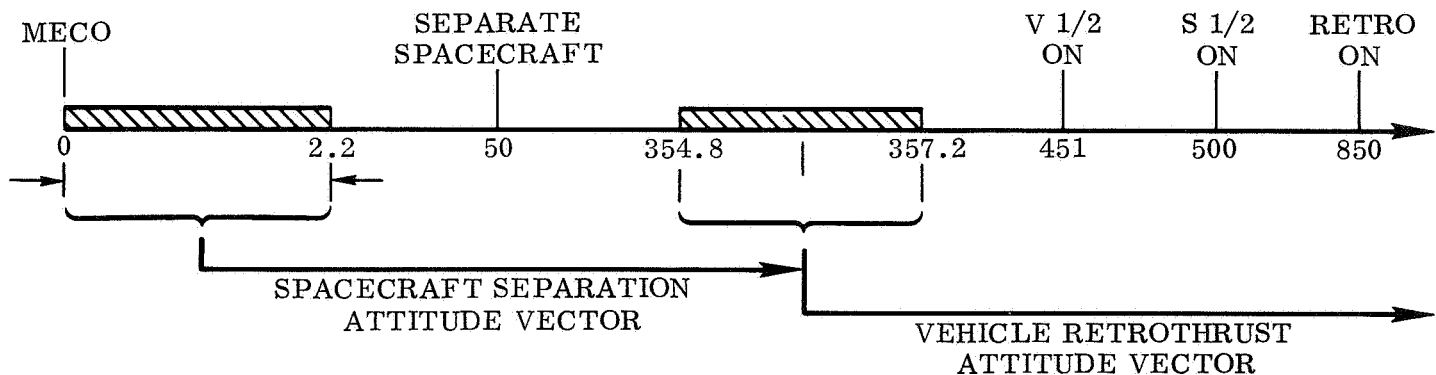


Figure 8-5. Guidance and Autopilot Reorient Compatibility

## 8.6 COMPATIBILITY OF DOGLEG MANEUVER AND FAIRING JETTISON TIMES

The guidance equations are required to provide a constant attitude steering vector from MES until the nose fairings are out of range of impact with vehicle and payload. This period is from MES until MES+16 seconds, allowing 4 seconds for fairing clearance of the vehicle.



Since both MES and fairing jettison times are relative to SECO (start upper stage timer), the start of the dogleg maneuver must also be referenced to SECO. This is accomplished by the guidance  $E_8$  test (see Figure A-7) which senses the SECO decay thus providing a SECO time reference for initiating dogleg steering.

In the nominal case, the upper stage timer is started by the autopilot SECO discrete, followed by guidance-sensing of SECO occurrence within the uncertainty range given in Section 8.2. The start of the dogleg maneuver therefore has the same uncertainty in the nominal case as the time of the L6 guidance discrete.

In the case where the guidance L6 discrete starts the upper stage timer (i.e., a failure mode), all post-SECO events are timed relative to the L6 discrete. In this case, the uncertainty in the time of starting the dogleg maneuver is a function of guidance cycle time only.

The  $E_{yaw}$  time test (Figure A-10) which allows dogleg steering is initialized by a constant,  $J_{40}$ , representing the elapsed time from the start of the upper stage timer for this event. This constant has been selected so that the initiation of the dogleg maneuver satisfies the design requirements for both nominal and backup SECO (start upper timer) cases.

The compatibility of guidance and autopilot sequences relative to fairing jettison and enable dogleg times is illustrated by Figure 8-6. The nominal time of guidance enabling dogleg steering is 35.4 seconds relative to the start of the upper stage timer. Cycle time lags and consideration of a SECO backup sequence account for the uncertainty range. It is seen that the earliest time for initiating dogleg steering is 5 seconds after fairing jettison time, which satisfies the design constraint of 4 seconds.

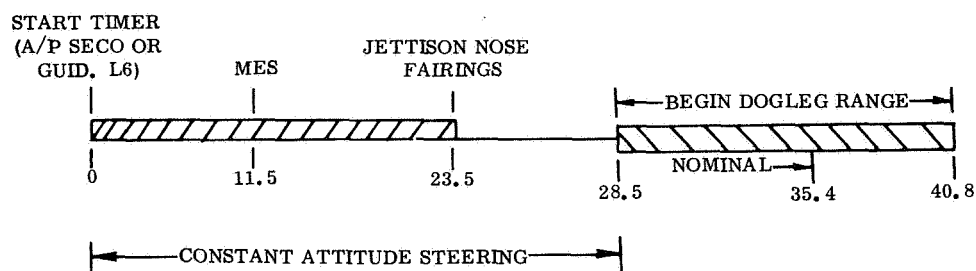


Figure 8-6. Compatibility of Dogleg Maneuver and Fairing Jettison Times

SECTION 9  
REFERENCES

1. Approximations for Digital Computers; Cecil Hastings, Jr.; Princeton University Press, Princeton, N. J., 1955.
2. OAO Target Specification, NASA T.D. No. CPO 250, 18 June 1968.
3. Centaur Configuration, Performance, and Weight Status Report, GDC63-0495-53, June 1968.
4. Guidance and Control System Requirements, Atlas-Centaur 16, AY63-0071-16, Revision B, 27 June 1968.
5. Atlas SLV-3C/Centaur Error Sources and Trajectory Dispersion Simulation Data, GDC-BKM67-043, 15 December 1967.
6. Analysis of Guidance MECO Error Sources for Atlas/Centaur Missions, GDC-BKM68-030, 15 June 1968.
7. Design Criteria and Requirements Document, Atlas/Centaur OAO-A2 Mission, GDC-BTD-67-098-4, Revision D, 22 April 1968.
8. AC-17 Final Guidance Equations and Performance Analysis, GDC-BKM68-020, June 1968.
9. AC-17 Airborne Computer Preflight Program for the Centaur Inertial Guidance System, GDC-BKM68-042, 1 July 1968.

APPENDIX A  
GUIDANCE EQUATION FLOW DIAGRAMS FOR AC-16

<u>Figure</u>		<u>Page</u>
A-1	Explicit Equation Modular Blocks	A-2
A-2	Initialization	A-3
A-3	Initialization, Contd	A-4
A-4	Navigation Equations	A-5
A-5	Coordinate System Equations	A-6
A-6	Booster Logic	A-7
A-7	Sustainer-Centaur Logic	A-8
A-8	Time-to-go Equations	A-9
A-9	Pitch Steering Coefficients	A-10
A-10	Yaw Steering Coefficients	A-11
A-11	Steering Equations	A-12
A-12	Parking Orbit Equations	A-13
A-13	Post-Injection Equations	A-14

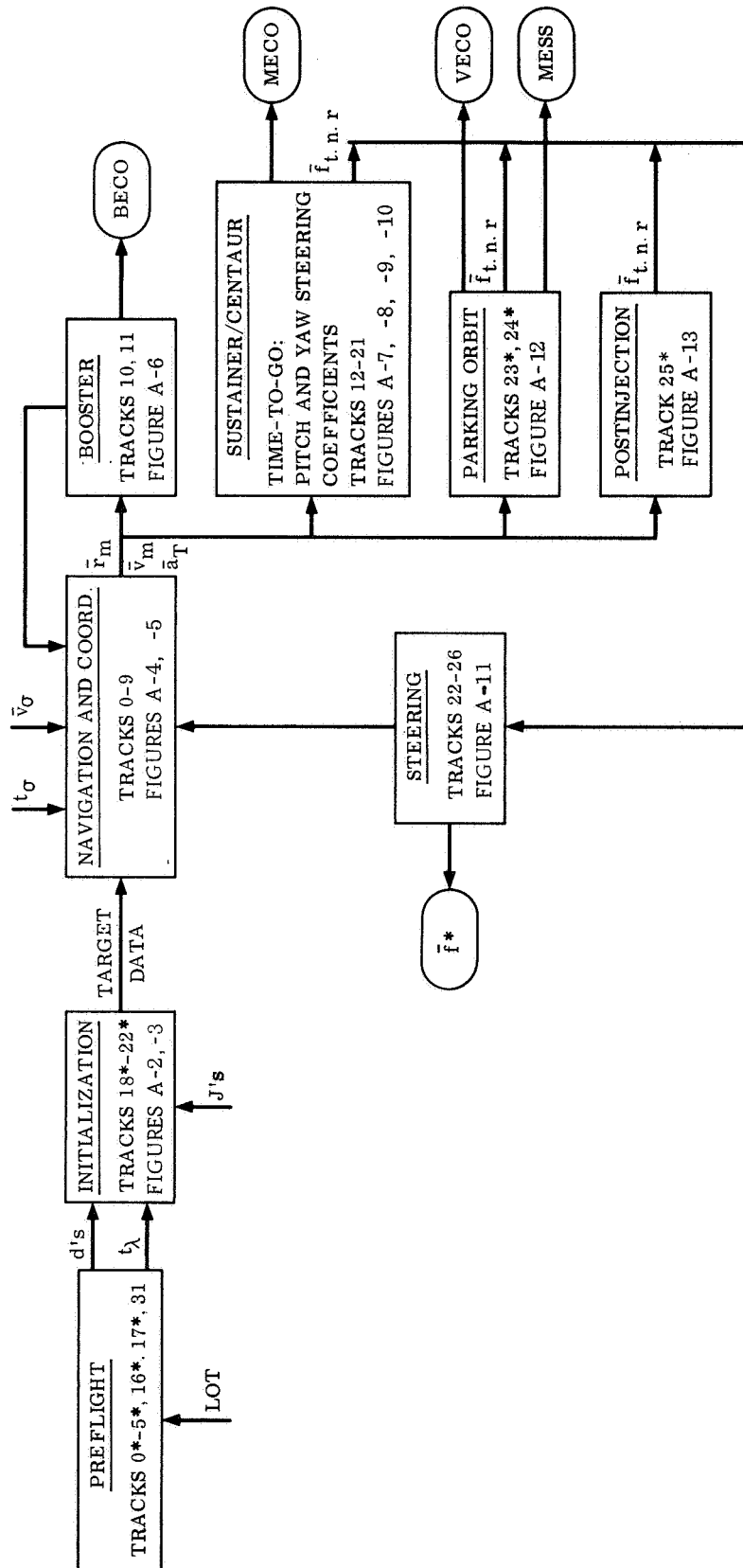


Figure A-1. Explicit Equation Modular Blocks

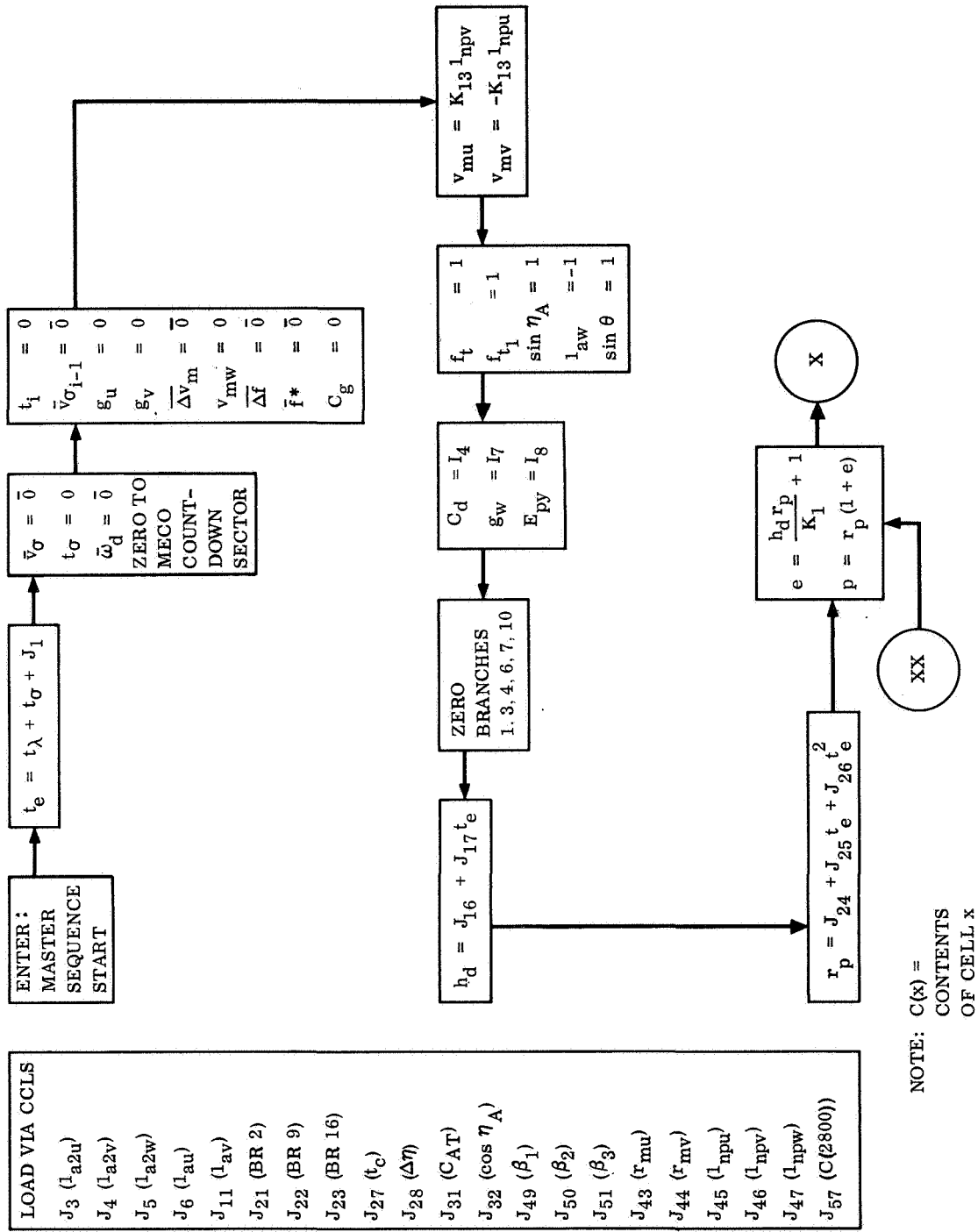


Figure A-2. Initialization

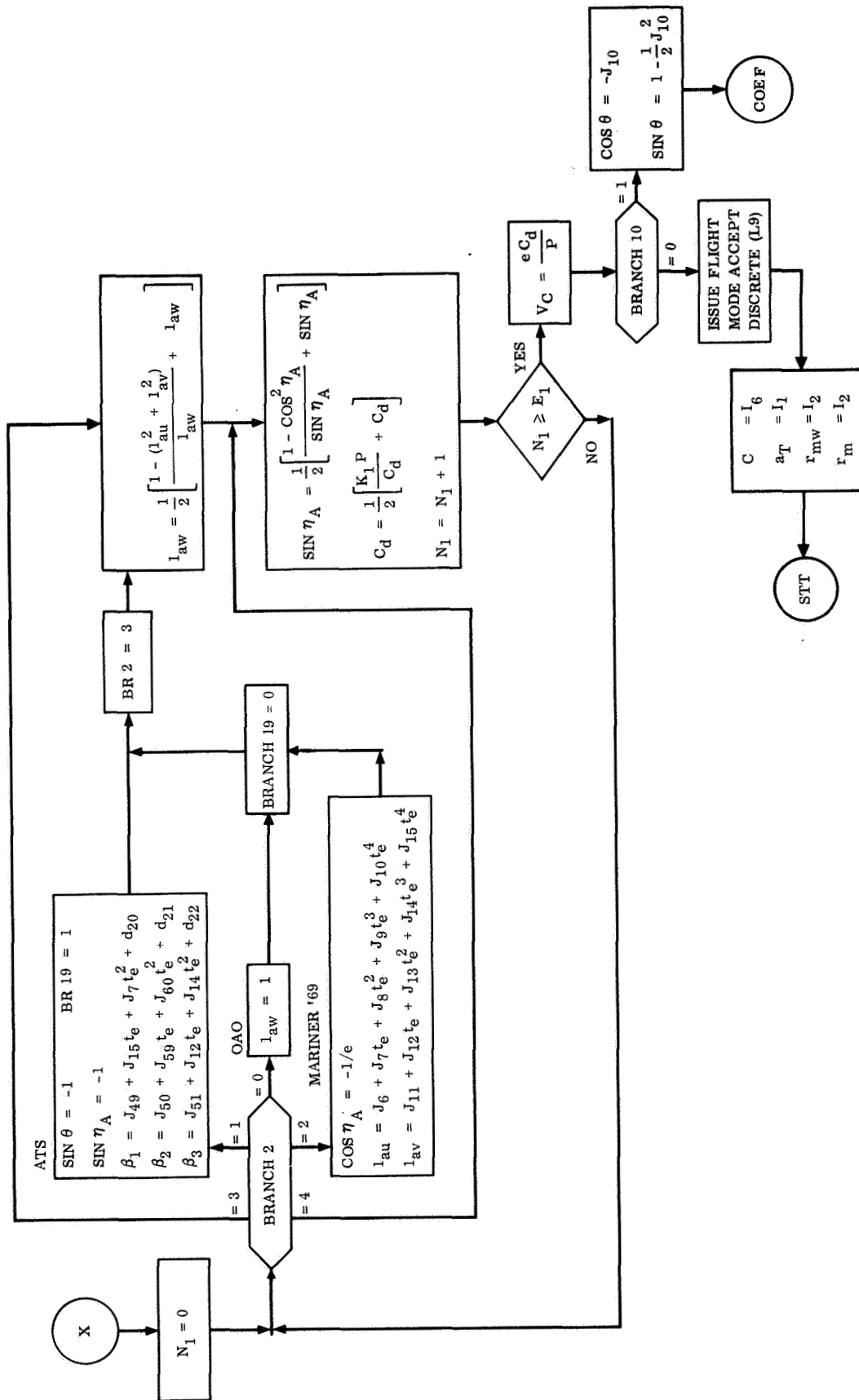


Figure A-3. Initialization, Contd

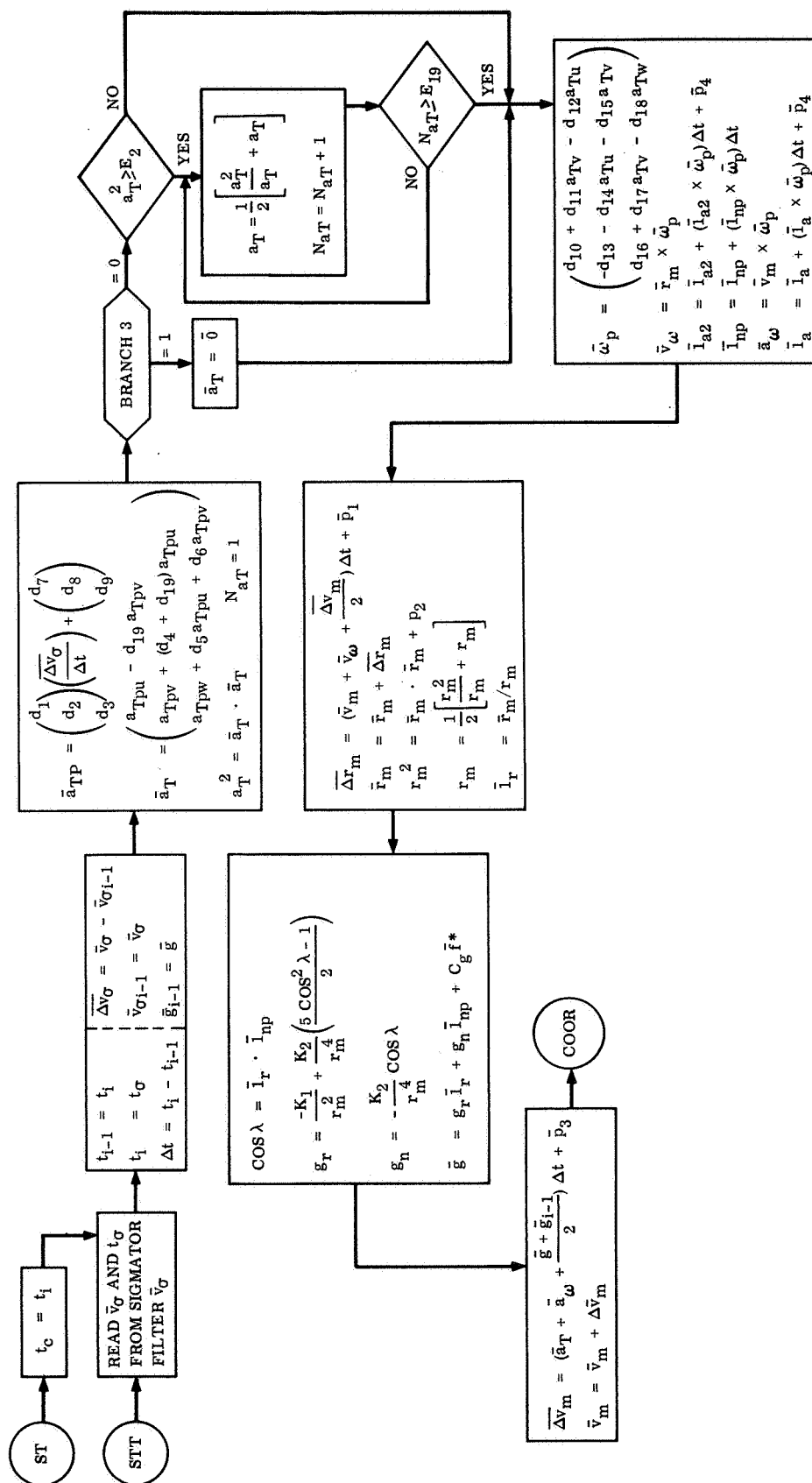


Figure A-4. Navigation Equations

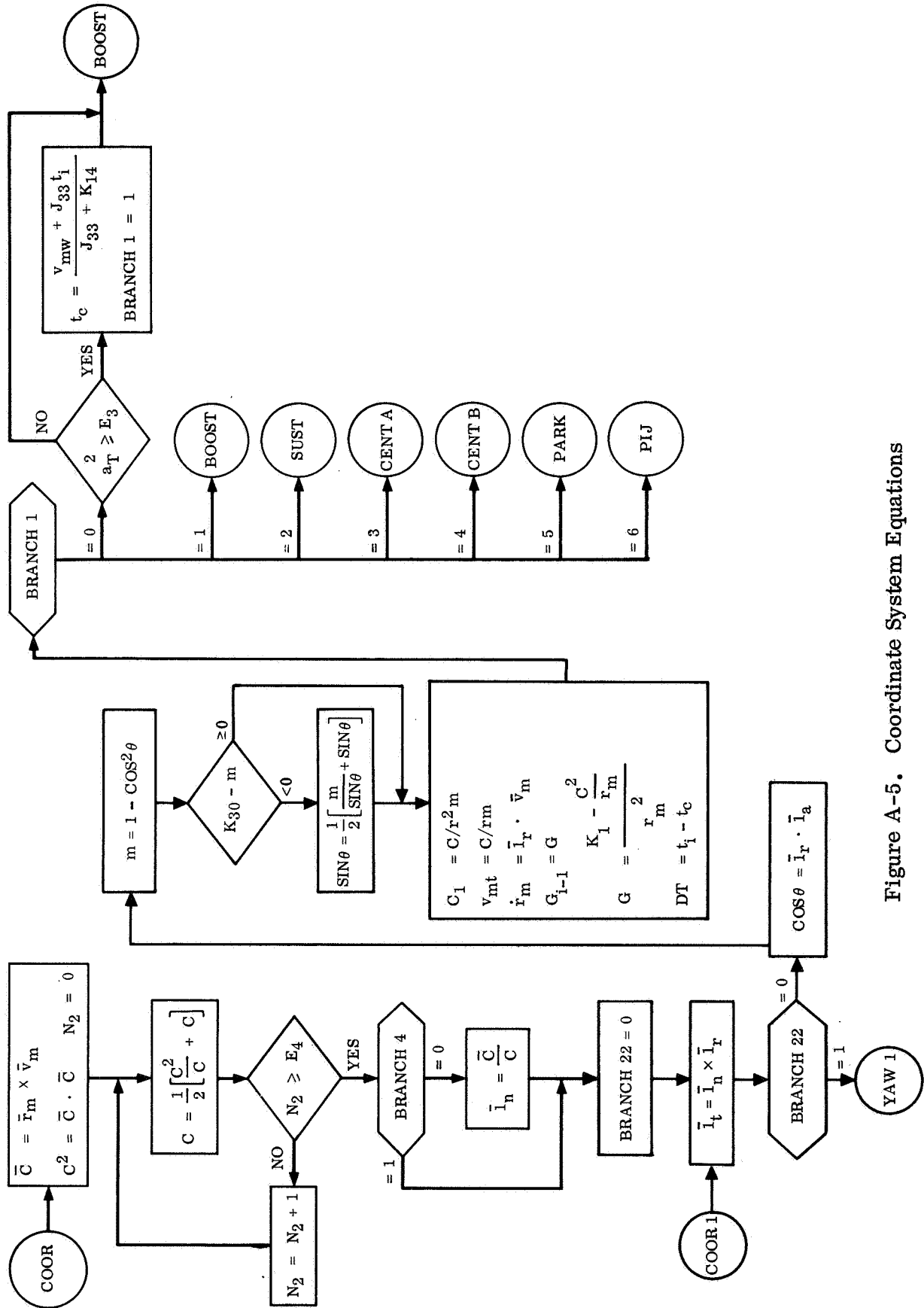


Figure A-5. Coordinate System Equations



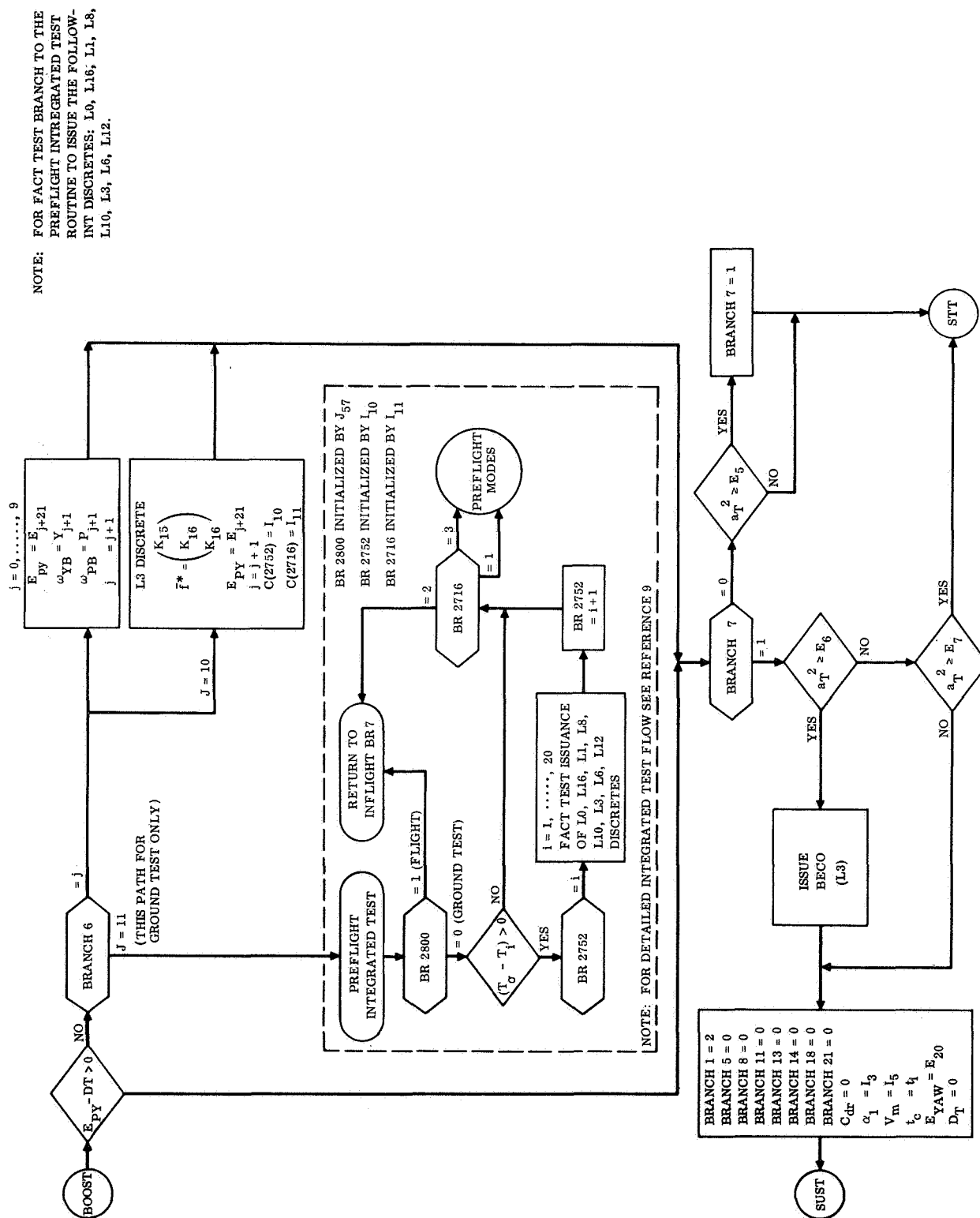


Figure A-6. Booster Logic

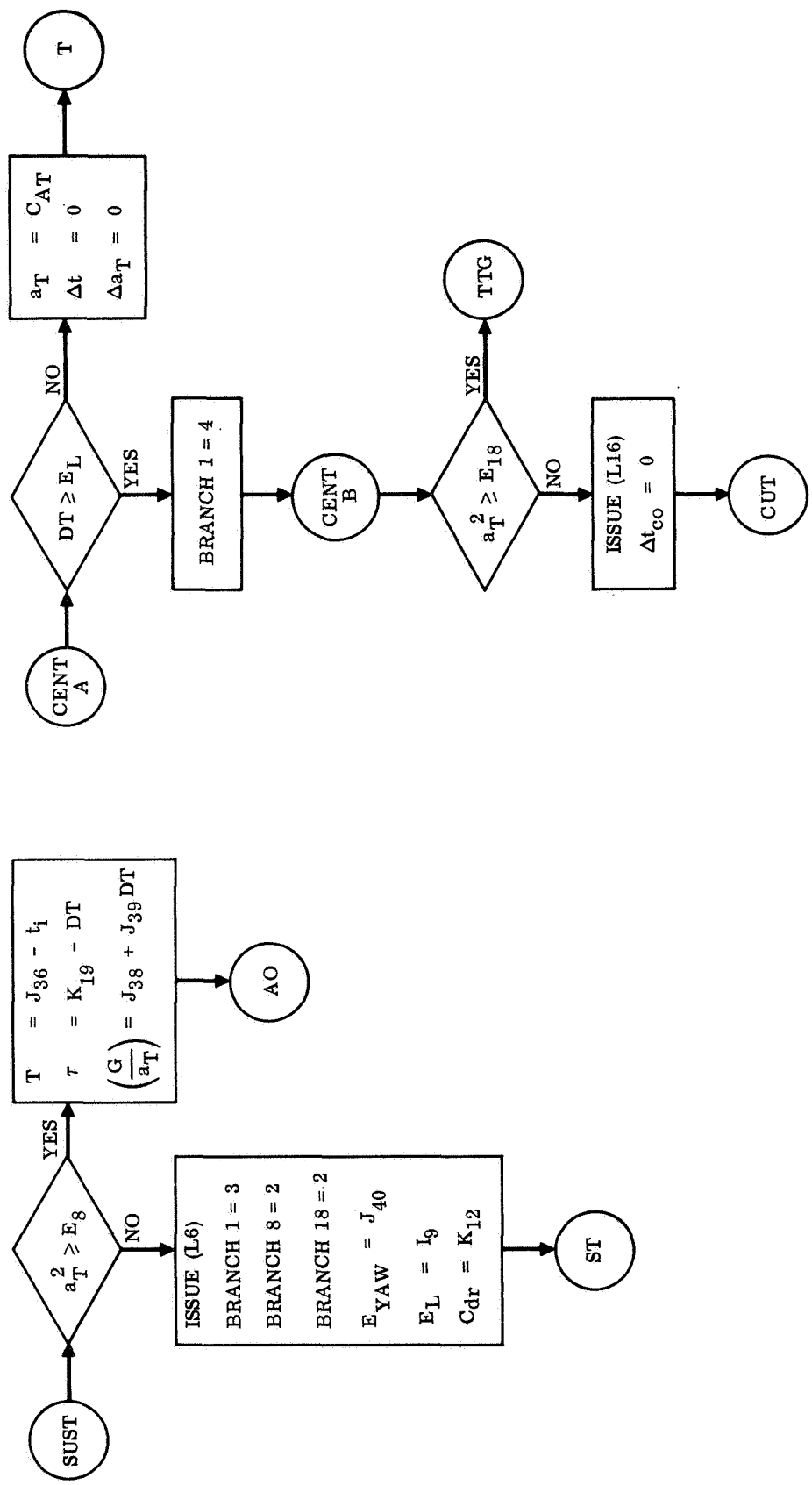


Figure A-7. Sustainer-Centaur Logic



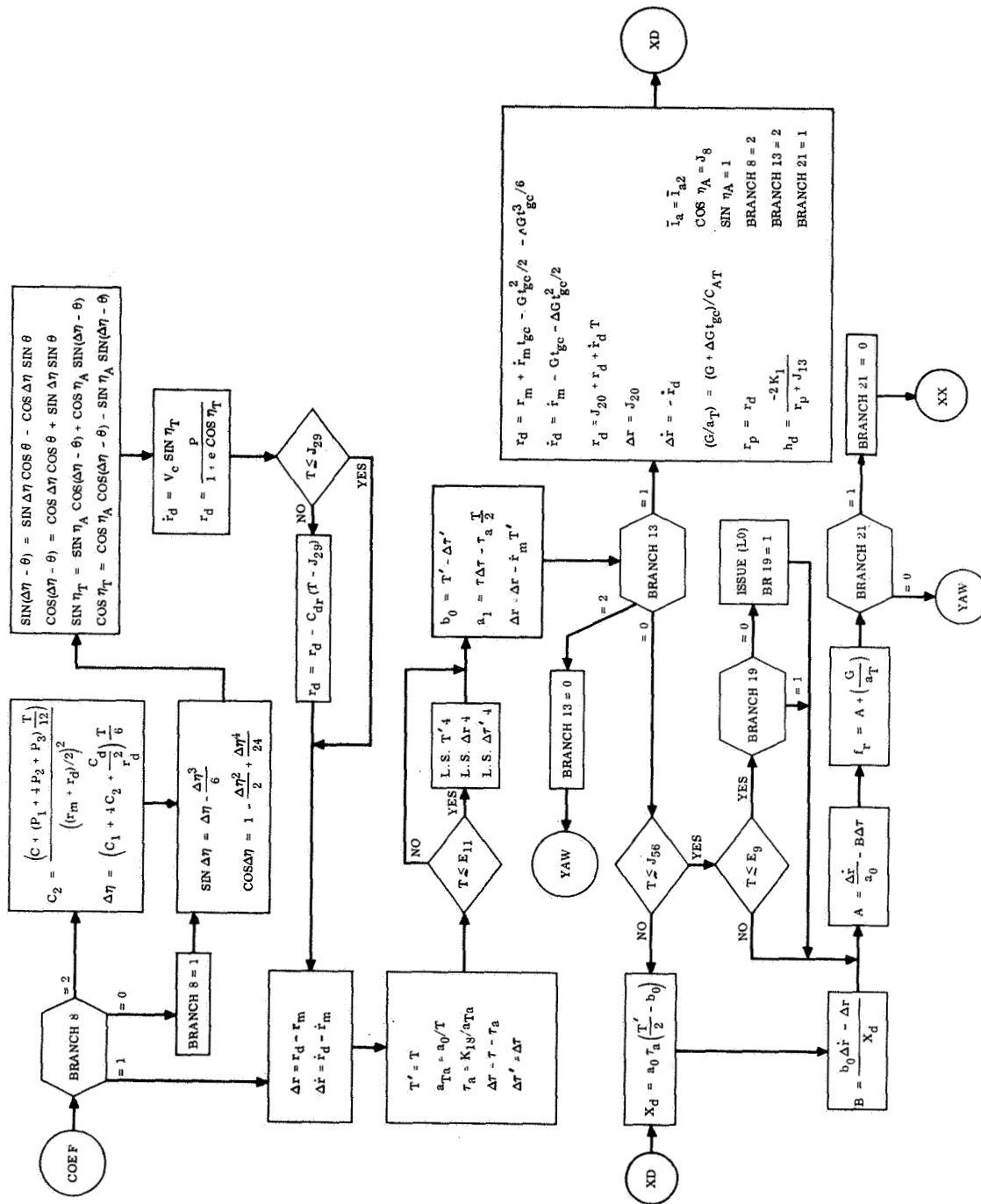


Figure A-9. Pitch Steering Coefficients

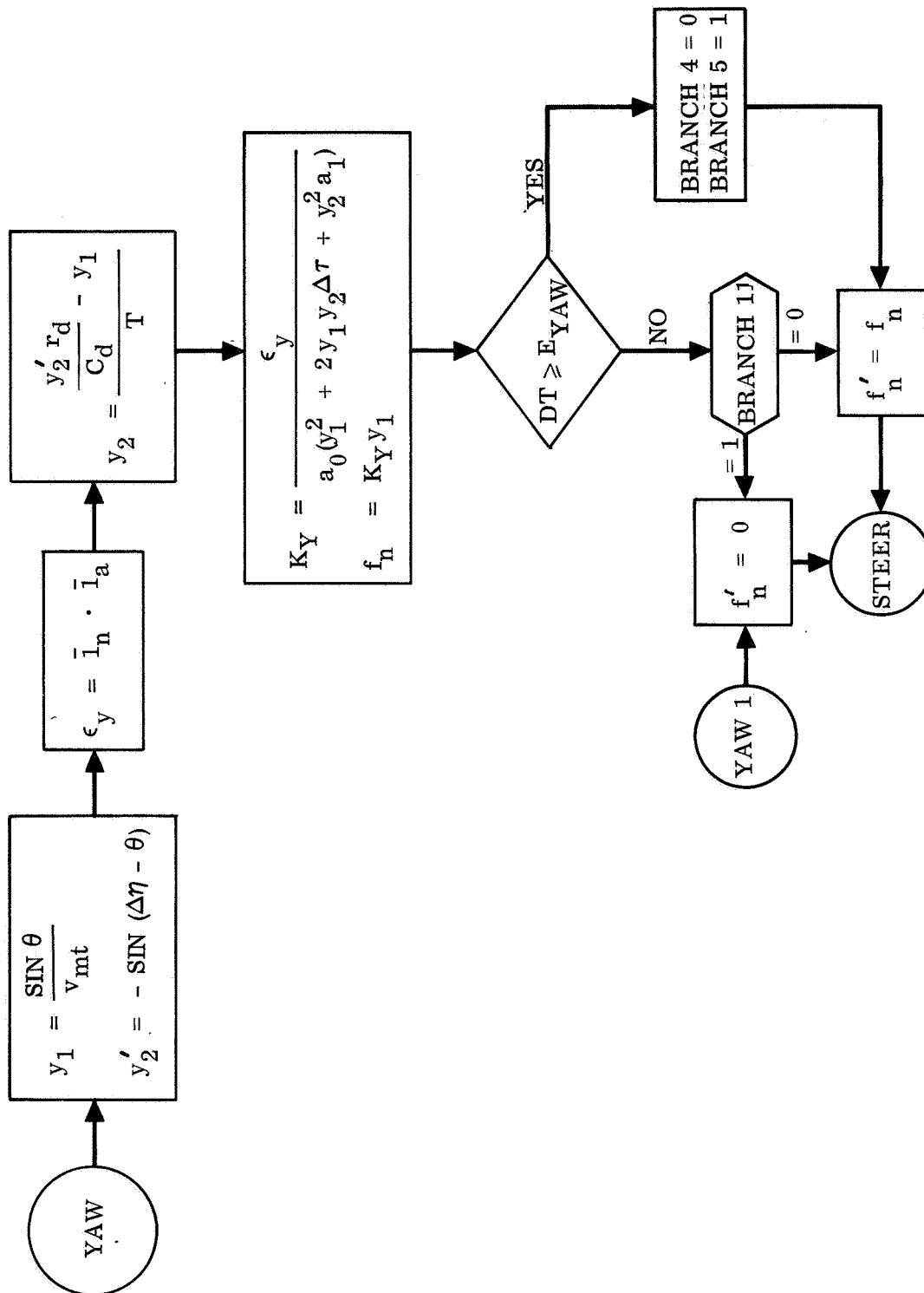


Figure A-10. Yaw Steering Coefficients

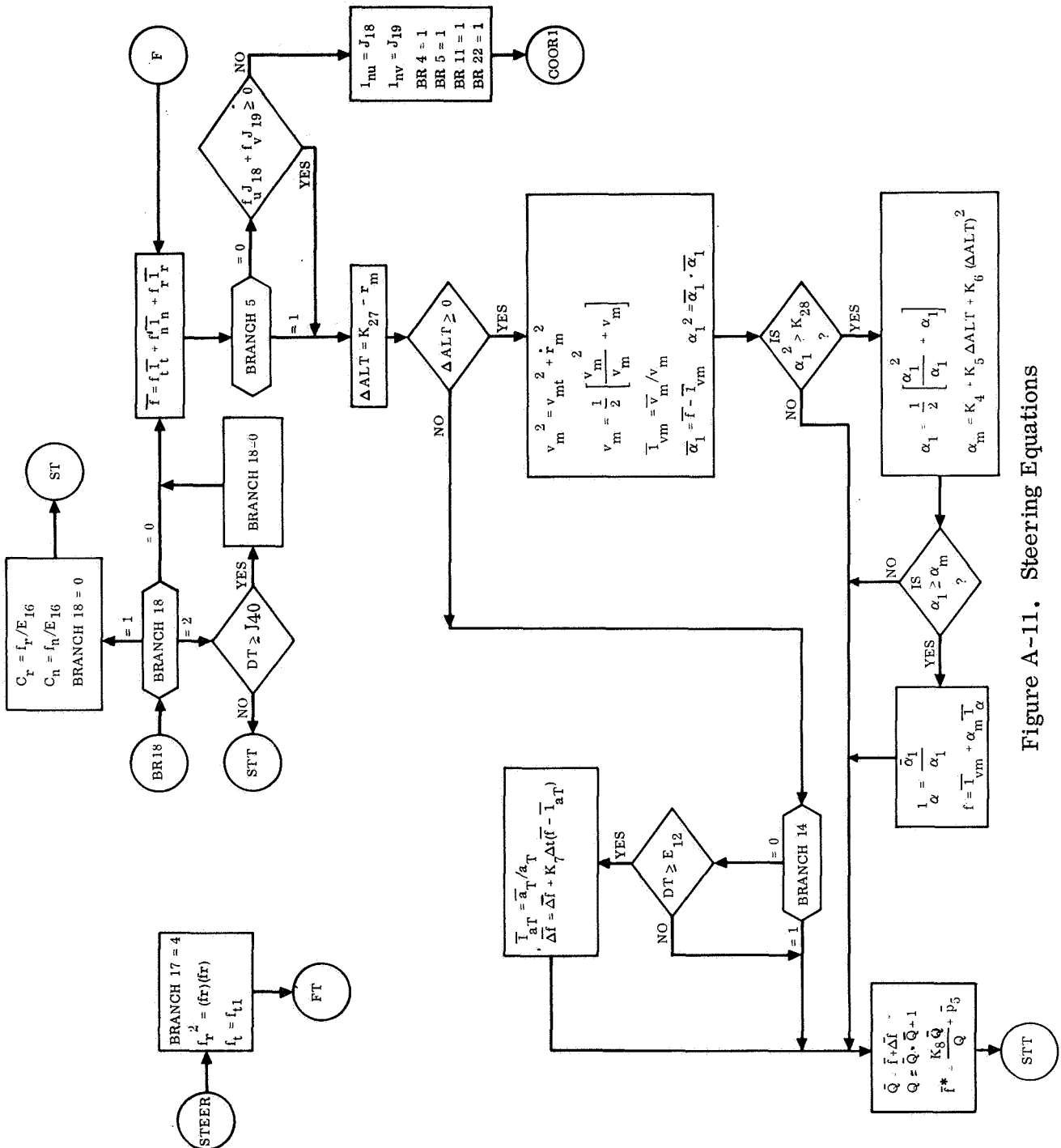


Figure A-11. Steering Equations

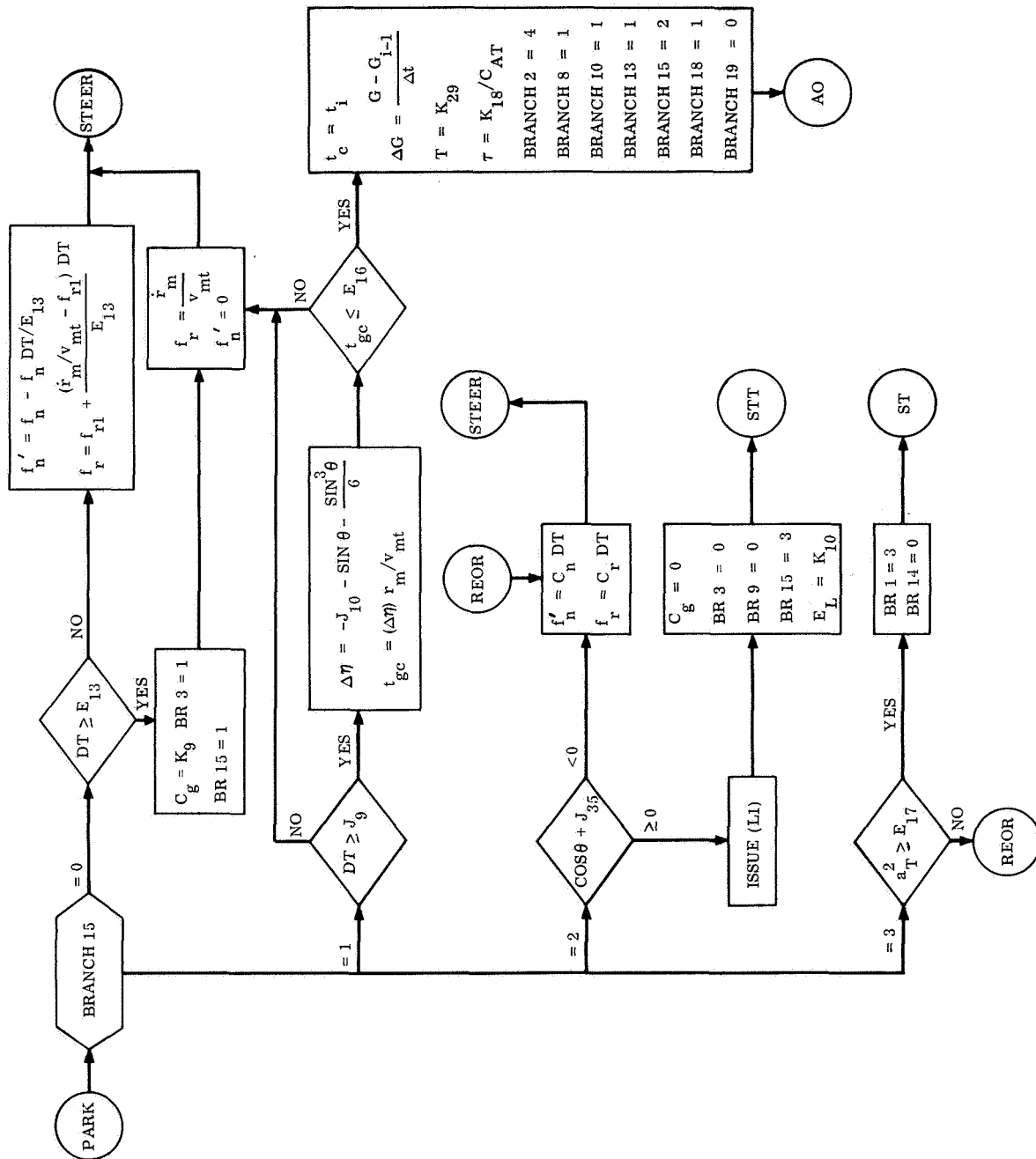


Figure A-12. Parking Orbit Equations

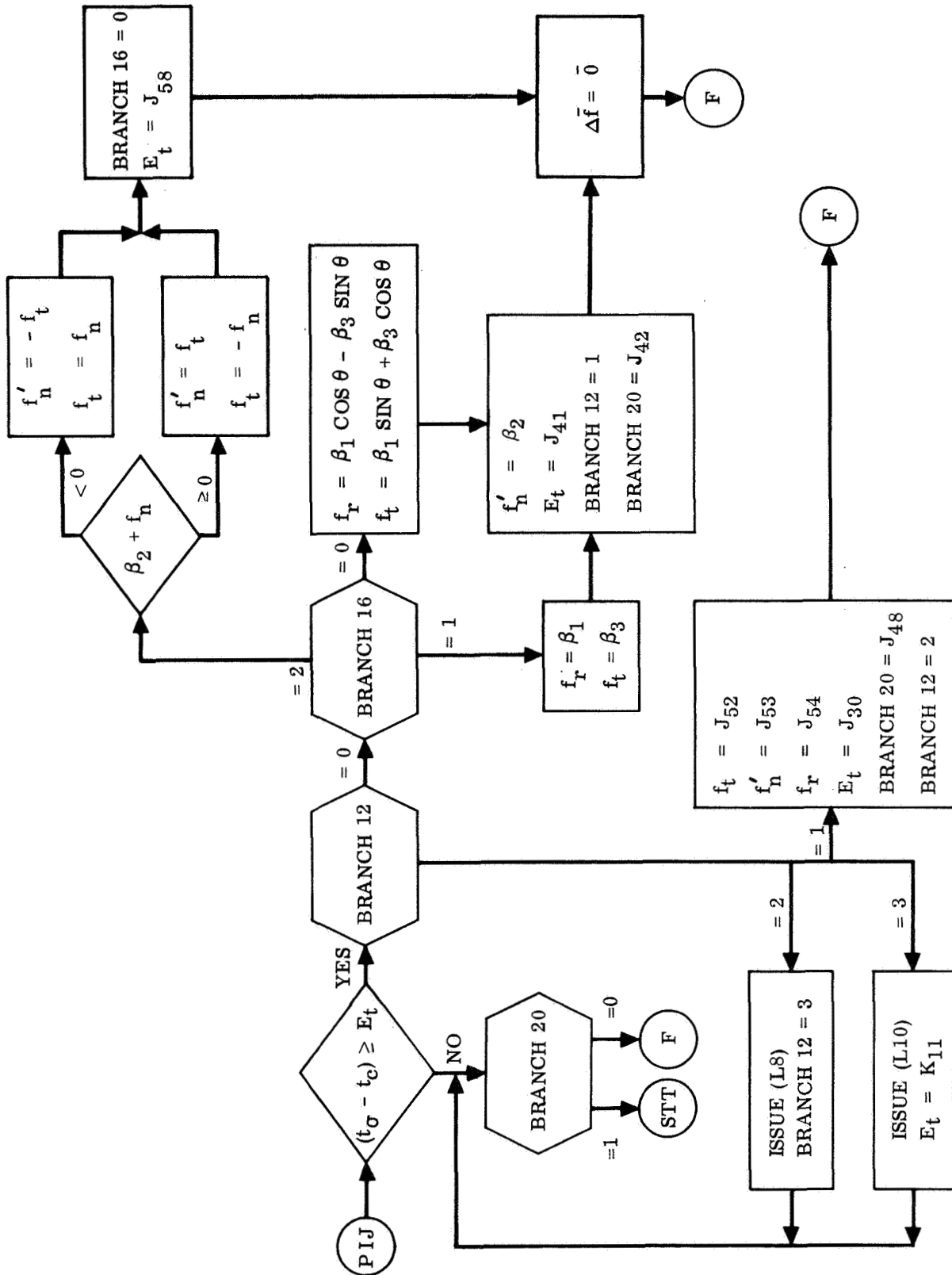


Figure A-13. Post-Injection Equations



APPENDIX B  
GUIDANCE CONSTANTS

Table B-1	Switching Constants . . . . .	B-2
Table B-2	Initialization Constants . . . . .	B-4
Table B-3	Equation Input Constants . . . . .	B-5
Table B-4	Definition of J Constants . . . . .	B-8

Table B-1. Switching Constants

Constant	Value	Units	Scale Factor	Definition
E <sub>1</sub>	10.	none	16.	Iteration counter for initialization square roots.
E <sub>2</sub>	480.	(ft/sec <sup>2</sup> ) <sup>2</sup>	270400.	Acceleration test for $ \bar{a}_T $ computation.
E <sub>3</sub>	1300.	(ft/sec <sup>2</sup> ) <sup>2</sup>	270400.	Acceleration test for 2 in. motion computation.
E <sub>4</sub>	2.	none	32768.	Iteration counter for $ \bar{c} $ computation.
E <sub>5</sub>	10000.	(ft/sec <sup>2</sup> ) <sup>2</sup>	270400.	BECO enable acceleration.
E <sub>6</sub>	28500	(ft/sec <sup>2</sup> ) <sup>2</sup>	270400.	BECO acceleration.
E <sub>7</sub>	2500.	(ft/sec <sup>2</sup> ) <sup>2</sup>	270400.	Booster-sustainer equation switching acceleration.
E <sub>8</sub>	550.	(ft/sec <sup>2</sup> ) <sup>2</sup>	270400.	SECO backup acceleration.
E <sub>9</sub>	20.8	sec	806.59692	Time to go for LO (PU null) discrete.
E <sub>10</sub>	4.	none	16.	Iteration counter for $f_t$ computation.
E <sub>11</sub>	50.	sec	806.59692	Time to go for steering coefficient rescaling.
E <sub>12</sub>	30.	sec	12905.551	Time lock out for integral control.
E <sub>13</sub>	78.	sec	12905.551	Time from MECO I to VECO.

Table B-1. Switching Constants, Contd

Constant	Value	Units	Scale Factor	Definition
E <sub>14</sub>	not used	—	—	
E <sub>15</sub>	not used	—	—	
E <sub>16</sub>	600.	sec	806.59692	Time to go to MES II to begin second burn reorient.
E <sub>17</sub>	400.	(ft/sec <sup>2</sup> ) <sup>2</sup>	270400.	Acceleration level for switching from parking orbit to second burn equations.
E <sub>18</sub>	100.	(ft/sec <sup>2</sup> ) <sup>2</sup>	270400.	MECO backup acceleration.
E <sub>19</sub>	3.	none	256.	Iteration counter for $ \bar{a}_T $ square root.
E <sub>20</sub>	200.	sec	12905.551	Time from BECO to begin dog-leg maneuver.
E <sub>21</sub>	21.9	sec	12905.551	} Booster steering switching times.
E <sub>22</sub>	41.9	sec	12905.551	
E <sub>23</sub>	46.9	sec	12905.551	
E <sub>24</sub>	56.9	sec	12905.551	
E <sub>25</sub>	71.9	sec	12905.551	
E <sub>26</sub>	75.9	sec	12905.551	
E <sub>27</sub>	83.9	sec	12905.551	
E <sub>28</sub>	99.9	sec	12905.551	
E <sub>29</sub>	126.9	sec	12905.551	

Table B-1. Switching Constants, Contd

Constant	Value	Units	Scale Factor	Definition
E <sub>30</sub>	167.	sec	12905.551	Time for outputting ground test steering vector.
E <sub>31</sub>	222.	sec	12905.551	Time for branching to Integrated Test routine for ground tests.

Table B-2. Initialization Constants

Constant	Value	Units	Scale Factor	Definition
I <sub>1</sub>	36.	ft/sec <sup>2</sup>	520.	$ \bar{a}_T $
I <sub>2</sub>	20909819.	ft	42288909.	r <sub>m</sub> , r <sub>mw</sub>
I <sub>3</sub>	0.5	none	2.	Angle of attack
I <sub>4</sub>	$0.6 \times 10^{12}$	ft <sup>2</sup> /sec	$0.22171567 \times 10^{13}$	Desired angular momentum
I <sub>5</sub>	10000.	ft/sec	52428.8	Relative velocity
I <sub>6</sub>	$0.3 \times 10^{11}$	ft <sup>2</sup> /sec	$0.22171567 \times 10^{13}$	Angular momentum
I <sub>7</sub>	-32.176	ft/sec <sup>2</sup>	130.	g <sub>wi-1</sub>
I <sub>8</sub>	11.9	sec	12905.551	Booster switching constant
I <sub>9</sub>	23.5	sec	12905.551	Steering time lockout from SECO
I <sub>10</sub>	27 17 38 15 6	-	-	} Instructions for use in the Integrated Test routine
I <sub>11</sub>	10 20 17 57 7	-	-	

Table B-3. Equation Input Constants

Constant	Value	Units	Scale Factor	Definition
$K_1$	$0.14076471 \times 10^{17}$	$\text{ft}^3/\text{sec}^2$	$0.11624286 \times 10^{18}$	Gravitational constant
$K_2$	$0.20012690 \times 10^{29}$	$\text{ft}^5/\text{sec}^2$	$0.25985391 \times 10^{32}$	Gravitational- oblateness constant
$K_3$	5.	$\text{ft}/\text{sec}^2$	520.	Change in acceleration from MECO I to MES II
$K_4$	0.58580684	none	8.	Angle of attack con- straint polynomial coefficients
$K_5$	$-0.84494017 \times 10^{-5}$	1/ft	$0.24214387 \times 10^{-4}$	
$K_6$	$0.44423320 \times 10^{-10}$	$1/\text{ft}^2$	$0.73292068 \times 10^{-10}$	
$K_7$	0.04	1/sec	0.1586914	Integral gain
$K_8$	0.81851792	none	2.	Steering gain
$K_9$	0.03284	$\text{ft}/\text{sec}^2$	130.	Nominal ullage acceleration
$K_{10}$	0.	sec	12905.551	Steering lockout at MES II
$K_{11}$	12900.	sec	12905.551	Time lockout in post injection after L10 discrete
$K_{12}$	1200.	$\text{ft}/\text{sec}$	52428.8	Depressed $r_d$ coefficient (OAO)
$K_{13}$	1527.1368	$\text{ft}/\text{sec}$	26214.4	Initial velocity multiplier
$K_{14}$	-0.085	$\text{ft}/\text{sec}^2$	16.25	w component of total acceleration prior to 2-in. motion

Table B-3. Equation Input Constants, Contd

Constant	Value	Units	Scale Factor	Definition
K <sub>15</sub>	0.03515625	none	1.	$f_u^*$ in Booster } ground $f_v^*, f_w^*$ in } checkout Booster } only
K <sub>16</sub>	0.013671875	none	1.	
K <sub>17</sub>	6258.8758	ft/sec	52428.8	Polynomial coefficient in $a_o \ln$ expansion
K <sub>18</sub>	14206.27	ft/sec	419430.40	Centaur exhaust velocity ( $g I_{sp}$ )
K <sub>19</sub>	630.	sec	12905.551	Initial value of $\tau$ for sustainer steering
K <sub>20</sub>	3.162278	none	16.	$\sqrt{10}$ ; used in $\ln$ expansion for $a_o$
K <sub>21</sub>	16355.573	ft/sec	52428.8	Polynomial coeffi- cients in $a_o \ln$ expansion
K <sub>22</sub>	28412.630	ft/sec	52428.8	
K <sub>23</sub>	9464.4964	ft/sec	52428.8	
K <sub>24</sub>	5806.9503	ft/sec	52428.8	
K <sub>25</sub>	3087.1626	ft/sec	52428.8	
K <sub>26</sub>	0.04	none	8.	$f_t^2$ lower limit value
K <sub>27</sub>	21209819.	ft	42288909.	Radial limit for re- quired angle of attack control
K <sub>28</sub>	0.01	none	4.	Minimum value of $\alpha_1^2$ for computation of $ \bar{\alpha}_1 $
K <sub>29</sub>	103.	sec	806.59692	Initial value for T in second burn

Table B-3. Equation Input Constants, Contd

Constant	Value	Units	Scale Factor	Definition
$K_{30}$	0.01	none	2.	Minimum value for $\sin^2 \theta$ in computation of $\sin \theta$
$K_{31}$	0.2	none	2.	Lower limit for $f_t$
$P_1$	00 02 00 00 0	-	-	Roundoff bit for $\overline{\Delta r}_m$
$P_2$	12 00 00 00 0	-	-	Roundoff bit for $r_m^2$
$P_3$	10 00 00 00 0	-	-	Roundoff bit for $\overline{\Delta v}_m$
$P_4$	00 08 00 00 0	-	-	Roundoff bit for $\bar{l}_a, \bar{l}_{a2}$
$P_5$	00 00 08 00 0	-	-	Roundoff bit for $\bar{f}^*$

Table B-4. J Constants

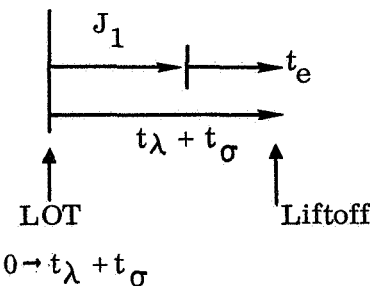
J Number	Function
$J_1$	<p>Initializes launch on time polynomials for <math>t_e</math> computation required only for launch-on-time missions.</p>  <p style="text-align: center;"><math>0 \rightarrow t_\lambda + t_\sigma</math></p> <p><math>J_1</math> orients the 0 point of the launch on time polynomials relative to LOT issuing time.</p> <p><math>J_1</math> is the negative of the time shown in the diagram because the airborne computer adds rather than subtracts <math>J_1</math> when computing <math>t_e</math>; i.e.,</p> $t_e = t_\lambda + t_\sigma + J_1$
$J_2$	Biases time to go for engine shutdown impulse (vehicle dependent) plus fixed program lags.
$J_3, J_4, J_5$	ATS second burn target vector, $\bar{l}_{a2}$ . $\bar{l}_{a2}$ is stored into $\bar{l}_a$ just prior to second burn. It is integrated from launch because of the drifting platform.
$J_6$	<ol style="list-style-type: none"> <li><math>l_{au}</math> target vector component for ATS first burn and OAO.</li> <li>Constant term in <math>l_{au}</math> polynomial for Mariner.</li> </ol>
$J_7$	<ol style="list-style-type: none"> <li><math>\beta_1</math> component polynomial coefficient on ATS mission.</li> <li><math>l_{au} t_e</math> polynomial coefficient for Mariner.</li> </ol>
$J_8$	<ol style="list-style-type: none"> <li><math>l_{au} t_e</math> polynomial coefficient for Mariner.</li> <li>Cosine of the target vector true anomaly for ATS second burn target vector.</li> </ol>
$J_9$	<ol style="list-style-type: none"> <li><math>l_{au} t_e</math> polynomial coefficient for Mariner.</li> <li>Elapsed time from first MECO until vehicle is in proper quadrant for interrogating range angle test on ATS parking orbit.</li> </ol>
$J_{10}$	<ol style="list-style-type: none"> <li><math>l_{au} t_e</math> polynomial coefficient for Mariner.</li> <li>Nominal value of <math>\cos \theta</math> at ATS second burn startup, where <math>\theta</math> is measured from second target vector.</li> </ol>



Table B-4. J Constants, Contd

J Number	Function
$J_{11}$	<ol style="list-style-type: none"> <li>1. <math>l_{av}</math> target vector component for ATS first burn and OAO.</li> <li>2. Constant term in <math>l_{av}</math> polynomial for Mariner.</li> </ol>
$J_{12}$	<ol style="list-style-type: none"> <li>1. <math>l_{av} t_e</math> polynomial coefficient for Mariner.</li> <li>2. <math>\beta_3</math> component polynomial coefficient for ATS mission.</li> </ol>
$J_{13}$	<ol style="list-style-type: none"> <li>1. <math>l_{av} t_e</math> polynomial coefficient for Mariner.</li> <li>2. Radius of apogee for ATS transfer orbit.</li> </ol>
$J_{14}$	<ol style="list-style-type: none"> <li>1. <math>l_{av} t_e</math> polynomial coefficient for Mariner.</li> <li>2. <math>\beta_3</math> component polynomial coefficient for ATS mission.</li> </ol>
$J_{15}$	<ol style="list-style-type: none"> <li>1. <math>l_{av} t_e</math> polynomial coefficient for Mariner.</li> <li>2. <math>\beta_1</math> component polynomial coefficient for ATS.</li> </ol>
$J_{16}$	Desired orbital energy constant term for all missions.
$J_{17}$	Launch time rate of change of orbital energy for Mariner.
$J_{18}, J_{19}$	u, v components of dogleg limited $\bar{l}_n$ vector ( $l_{nw}$ component same as true $l_{nw}$ calculated in COORDINATES). The dogleg limited $\bar{l}_n$ vector is perpendicular to the thrust plane determined by range safety considerations.
$J_{20}$	Predicted $\Delta r$ at ATS second burn startup, chosen so as to optimize payload delivered at end of second burn; depends mainly on parking orbit/transfer orbit relative geometry.
$J_{21}$	Mission targeting branch 2 =0 OAO mission =1 ATS mission =2 Mariner mission
$J_{22}$	Mission MECO switching branch 9 =0 OAO, Mariner missions =1 ATS mission
$J_{23}$	Mission post injection switching branch 16 =2 ATS mission =1 OAO or Mariner mission

Table B-4. J Constants, Contd

J Number	Function
$J_{24}, J_{25}, J_{26}$	$t_e$ polynomial for perigee on all missions (only constant term, $J_{24}$ , required for OAO and ATS)
$J_{27}$	Sets $t_c$ , which is a simulated liftoff time, so that when on-pad earth spin tests are run, the booster steering rates will be issued at times which satisfy flight control system requirements.  Note: $J_{27}$ is set high for flight so as to not constrain holddown time.
$J_{28}$	Mission-dependent initial $\Delta\eta$ , estimate of BECO to MECOI burn arc used for sustainer phase computation of $r_d, \dot{r}_d$ ; independent of launch day, but changes with mission.
$J_{29}$	Used only on OAO mission; time to switch out depressed $r_d$ computation.
$J_{30}$	Post injection $E_t$ switching time; controls elapsed time from MECO that "unlock vent valve", and "power changeover" discrettes are issued.  = 12,900 sec OAO = 12,900 sec Mariner = 2,298 sec ATS
$J_{31}$	Initial Centaur startup acceleration value used by time to go computations between SECO and first Centaur MES; slightly different for each mission.
$J_{32}$	$\cos \eta_A$ for ATS — first burn target vector. ( $\eta_A$ is the true anomaly of the target vector.)  $\eta_A$ is selected so that first burn injection occurs approximately at perigee.
$J_{33}$	Negative of the upward acceleration occurring just after liftoff. $J_{33}$ is used to determine 2-in. liftoff time.
$J_{34}$	Not used
$J_{35}$	Range angle used (in parking orbit section) for issuing second burn MES discrete for ATS second burn.
$J_{36}$	Initial time to go at start of sustainer guidance.
$J_{37}$	Not used
$J_{38}, J_{39}$	Sustainer guidance steering continuity constants; $J_{38}, J_{39}$ approximate a pseudo $\frac{G}{a_T}$ that is required for smooth steering between SECO and MES I.

Table B-4. J Constants, Contd

J Number	Function
J <sub>40</sub>	Elapsed time from SECO that controls the fixed attitude time after MESI; gives a mission dependent time of admitting steering vector during first Centaur burn.
J <sub>41</sub>	Post-injection E <sub>t</sub> switching constant; controls time (from MECO) of admitting the reorient vector during post injection; mission dependent.
J <sub>42</sub>	Post-injection setting of branch 20; mission dependent branch which determines if steering vector (spacecraft separation vector) is rotated with coordinate system or left inertially fixed.  = 1 ATS and Mariner (fixed inertially; by-passes STEER) = 0 OAO (rotated; execute STEER)
J <sub>43</sub> , J <sub>44</sub>	Initial values of r <sub>mu</sub> , r <sub>mv</sub> ; depends on launch pad.
J <sub>45</sub> , J <sub>46</sub> , J <sub>47</sub>	Initial values of l <sub>npu</sub> , l <sub>npv</sub> , l <sub>npw</sub> ; the north pole; depends on launch pad
J <sub>48</sub>	Post-injection setting of branch 20 used after reorient vector is issued; determines whether reorient vector is rotated or fixed inertially  = 1 Mariner (fix inertially) = 0 OAO, ATS (rotate)
J <sub>49</sub> , J <sub>50</sub> , J <sub>51</sub>	$\beta_1, \beta_2, \beta_3$ component (respectively) of the spacecraft separation attitude vector.
J <sub>52</sub> , J <sub>53</sub> , J <sub>54</sub>	Post-injection reorient vector for all missions; different for each mission; on Mariner may be different for different launch days.
J <sub>55</sub>	Value of time to go when exit to MECO countdown is performed; a J constant because of ground test constraints.
J <sub>56</sub>	Value of time to go when B (steering coefficient) is frozen; a J constant because of ground test constraints.
J <sub>57</sub>	An initialization instruction used in the preflight section integrated test.
J <sub>58</sub>	Time from MECO when switching from 90-degree to final third burn pointing vector occurs on ATS.
J <sub>59</sub> , J <sub>60</sub>	$\beta_2$ component t <sub>e</sub> polynomial coefficients used on ATS.

APPENDIX C  
TELEMETRY SEQUENCE

Table C-1. Telemetry Sequence

Word Order	Symbol *	Scale Factor	Units	Definition
1	$a_T$	520.0	ft/sec <sup>2</sup>	Thrust acceleration magnitude
2	$r_{mu_{i-1}}$	42288908.0	ft	u component of position
3	$l_{npv_{i-1}}$	2.0	none	v component of the earth rotational vector
4	$l_{av_{i-1}}$	2.0	none	v component of the target vector
5	$r_{mv}$	42288908.0	ft	v component of position
6	$C_{i-1}$	$0.22171567 \times 10^{13}$	ft <sup>2</sup> /sec	Angular momentum
7	$v_{mw_{i-1}}$	52428.8	ft/sec	w component of velocity
8	$l_{aw_{i-1}}$	2.0	none	w component of the target vector
9	$l_{npu}$	2.0	none	u component of the earth rotational vector
10a	$t_e$	12905.551	sec	Time in the launch window (telemetered from GO INERTIAL to BECO)
10b	$T_{i-1}$	806.59692	sec	Time to go (telemetered from BECO to end)
11	$v_{mu_{i-1}}$	52428.8	ft/sec	u component of velocity
12	$l_{au_{i-1}}$	2.0	none	u component of the target vector
13	$l_{npw}$	2.0	none	w component of the earth rotational vector

Table C-1. Telemetry Sequence, Contd

Word Order	Symbol	Scale Factor	Units	Definition
14	$v_{mv_{i-1}}$	52428.8	ft/sec	v component of velocity
15	$r_{mw}$	42288908.0	ft	w component of position
16	$r_m$	42288908.0	ft	Position magnitude
17	$f_{u_{i-1}}^*$	1.0	none	u component of the steering vector
18	$v_{ow}$	104857.6	ft/sec	w component of sigmator velocity
19	$f_{w_{i-1}}^*$	1.0	none	w component of the steering vector
20	$v_{ov}$	104857.6	ft/sec	v component of sigmator velocity
21	$f_{v_{i-1}}^*$	1.0	none	v component of the steering vector
22	$\sin \theta_{i-1}$	2.0	none	Sine of the central angle
23	$f_{t_{i-1}}$	2.0	none	Tangential steering component
24	$t_i$	12905.551	sec	Guidance compute cycle time
25	$v_{ou}$	104857.6	ft/sec	u component of sigmator velocity

\* Those quantities having an  $i-1$  subscript are parameter values for the previous compute cycle. That is they are effective for  $t_{i-1}$  time. All other quantities are effective for the telemetered  $t_i$  time (Word 24).

APPENDIX D  
INFLIGHT DISCRETES

Table D-1. Inflight Discretes

Discrete	Line	Track $\beta$ Code	Length
Flight mode accept	L9	25	63 W. T.
BECO	L3	19	60 W. T.
SECO backup	L6	22	64 W. T.
PU null	L0	16	64 W. T.
MECO	L16	00	1.1 msec

## APPENDIX E

TIME-TO-GO ERROR RESULTING FROM THRUST PERTURBATION  
DUE TO NULLING PROPELLANT UTILIZATION VALVE

The propellant utilization valve is nulled upon issuing the LO discrete when "Time-To-Go" (T) has been tested and found to be less than the constant  $E_9$ . Thus, the latest possible time for issuing LO is obtained by assuming guidance sampling to be phased such that T is just slightly larger than  $E_9$  on the second to last test. This situation is illustrated in Figure E-1.

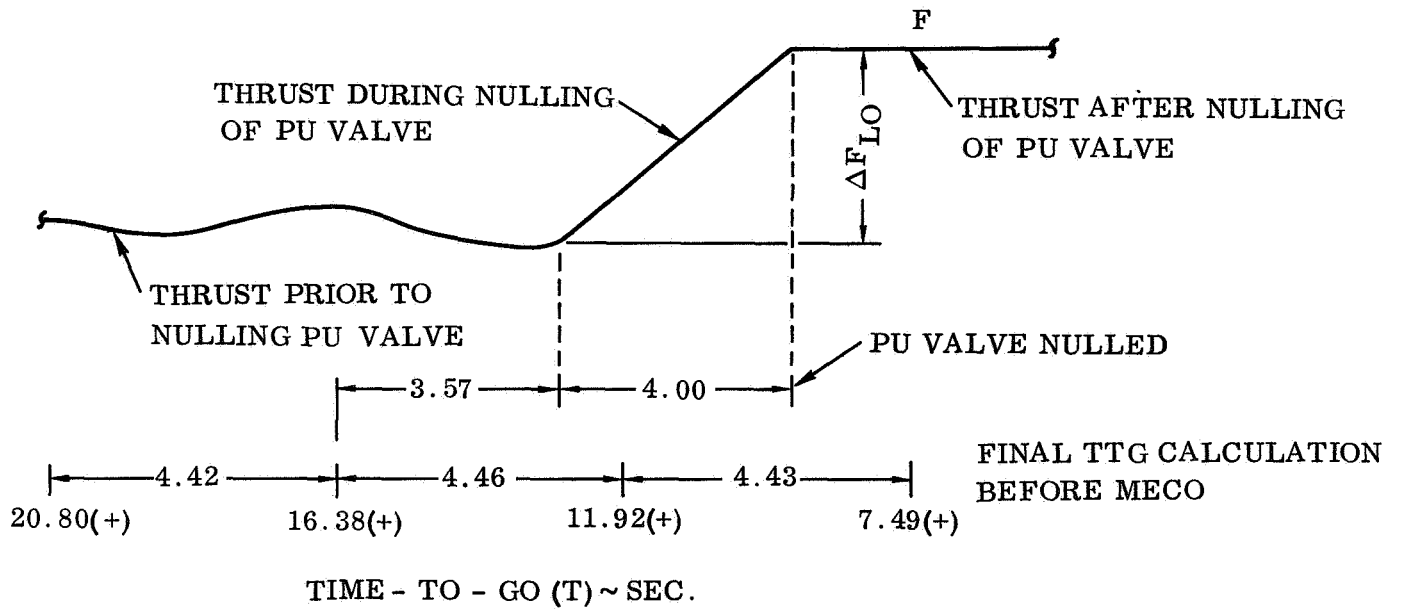


Figure E-1

The Time-To-Go calculation is given by

$$\begin{aligned}
 T &= T' + T_A \\
 &= T' + \frac{C_d - C - \Delta C'}{P_5}
 \end{aligned}
 \tag{E-1}$$

where

$$\Delta C' = (P_1 + 4P_2 + 2P_3 + 4P_4 + P_5) \frac{T'}{12}
 \tag{E-2}$$

The error in T,  $\delta T$ , is

$$\begin{aligned}\delta T &= -\frac{Cd - C - \Delta C'}{P_5^2} \delta P_5 - \frac{\delta(\Delta C')}{P_5} \\ &= -\left[\delta P_1 + 4\delta P_2 + 2\delta P_3 + 4\delta P_4 + \left(1 + 12\frac{T_A}{T'}\right)\delta P_5\right] \frac{T'}{12P_5}\end{aligned}\quad (E-3)$$

The derivative of angular momentum,  $P_i \triangleq P(t_i)$ , is computed as

$$P_i = f_t(t_i) a_T(t_i) r_m(t_i) \quad (E-4)$$

Hence, the error in computing  $P_i$  is

$$\delta P_i = P_i \left[ \frac{\delta f_t(t_i)}{f_t(t_i)} + \frac{\delta a_T(t_i)}{a_T(t_i)} + \frac{\delta r_m(t_i)}{r_m(t_i)} \right] \quad (E-5)$$

Now, assuming the errors  $\delta f_t/f_t$  and  $\delta r_m/r_m$  to be small in comparison to  $\delta a_T/a_T$ , the error in  $P_i$  is approximately

$$\delta P_i = P_i \frac{\delta a_T(t_i)}{a_T(t_i)} \quad (E-6)$$

The predicted thrust acceleration  $a_T(t_i)$  is

$$\begin{aligned}a_T(t_i) &= \frac{K_{18}}{t_i} \\ &= \frac{K_{18}}{\frac{K_{18}}{a_{T_o}} - t_i}\end{aligned}\quad (E-7)$$

The error in  $a_T(t_i)$  is therefore

$$\delta a_T(t_i) = \frac{a_T^2(t_i)}{a_{T_o}} \frac{\delta a_{T_o}}{a_{T_o}}$$



or

$$\frac{\delta a_T(t_i)}{a_T(t_i)} = \frac{a_T(t_i)}{a_{T_0}} \frac{\delta a_{T_0}}{a_{T_0}} \quad (E-8)$$

Since the ratio  $a_T(t_i)/a_{T_0}$  does not differ significantly from unity for  $t_1 = t_2, t_3, t_4$ , and  $t_5$  during the eight seconds preceding MECO, the approximation

$$\frac{\delta a_T(t_i)}{a_T(t_i)} \approx \frac{\delta a_{T_0}}{a_{T_0}} \quad (E-9)$$

is adequate. Using Equations E-6 and E-9, Equation E-3 may be written as

$$\delta T = - \left[ P_1 + 4P_2 + 2P_3 + 4P_4 + \left( 1 + 12 \frac{T_A}{T'} \right) P_5 \right] \frac{T'}{12P_5} \frac{\delta a_{T_0}}{a_{T_0}} \quad (E-10)$$

In addition, since  $P_1 \approx P_2 \approx \dots \approx P_5$  for  $T < 8$ , Equation E-10 may be simplified to read

$$\delta T = - \left( 1 + \frac{T_A}{T'} \right) \frac{\delta a_{T_0}}{a_{T_0}} T' \quad (E-11)$$

Finally, the ratio  $T_A/T'$  is insignificant (about 0.02 maximum) in comparison to unity. Thus, the error in the final TTG calculation is approximately

$$\delta T = - \frac{\delta a_{T_0}}{a_{T_0}} T' \quad (E-12)$$

The current up-dated acceleration,  $a_{T_0}$ , is calculated as

$$a_{T_0} = \left( 1 + \frac{\Delta t}{2\tau - \Delta t} \right) a_T \quad (E-13)$$

where  $a_T$  is effectively given by

$$a_T = \frac{1}{\Delta t} \int_{t-1}^{t_0} \frac{F}{M} dt \quad (E-14)$$

The error in the final computed  $a_{T_0}$  becomes

$$\begin{aligned}\delta a_{T_0} &= \left(1 + \frac{\Delta t}{2\tau - \Delta t}\right) \delta a_T \\ &= \frac{1}{\Delta t} \left(1 + \frac{\Delta t}{2\tau - \Delta t}\right) \int_{t-1}^{t_0} \frac{\delta F}{M} dt\end{aligned}\quad (E-15)$$

Here,  $\delta F$  is the perturbation in engine thrust due to nulling the PU valve and is referenced to the final thrust level attained after the valve has closed (4.0 seconds following the LO discrete). Using Figure E-1, Equation E-15 can be evaluated as

$$\delta a_{T_0} = -0.273 \frac{\Delta F_{LO}}{M} \quad (E-16)$$

where  $\Delta F_{LO}$  is the change in thrust level due to nulling the PU valve. Since the true value of the current acceleration is simply  $F/M$ , the error in the final TTG calculation becomes

$$\delta T = 0.273 \frac{\Delta F_{LO}}{F} T' \quad (E-17)$$

It should be noted (see Figure E-1) that a "critical" region exists for the final TTG calculation. This region, referenced to the CUT cycle, is defined by

$$8.00 > T > 7.49 \quad (E-18)$$

Obviously,  $T$  must be less than 8.00 (J<sub>55</sub>) by definition of the CUT cycle. On the other hand, if  $T$  is less than 7.49, the LO discrete is issued one cycle earlier resulting in an error free final  $a_{T_0}$  calculation.

Table E-1 presents the thrust shifts,  $\Delta F_{LO}$ , observed from post-flight data taken from the Surveyor program.

These data, together with our present understanding of the propellant utilization system, suggest that the thrust shift  $\Delta F_{LO}$  be considered as a random variable having a p.d.f. as shown in Figure E-2.

Table E-1. Thrust Shift,  $F_{LO}$ , Due to PU Valve  
Final Null Angle Shift

Vehicle AC-	No. of Burns	$\Delta F_{LO}$ (lb)
6	1	+314
7	1	+307
9	2	+360
10	1	+258
11	1	+263
12	2	+465
13	2	+260
14	2	+180
15	2	+300

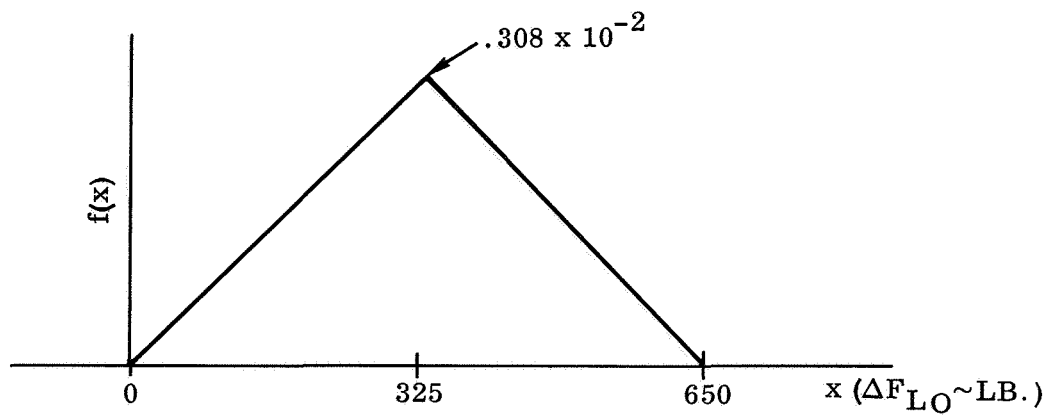


Figure E-2. Probability-Density-Function (p. d. f.) for Thrust Shift  
Due to PU Valve Final Null Angle Shift

Here, the upper limit of  $\Delta F_{LO} = 650$  lb represents the absolute physical limit of the PU/propulsion system.

Assuming the final Time-To-Go,  $T$ , to be uniformly distributed over the interval  $(3.57, 8.00)$ , the probability of  $T$  being in the critical region is  $0.51/4.43$  or  $0.115$ . Using Equation E-17 with  $F = 30,000$  lb and  $T' = 7.75$  seconds, the overall p.d.f. for the error  $\delta T$  due to the PU valve final null angle shift can be determined. The result is shown in Figure E-3.

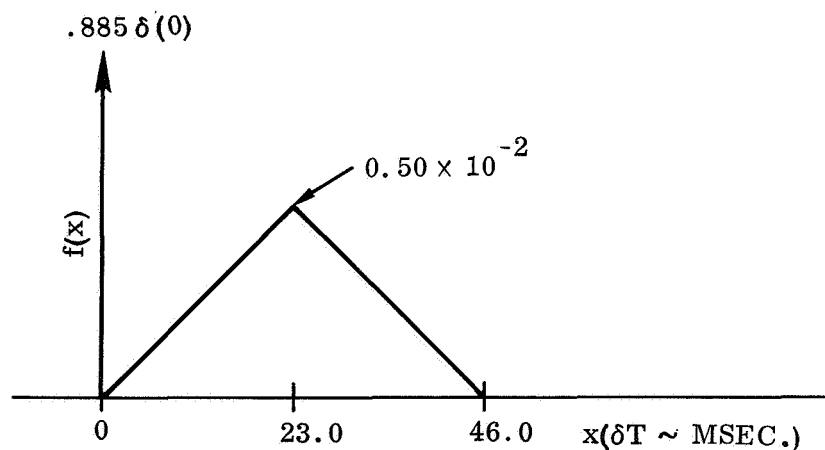


Figure E-3. Probability-Density-Function (p.d.f.) for Error in TTG Due to PU Valve Final Null Angle Shift

The delta function, corresponding to the event  $\delta T = 0$ , reflects the non-zero probability that the final value of  $T$  lies outside the critical region. The mean and standard deviations for this distribution are 2.65 and 7.93 msec respectively.

## APPENDIX F

### SIGMATOR VELOCITY FILTERING TECHNIQUE

In Section 2.1 it was pointed out that the velocity from the sigmator was read in a way which automatically provides a filter for accelerometer limit cycle noise. This section discusses that technique.

Accelerometer limit cycling introduces a random error into the sigmator velocity sampled by the inflight guidance equations. This random error propagates into the guidance computed steering vector and the time-to-go prediction. This has the two-fold result of producing a random error in both the vehicle turning rates and the cutoff time.

The problems caused by accelerometer limit cycling may be alleviated by the method of averaging. Averaging consists of taking the average value of repeated measurements of a quantity which reduces the random error in that quantity because the average of  $n$  data points has a standard deviation of  $\sigma/\sqrt{n}$ , where  $\sigma$  is the standard deviation of the individual data points.

A simple modification to the airborne computer SOT program enables the inflight guidance equations to average sigmator velocity. Recall that the equations use only the  $t_\sigma$  and  $\bar{v}_\sigma$  data, but not the  $\bar{r}_\sigma$  data, from the sigmator. Thus the  $\bar{r}_\sigma$  sectors are available to accumulate and average velocity pulses.

The sigmator of the GPK-33 computer integrates velocity to obtain position. The integration is approximated by a rectangular summation process as

$$\begin{aligned}
 r_\sigma &= v_{\sigma_0} \Delta t + v_{\sigma_1} \Delta t + v_{\sigma_2} \Delta t + \dots \\
 &= \Delta t (v_{\sigma_0} + v_{\sigma_1} + v_{\sigma_2} + \dots) \\
 &= \Delta t \sum_{i=1}^n v_{\sigma_i}
 \end{aligned}$$

The quantity  $\Delta t$  is chosen as the time necessary to accumulate eight time standard pulses. Since the time standard produces 1300 pulses per second,  $\Delta t$  equals  $8/1300$  second, and in 1 second it is then necessary to perform exactly  $1300/8$  summations of  $v_{\sigma}$  to maintain the accuracy of the  $r_{\sigma}$  computation. Since the nominal drum speed of 100 rps causes 200 summations per second to occur, it is necessary to delete some of these summations to maintain  $r_{\sigma}$  validity.

The multiplication of  $\Delta t$  times  $\sum_{i=1}^n v_{\sigma i}$  does not actually occur but rather is implied in the scale factor ultimately assigned to  $r_{\sigma}$ . Thus what really exists in the  $r_{\sigma}$  word of the sigmator is  $\sum_{i=1}^n v_{\sigma i}$ , precisely the quantity needed to average  $v_{\sigma}$  provided  $n$  is known.

The summation process occurs every one-half drum revolution; thus if the  $r_{\sigma}$  word is read at intervals which are precise multiples of one-half drum revolution, and no deletions occur during this interval, the exact number of  $v_{\sigma}$  samples contained in the  $r_{\sigma}$  word will be known. Therefore, in order to use the  $r_{\sigma}$  word as a velocity averager, it is necessary to cause the summation deletions not to occur.

The process for obtaining  $\bar{v}_{\sigma}$  on each compute cycle is then as follows:

1. Store 0 on the  $\bar{r}_{\sigma}$  sectors.
2. Exactly four drum revolutions later read  $t_{\sigma}$ .
3. Exactly eight drum revolutions after zeroing  $\bar{r}_{\sigma}$ , read  $\bar{r}_{\sigma}$  (thus  $n = 16$  in the summation process).

The  $\bar{r}_{\sigma}$  read in this manner is thus in fact the accumulation of 16 velocity data points. The scale factor associated with the lower word of  $\bar{r}_{\sigma}$  is  $0.16777216 \times 10^7$ . Thus by assigning the  $\bar{r}_{\sigma}$  data a scale factor of 104857.6 we are in fact averaging 16 velocity data points ( $104857.6 = 0.16777216 \times 10^7 / 16$ ). Therefore we have an averaged  $\bar{v}_{\sigma}$  by reading  $\bar{r}_{\sigma}$  and assigning the data the appropriate scale factor. This averaging method reduces the random noise on  $\bar{v}_{\sigma}$  by a factor of four, with no cost in inflight program storage.

This averaging process required a modification to the existing SOT program. Deletions in the  $r_{\sigma}$  process are normally determined by ORing SOT at bit  $P_{24}$  of the Phase II time word with a time accumulation dependent expression. If the output of the OR circuit is a one, a summation occurs; if it is a zero, a deletion occurs. The SOT program had a zero at bit  $P_{24}$  of the Phase II time word and as a result the summation or deletion was determined by the time accumulation dependent expression. The SOT bit  $P_{24}$  at bit  $P_{24}$  of the Phase II time word was changed to a one so that no deletions would occur. This had the desired effect of providing a true summation process, and subsequently reducing random noise by a factor of four.

**GENERAL DYNAMICS**  
*Convair Division*